Progress In Electromagnetics Research, PIER 70, 79–174, 2007

ANALYTICAL METHODS IN THEORY OF SLOT-HOLE COUPLING OF ELECTRODYNAMICS VOLUMES

M. V. Nesterenko, V. A. Katrich, Yu. M. Penkin and S. L. Berdnik

Department of Radiophysics
V.N. Karazin Kharkov National University
4, Svobody Sq., Kharkov 61077, Ukraine

Abstract—The approximate analytical solution of the integral equation concerning the equivalent magnetic current in the narrow slot, coupling two electrodynamic volumes, has been obtained by the averaging method. The formulas and the plots for currents and the coupling coefficients of longitudinal and transverse slots in the common walls of rectangular waveguides are represented. By means of the induced magnetomotive forces method using basis functions of current distribution, obtained by the averaging method, the following electrodynamic structures have been considered: the electrically long longitudinal slot in the common broad wall of rectangular waveguides; two symmetrical transverse slots in the common broad wall of rectangular waveguides; the transverse slots system in the common broad wall of rectangular waveguides. The problem about the resonant iris with the arbitrary oriented slot in the plane of cross-section of a rectangular waveguide has been solved by the averaging method. The problem about stepped junction of two semi-infinite rectangular waveguides with the impedance slotted iris has been solved by the induced magnetomotive forces method. The analytical formulas for the distributed surface impedance of homogeneous and inhomogeneous magnetodielectric coatings of iris surface have been obtained. For a greater number of the considered electrodynamic structures the calculated values are compared with the results, obtained by numerical methods (also using commercial programs) and the experimental data.

1. PROBLEM FORMULATION AND INITIAL INTEGRAL EQUATIONS; AVERAGING METHOD

The problem of electromagnetic coupling of two waveguides through apertures in their common walls is a classical problem which attracted the attention of many investigators starting from the paper written by Bethe in 1944 [1]. The narrow slots with the length of $2L$ commensurable with the operating wavelength of λ have especially been studied [2–13]. The investigations of the slots located both in broad and narrow walls of rectangular waveguides have been conducted by different methods, namely: analytical [2, 3], variational [4, 5], numerical [6–11], among which the most effective methods are the moments method and its particular case known as the Galerkin's method, the equivalent circuits method [12, 13], and also the finite elements method and the moments method [14].

At present, commercial finite elements software (e.g., "Ansoft's HFSS and Designer", "CST Microwave Studio", "Zeland" and others) is available to solve such problems. However, these programs need intensive memory, and sometimes they are very slow, for example, in electrically long slots and multi-slot systems analysis.

On the other hand, the approximate methods, mentioned above, have some drawbacks. The known analytical solutions have a limited range of applicability ($kL \cong \pi/2$, where $k = 2\pi/\lambda$) and the variational and equivalent circuits methods suppose the presence of the information a priori about the distribution function of the equivalent slot magnetic current. Even approximation of this information is unknown (for example, for electrically longitudinal slots) in some cases. That is why there exists a need to develop approximate methods which provide fast, sufficiently accurate calculations of simple waveguide-slot structures.

1.1. General Problem Formulation and Transition to the Case of a Narrow Slot

Let two volumes (limited by perfectly conducting flat surfaces) be coupled between each other by the slot in the common unlimited thin wall. Using the boundary condition of the tangential magnetic field continuity on the S_{sl} surface of the coupling aperture, we obtain the following integral equation concerning the equivalent magnetic current (time dependence $e^{i\omega t}$ throughout the book is used, ω is the circular

frequency) [15]:

$$(\text{graddiv} + k^2) \int\limits_{S_{sl}} \hat{G}_m^{\Sigma}(\vec{r}, \vec{r}\,')\vec{J}^m(\vec{r}\,')d\vec{r}\,' = -i\omega\vec{H}_0^{\Sigma}(\vec{r}). \tag{1}$$

Here: $\vec{r}$ is the observation point radius-vector; $\vec{r}\,'$ is the source radius-vector; $\vec{J}^m(\vec{r})$ is the magnetic current surface density on the aperture; $\hat{G}_m^{\Sigma}(\vec{r}, \vec{r}\,') = \hat{G}_m^e(\vec{r}, \vec{r}\,') + \hat{G}_m^i(\vec{r}, \vec{r}\,')$, $\hat{G}_m^{e,i}(\vec{r}, \vec{r}\,')$ are the magnetic dyadic Green's functions; $\vec{H}_0^{\Sigma}(\vec{r}) = \vec{H}_0^i(\vec{r}) - \vec{H}_0^e(\vec{r})$ are the impressed sources fields in the internal (index "i" for the region 1 and 2) and the external (index "e" for regions 3 and 4) volumes.

The $\hat{G}_m^{e,i}(\vec{r}, \vec{r}\,')$ functions are the following [16]:

$$\hat{G}_m^{e,i}(\vec{r}, \vec{r}\,') = \hat{I}G(\vec{r}, \vec{r}\,') + \hat{G}_{0m}^{e,i}(\vec{r}, \vec{r}\,'), \tag{2}$$

where $\hat{I}$ is the unit dyadic, $G(\vec{r}, \vec{r}\,') = \frac{e^{-ik|\vec{r}-\vec{r}\,'|}}{|\vec{r}-\vec{r}\,'|}$ is the Green's free space function and $\hat{G}_{0m}^{e,i}(\vec{r}, \vec{r}\,')$ are the regular everywhere dyadic functions providing satisfaction of boundary conditions for $\hat{G}_m^{e,i}(\vec{r}, \vec{r}\,')$ functions on the internal surface of the volumes coupled.

The Equation (1) is rather difficult to analyze in a general case; however, for the narrow slots ($d/2L \ll 1$, $d/\lambda \ll 1$), where d is the slot width, the equation is sufficiently simplified. In this case the slot current can be written in the following way (index "m" is omitted):

$$\vec{J}(\vec{r}) = \vec{e}_s J(s)\chi(\xi), \quad J(\pm L) = 0, \quad \int\limits_{\xi} \chi(\xi)d\xi = 1, \tag{3}$$

where s and ξ are the longitudinal and transverse local slot coordinates (Figure 1); $\vec{e}_s$ is the unit vector; $\chi(\xi)$ is the set function accounting the peculiarities of the electrostatic field on the slot edge [17]:

$$\chi(\xi) = \frac{1/\pi}{\sqrt{(d/2)^2 - \xi^2}}. \tag{4}$$

Thus, the $\vec{J}(\vec{r})$ current problem in the $\vec{H}_0^{\Sigma}(\vec{r})$ field given reduces to the determination of the $J(s)$ current distribution function.

Let us consider the slot to be rectilinear and the impressed field in the external volume to be absent, that is $\vec{H}_o^e(\vec{r}) = 0$. Then substituting

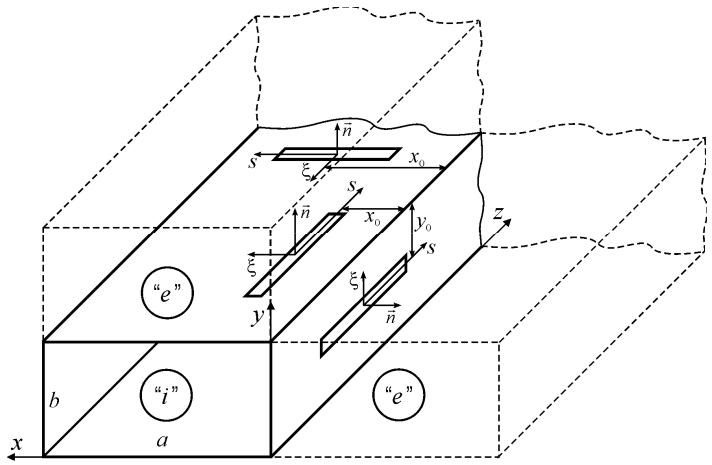

Figure 1. The problem formulation and the symbols used.

(3) and (4) into (1) we get:

$$\left(\frac{d^2}{ds^2}+k^2\right)\int\limits_{-L}^{L} J(s')[G_s^e(s,s')+G_s^i(s,s')]ds' = -i\omega H_{0s}^i(s), \tag{5}$$

$$G_s^{e,i}(s,s') = 2\frac{e^{-ikR(s,s')}}{R(s,s')}+G_{0s}^{e,i}(s,s'),\ R(s,s')=\sqrt{(s-s')^2+(d/4)^2}. \tag{6}$$

Here we take into account the fact that for the sources on the flat surface $\hat{G}^{e,i}(s,\xi;s',\xi')=2\hat{I}G(s,\xi;s',\xi')+\hat{G}_0^{e,i}(s,\xi;s',\xi')$ we have:

$$G(s,s')=\int\limits_{\xi} G(s,\xi;s',\xi')\chi(\xi')d\xi',\ \hat{G}_0^{e,i}(s,s') = \int\limits_{\xi} \hat{G}_0^{e,i}(s,\xi;s',\xi')\chi(\xi')d\xi'.$$

It must be noted that in the kernel (6) of the integral Equation (5) the approximate expression for $|\vec{r}-\vec{r}\,'|$ in the transverse coordinate dependence is chosen in the form of $(\xi-\xi')^2 \cong (d/4)^2$, as it is usually used in the vibrator antenna theory [18] and it is precisely the form for the slots on metallic surfaces [15, 17, 19].

Isolating the logarithmic peculiarity in the Equation (5) analogically with [2, 15, 18], we obtain:

$$\int\limits_{-L}^{L} J(s')\frac{e^{-ikR(s,s')}}{R(s,s')}ds' = J(s)\Omega(s) + \int\limits_{-L}^{L}\frac{J(s')e^{-ikR(s,s')}-J(s)}{R(s,s')}ds', \tag{7}$$

where $\Omega(s) = \int\limits_{-L}^{L} \frac{ds'}{R(s,s')}$. Suppose due to [2] $\Omega(s) \approx \Omega(0) = 2\ln\frac{8L}{d}$, we obtain the integral-differential equation with a small parameter:

$$\frac{\mathrm{d}^2 J(s)}{\mathrm{d}s^2} + k^2 J(s) = \alpha\left\{i\omega H_{0s}(s) + F[s, J(s)] + F_0[s, J(s)]\right\}, \qquad (8)$$

where $\alpha = \frac{1}{8\ln(d/(8L))}$ is the natural small ($|\alpha| \ll 1$) parameter of the problem; $H_{0s}(s)$ is the component of the field of the impressed sources on the slot axis;

$$F[s, J(s)] = 4\left[-\frac{\mathrm{d}J(s')}{\mathrm{d}s'}\frac{e^{-ikR(s,s')}}{R(s,s')}\bigg|_{-L}^{L} + \left(\frac{2\mathrm{d}J(s)}{\mathrm{d}s} + J(s)\frac{\mathrm{d}}{\mathrm{d}s}\right)\frac{1}{R(s,s')}\right] + 4\int\limits_{-L}^{L}\frac{\left[\frac{\mathrm{d}^2 J(s')}{\mathrm{d}s'^2} + k^2 J(s')\right]e^{-ikR(s,s')} - \left[\frac{\mathrm{d}^2 J(s)}{\mathrm{d}s^2} + k^2 J(s)\right]}{R(s,s')}\mathrm{d}s' \qquad (9)$$

is the slot own field in the infinite screen;

$$F_0[s, J(s)] = -\frac{\mathrm{d}J(s')}{\mathrm{d}s'}[G^e_{0s}(s,s') + G^i_{0s}(s,s')]\bigg|_{-L}^{L} + \int\limits_{-L}^{L}\left[\frac{\mathrm{d}^2 J(s')}{\mathrm{d}s'^2 + k^2 J(s')}\right][G^e_{0s}(s,s') + G^i_{0s}(s,s')]\mathrm{d}s' \qquad (10)$$

is the slot own field repeatedly reflected from the coupled volumes walls.

We must note that the inequality $|\alpha| \ll 1$ is valid in sufficiently wide limits of the ratio $(d/2L)$ variation: for example, for $(d/2L) = 0.1$ we have $|\alpha| = 0.034$ and for $(d/2L) = 0.3$ we have $|\alpha| = 0.048$.

1.2. Asymptotic Averaging Method

The questions of a strict ground of the asymptotic averaging method are a pure mathematic problem investigated in details in the monographs [20, 21], where the corresponding theorems of averages are proved. Let us consider briefly those their principes we need further.

Let the system of ordinary differential equations in a standard form (x- the n-dimensional vector, $0 < \alpha \ll 1$ — the small parameter) be set

$$\frac{\mathrm{d}x}{\mathrm{d}s} = \alpha X(s, x), \qquad (11)$$

which is characterized by that, that the first derivatives $\frac{\mathrm{d}x}{\mathrm{d}s}$ are proportional to the small parameter, that is, x variables change slowly. Different methods exist to reduce the equations to form (11), at the same time the method of variation of arbitrary constants is oftener used [21]. Considering that, reduction of the initial equations system to the standard form has been done, we change the variables in (11)

$$x = \zeta + \alpha\tilde{X}(s, \zeta), \tag{12}$$

where ζ are considered as new unknowns, $\frac{\partial\tilde{X}}{\partial s} = X(s, \zeta) - \overline{X}(\zeta)$, and the bar symbol means average on the explicitly containing variable s

$$\overline{X}(\zeta) = \lim_{l\to\infty} \frac{1}{l} \int_0^l X(s, \zeta)ds. \tag{13}$$

Then, after some transformations, we can get [20]

$$\frac{\mathrm{d}\zeta}{\mathrm{d}s} = \alpha\overline{X}(\zeta) + \alpha^2 \dots, \tag{14}$$

that is, if ζ satisfies the Equations (14), the right part of which differs from the right part of averaging equations

$$\frac{\mathrm{d}\zeta}{\mathrm{d}s} = \alpha\overline{X}(\zeta) \tag{15}$$

at the values of the α^2 order; then the expression (12) is an accurate development of the input equations (11). That is why, we can accept $x = \zeta$, as the first approximation where ζ is solution of the Equations (15), which satisfies the Equations (11) precisely to the values of the infinitesimal second order.

Thus, the equations in the first approximation (15) are obtained from the exact Equations (11) by means of averaging the last on the s-variable and ζ are considered to be constants. This formal process, which consists of changing the exact equations by averaging ones, is called the averaging principle. Its essence was brought to light by N. Bogolyubov [20], who showed that the averaging method was connected with the existence of some change of variables which allow to omit s from the right part of equations with any accuracy grade relatively to the α-small parameter. It gives the opportunity to form not only the system of the first approximation (15) but to find the averaging system of higher orders, solution of which approximate the solutions of (11) with arbitrary fixed precision though, practically, because of quick complication of formulas the first approximation can effectively

be mainly used. The proof of the smallness of the first approximation error was also obtained by N. Bogolyubov [20], who determined, that under rather general conditions the difference $x(s)-\zeta(s)$ could be done as small as possible for sufficiently small α on any big but finite interval $0 < s < l$. Thus, the following basic theorem of average takes place [20, 21].

The theorem I. Let the function $X(s,x)$ be determined and continuous in domain Q ($s \geq 0$, $x \in D$), and in this domain:

1. $X(s,x) \in Lip_x(\lambda, Q)$, that is, $X(s,x)$ satisfies the Lipshits condition with the constant λ at x;
2. $\|X(s,x)\| < M$, that is, $X(s,x)$ is limited;
3. in each point $x \in D$ the limit (13) exists;
4. the solution $\zeta(s)$ of the averaging system (15) is determined for all $s \geq 0$ and is situated in the D-domain with some ρ-neighborhood.

Then for any possibly small $\eta > 0$ and any possibly big $L > 0$ we can indicate such α_0, that at $0 < \alpha < \alpha_0$ the unequation will be fulfilled on the segment $0 \leq s \leq L\alpha^{-1}$

$$\|x(s) - \zeta(s)\| < \eta,$$

where $x(s)$ and $\zeta(s)$ — the solutions of the systems (11) and (15), correspondingly, coinciding at $s = 0$.

This theorem is also generalized in the integral-differential equations in a standard form

$$\frac{\mathrm{d}x}{\mathrm{d}s} = \alpha X\left(s, x, \int_0^s \phi\left(s, s', x(s')\right) ds'\right), \tag{16}$$

for which the following scheme of averages is possible [21]. Let us calculate the integral

$$\psi(s,x) = \int_0^s \phi(s, s', x)\mathrm{d}s' \tag{17}$$

on the explicitly entering variable s' (here s and x are considered to be parameters). Now alongside with (16) let us consider the differential equations system

$$\frac{\mathrm{d}y}{\mathrm{d}s} = \alpha X\left(s, y, \psi(s,y)\right), \tag{18}$$

which subject to averaging, namely: let the limit exist

$$\lim_{l\to\infty}\frac{1}{l}\int\limits_0^l X\left(s,y,\psi(s,y)\right)\mathrm{d}s=\overline{X}(y). \tag{19}$$

Then we obtain the following differential equations system

$$\frac{\mathrm{d}\zeta}{\mathrm{d}s}=\alpha\overline{X}(\zeta). \tag{20}$$

The system (20) is averaged, corresponding to the integral-differential equations system (16). Thus, the idea of average in the systems of the form (16) is to approximate solutions of this system by solutions of a specially selected system of differential equations of the form (20), which, probably, it is easier to investigate than the initial integral-differential equations system. The conditions under which the proximity of solutions (16), (18) and (20) take place are given in [21].

In the integral-differential systems (as different from the average in the differential systems) different variants of average are possible. In a general case for one system of the integral-differential equations it is possible to put into accordance some different systems of the averaged equations. Some of these averaged systems are the differential equations systems, others — integral-differential equations systems. The possibility of choice of a more suitable averaged system defines high efficiency of the method of average at applied problems solutions.

Let us consider the following integral-differential equations systems

$$\frac{\mathrm{d}x}{\mathrm{d}s}=\alpha X\left(s,x,\frac{\mathrm{d}x}{\mathrm{d}s},\int\limits_0^s\phi\left(s,s',x(s'),\frac{\mathrm{d}x(s')}{\mathrm{d}s'}\right)\mathrm{d}s'\right), \tag{21}$$

which is the system of a standard form unsolved relating to the derivative. Practically, the attempt to solve the system relatively to $\frac{\mathrm{d}x}{\mathrm{d}s}$ often runs into the necessity to fulfill intricate and laborious computations. That is why the corresponding schemes of averages which allow to avoid this [21]. Thus, in the first approximation instead of (21) we can consider the simplified system

$$\frac{\mathrm{d}y}{\mathrm{d}s}=\alpha X\left(s,y,0,\int\limits_0^s\phi\left(s,s',y(s'),0\right)\mathrm{d}s'\right), \tag{22}$$

because availability of the derivates in the right part (21) begins to affect the second and further asymptotic approximations. The solutions (21) and (22) are arbitrarily near on the segment of the $L\alpha^{-1}$ order at sufficiently general conditions and small α.

Both in the integral-differential equations systems and in the differential equations ones different variants of partial average are possible, that is, only several addendums or individual equations in the fixed system [21] undergo average. Particularly, if the initial system has the form

$$\frac{\mathrm{d}x}{\mathrm{d}s} = \alpha X_1(s,x) + \alpha X_2(s,x) \tag{23}$$

and the limit exists

$$\lim_{l\to\infty} \frac{1}{l} \int_0^l X_1(s,x)\mathrm{d}s = \overline{X}_1(x), \tag{24}$$

then the partially averaged system corresponds to the system (23)

$$\frac{d\zeta}{ds} = \alpha\overline{X}_1(\zeta) + \alpha X_2(s,\zeta). \tag{25}$$

Variants of partial averaging are rather various and also stretch on the systems of the form (16) and (21).

2. ANALYTICAL SOLUTION OF THE INTEGRAL EQUATIONS FOR THE CURRENT

In this section the asymptotic averaging method has been used to obtain the general approximate analytical expression for the magnetic current in the slot applied both for the adjusted slots ($kL = n\pi/2$, $n = 1, 2, 3\ldots$) and for the unadjusted ones ($kL \neq n\pi/2$) coupling two waveguides of different cross-section sizes in a common case which are exited by the arbitrary field of impressed sources.

2.1. Solution of the Equation for the Current in a General Form

Due to the constants variation method [20] let us change the variables:

$$\begin{aligned} J(s) &= A(s)\cos ks + B(s)\sin ks, \\ \frac{\mathrm{d}J(s)}{\mathrm{d}s} &= -A(s)k\sin ks + B(s)k\cos ks, \\ &\quad \times \left(\frac{\mathrm{d}A(s)}{\mathrm{d}s}\cos ks + \frac{\mathrm{d}B(s)}{\mathrm{d}s}\sin ks = 0\right), \end{aligned}$$

$$\begin{aligned}\frac{\mathrm{d}^2J(s)}{\mathrm{d}s^2}+k^2J(s) &= -\frac{\mathrm{d}A(s)}{\mathrm{d}s}\sin ks+\frac{\mathrm{d}B(s)}{\mathrm{d}s}\cos ks \\ &= \frac{\alpha}{k}\left\{i\omega H_{0s}(s)+F_N[s,J(s)]\right\}. \qquad (26)\end{aligned}$$

The Equation (8) goes to the next system of the integral-differential equations for the unknown functions $A(s)$ and $B(s)$:

$$\begin{aligned}\frac{\mathrm{d}A(s)}{\mathrm{d}s} &= -\frac{\alpha}{k}\left\{i\omega H_{0s}(s)+F_N\left[s,A(s),\frac{\mathrm{d}A(s)}{\mathrm{d}s},B(s),\frac{\mathrm{d}B(s)}{\mathrm{d}s}\right]\right\}\sin ks, \\ \frac{\mathrm{d}B(s)}{\mathrm{d}s} &= +\frac{\alpha}{k}\left\{i\omega H_{0s}(s)+F_N\left[s,A(s),\frac{\mathrm{d}A(s)}{\mathrm{d}s},B(s),\frac{\mathrm{d}B(s)}{\mathrm{d}s}\right]\right\}\cos ks, \quad (27)\end{aligned}$$

where $F_N = F + F_0$ and it is the slot full own field.

The equations obtained are fully equivalent to the Equation (8), and they are the system of the integral-differential equations of standard type unsolved for a derivative. The right-hand parts of these equations are proportional to the α small parameter. Therefore, the $A(s)$ and $B(s)$ functions in the right-hand parts of the Equations (27) can be regarded as slowly changing functions. To solve the system of the equations in (27) it is possible to use the asymptotic averaging method. Then when we put the system of the Equations (27) in accordance with the simplified system [20] where in the right-hand parts of the equations $\frac{\mathrm{d}A(s)}{\mathrm{d}s}=0$, $\frac{\mathrm{d}B(s)}{\mathrm{d}s}=0$. When we make partial averaging [21] in (27) along the s explicitly entering variable we obtain two equations of the first approximation:

$$\begin{aligned}\frac{\mathrm{d}\overline{A}(s)}{\mathrm{d}s} &= -\alpha\left\{\frac{i\omega}{k}H_{0s}(s)+\overline{F}_N[s,\overline{A},\overline{B}]\right\}\sin ks, \\ \frac{\mathrm{d}\overline{B}(s)}{\mathrm{d}s} &= +\alpha\left\{\frac{i\omega}{k}H_{0s}(s)+\overline{F}_N[s,\overline{A},\overline{B}]\right\}\cos ks, \qquad (28)\end{aligned}$$

where

$$\begin{aligned}\overline{F}_N[s,\overline{A},\overline{B}] &= \left[\overline{A}(s')\sin ks'-\overline{B}(s')\cos ks'\right]G_s^{\Sigma}(s,s')\Big|_{-L}^{L}, \\ G_s^{\Sigma}(s,s') &= 4\frac{e^{-ikR(s,s')}}{R(s,s')}+G_{0s}^{e}(s,s')+G_{0s}^{i}(s,s') \\ &= G_s^{e}(s,s')+G_s^{i}(s,s'). \qquad (29)\end{aligned}$$

Integrating the system (28) and substituting the obtained values $\overline{A}(s)$ and $\overline{B}(s)$ as the approximating functions for $A(s)$ and $B(s)$ in

(26) we get the most general asymptotic expression for the narrow slot current in the arbitrary position relative to coupled volumes walls:

$$J(s) = \overline{A}(-L)\cos ks + \overline{B}(-L)\sin ks + \alpha \int_{-L}^{s} \left\{ \frac{i\omega}{k} H_{0s}(s') + \overline{F}_N[s', \overline{A}, \overline{B}] \right\} \sin k(s-s')\mathrm{d}s'. \quad (30)$$

To define the constants $\overline{A}(\pm L)$ and $\overline{B}(\pm L)$ it is necessary to use the boundary conditions $J(\pm L) = 0$ and the symmetrical conditions [18] which are uniquely connected with the slot excitation technique. Then taking into consideration the symmetrical (index "s") and the antisymmetrical (index "a") current components at arbitrary excitation $H_{0s}(s) = H_{0s}^s(s) + H_{0s}^a(s)$ of the slot with the accuracy not more than the terms of the α^2 order, we, finally, have:

$$J(s) = J^s(s) + J^a(s) = \alpha \frac{i\omega}{k} \times \left\{ \int_{-L}^{s} H_{0s}(s') \sin k(s-s')\mathrm{d}s' - \frac{\sin k(L+s) \int_{-L}^{L} H_{0s}^s(s') \sin k(L-s')\mathrm{d}s'}{\sin 2kL + \alpha N^s(kd, 2kL)} - \frac{\sin k(L+s) \int_{-L}^{L} H_{0s}^a(s') \sin k(L-s')\mathrm{d}s'}{\sin 2kL + \alpha N^a(kd, 2kL)} \right\}, \quad (31)$$

where $N^s(kd, 2kL)$ and $N^a(kd, 2kL)$ are the functions of the slot own field which are equal, respectively:

$$N^s(kd, 2kL) = \int_{-L}^{L} [G_s^{\Sigma}(s, -L) + G_s^{\Sigma}(s, L)] \sin k(L-s) ds,$$

$$N^a(kd, 2kL) = \int_{-L}^{L} [G_s^{\Sigma}(s, -L) - G_s^{\Sigma}(s, L)] \sin k(L-s) ds, \quad (32)$$

and which are completely defined by the Green's functions of the coupled volumes representing infinite and half-infinite waveguides, resonators and etc.

It is necessary to note that near the resonance ($\sin 2kL \approx 0$) the main contribution to the current amplitude is made by the functions of the slot own field $N^s(kd, 2kL)$ and $N^a(kd, 2kL)$, which take into account both the basic oscillation mode and high wave modes in the surroundings of the slot. Stevenson [2] obtained the expression for the magnetic current in a case of the arbitrary oriented narrow slot situated on the common wall of rectangular waveguides by the iterations method, which King used for thin vibrators [18]. However, in [2] (unlike the formula (31)) the $kL = \pi/2$ assumption was made for the current distribution function and the slot own field function.

2.2. Single Slots in the Common Walls of Rectangular Waveguides

As an example, let us consider the coupling of two identical rectangular waveguides by the $\{a \times b\}$ cross sections through the symmetrical transverse slot in the common broad wall and via the longitudinal slot in the common narrow wall. We also consider the coupling of two mutually perpendicular waveguides in the H-plane through the longitudinal/transverse slot in the common broad wall.

2.2.1. Symmetrical Transverse Slot in a Common Broad Wall of Waveguides

In this case $H_{0s}(s) = H^s_{0s}(s) = H_0 \cos\frac{\pi s}{a}$. Taking into account that for coupling of two waveguides of equal sizes $N^s = 2W^s,\ N^a = 2W^a$, we get:

$$J(s) = -\alpha H_0 \frac{i\omega \left\{\cos ks \cos\left(\frac{\pi L}{a}\right) - \cos kL \cos\left(\frac{\pi s}{a}\right)\right\}}{\gamma^2[\cos kL + \alpha 2W^s_t\,(kd, kL)]}, \qquad (33)$$

where $\gamma^2 = k^2 - (\pi/a)^2$, H_0 is the amplitude of the incident H_{10}-wave, falling from $z = -\infty$ (a region 1).

The $|S_{11}|$ reflection coefficient, the $|S_{12}|$ transmission ones in the first waveguide and the transmission coefficients $|S_{13}|$ and $|S_{14}|$ in the second waveguide are equal, respectively:

$$\begin{aligned} |S_{11}| &= |S_{13}| = |S_{14}| = \left|\frac{4\pi\alpha f\left(kL, \frac{\pi}{a}L\right)}{abk\gamma[\cos kL + \alpha 2W^s_t(kd, kL)]}\right|, \\ |S_{12}| &= \left|1 - \frac{4\pi\alpha f\left(kL, \frac{\pi}{a}L\right)}{iabk\gamma[\cos kL + \alpha 2W^s_t(kd, kL)]}\right|, \end{aligned} \qquad (34)$$

where

$$f\left(kL, \frac{\pi}{a}L\right) = 2\cos\frac{\pi}{a}L\frac{\sin kL\cos\frac{\pi}{a}L - \frac{\pi}{ka}\cos kL\sin\frac{\pi}{a}L}{1-(\pi/ka)^2} - \frac{\cos kL}{(2\pi/ka)}\left(\sin\frac{2\pi L}{a} + \frac{2\pi L}{a}\right).$$

2.2.2. Longitudinal Slot in a Common Narrow Wall of Waveguides

For a longitudinal slot, the field projection of impressed sources on the slot axis equals $H_{0s}(s) = H_0\exp(-i\gamma s)$, and we have

$$J(s) = J^s(s) + J^a(s) = \alpha H_0\frac{i\omega}{(\pi/a)^2} \left\{e^{-i\gamma s} - \frac{\cos ks\cos\gamma L}{\cos kL + \alpha 2W^s_{ln}(kd, kL)} + i\frac{\sin ks\sin\gamma L}{\sin kL + \alpha 2W^a_{ln}(kd, kL)}\right\}. \quad (35)$$

For the reflection, transmission and coupling coefficients we obtain the following expressions:

$$|S_{11}| = |S_{13}| = \left|\frac{4\pi\alpha}{abk\gamma}\left\{\begin{array}{l}\dfrac{f^s(kL,\gamma L)}{\cos kL + \alpha 2W^s_{ln}(kd,kL)} \\ +\dfrac{f^a(kL,\gamma L)}{\sin kL + \alpha 2W^a_{ln}(kd,kL)} - 2kL\dfrac{\sin 2\gamma L}{2\gamma L}\end{array}\right\}\right|,$$

$$|S_{12}| = \left|1 + \frac{i4\pi\alpha}{abk\gamma}\left\{\begin{array}{l}\dfrac{f^s(kL,\gamma L)}{\cos kL + \alpha 2W^s_{ln}(kd,kL)} \\ +\dfrac{f^a(kL,\gamma L)}{\sin kL + \alpha 2W^a_{ln}(kd,kL)} - 2kL\end{array}\right\}\right|,$$

$$|S_{14}| = |S_{12} - 1|, \quad (36)$$

where

$$f^s(kL,\gamma L) = 2\cos\gamma L\frac{\sin kL\cos\gamma L - (\gamma/k)\cos kL\sin\gamma L}{1-(\gamma/k)^2},$$

$$f^a(kL,\gamma L) = 2\sin\gamma L\frac{\cos kL\sin\gamma L - (\gamma/k)\sin kL\cos\gamma L}{1-(\gamma/k)^2}.$$

2.2.3. Longitudinal/Transverse Slot in a Common Broad Wall of Waveguides

In this case, the current distribution depends upon where the waveguide excitation sources are situated. If the H_{10} incident wave is

propagating in the waveguide for which the coupling slot is transverse, then we get:

$$J(s) = -\alpha H_0 \frac{i\omega \left\{\cos ks \cos\left(\frac{\pi L}{a}\right) - \cos kL \cos\left(\frac{\pi s}{a}\right)\right\}}{\gamma^2 \left\{\cos kL + \alpha[W_t^s(kd, kL) + W_{lb}^s(kd, kL)]\right\}}. \quad (37)$$

If the slot for the exciting field is longitudinal, then we have:

$$J(s) = J^s(s) + J^a(s)$$
$$= -\alpha H_0 \frac{i\omega \cos\frac{\pi x_0}{a}}{(\pi/a)^2} \left\{ \begin{array}{c} \dfrac{(\cos ks \cos\gamma L - \cos kL \cos\gamma s)}{\cos kL + \alpha[W_{lb}^s(kd, kL) + W_t^s(kd, kL)]} \\ -i\dfrac{(\sin ks \sin\gamma L - \sin kL \sin\gamma s)}{\sin kL + \alpha[W_{lb}^a(kd, kL) + W_t^a(kd, kL)]} \end{array} \right\}. \quad (38)$$

For the current in (37) the coupling coefficients are defined by the expressions (34), where it is necessary to make the following change $-2W_t^s \to W_t^s + W_{lb}^s$. For the current in (38) they equal, respectively, (the H_{10} incidence wave spreads from the region 3 into the region 4):

$$|S_{33}| = \left| \frac{4\pi\alpha \cos^2\frac{\pi x_0}{a}}{abk\gamma} \left\{ \begin{array}{c} \dfrac{f_1^s(kL, \gamma L)}{\cos kL + \alpha[W_{lb}^s(kd, kL) + W_t^s(kd, kL)]} \\ +\dfrac{f_1^a(kL, \gamma L)}{\sin kL + \alpha[W_{lb}^a(kd, kL) + W_t^a(kd, kL)]} \end{array} \right\} \right|,$$

$$|S_{34}| = \left| 1 - \frac{4\pi\alpha \cos^2\frac{\pi x_0}{a}}{iabk\gamma} \left\{ \begin{array}{c} \dfrac{f_1^s(kL, \gamma L)}{\cos kL + \alpha[W_{lb}^s(kd, kL) + W_t^s(kd, kL)]} \\ -\dfrac{f_1^a(kL, \gamma L)}{\sin kL + \alpha[W_{lb}^a(kd, kL) + W_t^a(kd, kL)]} \end{array} \right\} \right|,$$

$$|S_{31}|^2 = |S_{32}|^2 = \frac{1}{2}(1 - |S_{33}|^2 - |S_{34}|^2), \quad (39)$$

where

$$f_1^s(kL, \gamma L) = f^s(kL, \gamma L) - \frac{\cos kL}{2(\gamma/k)} (\sin 2\gamma L + 2\gamma L),$$
$$f_1^a(kL, \gamma L) = f^a(kL, \gamma L) - \frac{\sin kL}{2(\gamma/k)} (\sin 2\gamma L - 2\gamma L).$$

The expressions for $W_t^s(kd, kL)$, $W_t^a(kd, kL)$, $W_{ln}^s(kd, kL)$, $W_{ln}^a(kd, kL)$, $W_{lb}^s(kd, kL)$, $W_{lb}^a(kd, kL)$ functions are represented in Appendix B.

2.3. Finite Thickness of the Coupling Region Account

The h finite thickness of the wall between coupled volumes can be taken into account due to [22, 23] which introduces the d_e slot effective

width concept. Then at the $(h/\lambda) \ll 1$, precisely up to the terms of the $\{(hd)/\lambda^2\}$ order, we have [22]:

$$\begin{aligned} \frac{h}{d} \ll 1: \qquad & d_e = d\left(1 - \frac{1}{\pi}\frac{h}{d}\ln\frac{d}{h}\right); \\ \frac{h}{d} \gtrsim 1: \qquad & d_e = d\left(\frac{8}{\pi e}e^{-\frac{\pi}{2}\frac{h}{d}}\right). \end{aligned} \tag{40}$$

The expression in [23] is in good approximation for both cases:

$$d_e \cong de^{-\frac{\pi h}{2d}}. \tag{41}$$

The $|S_{13}|$ coefficient calculations, using the approximate ratios of (40) and (41) within the limits of $0 \leq h/2L \leq 0.2$, coincide with the result, obtained in [24] where the account of the rectangular waveguide wall thickness has been made by solving two coupling integral equations with moments method.

2.4. Numerical Results

The plots of the dependences of the $|S_\Sigma|^2 = |S_{13}|^2 + |S_{14}|^2$ coupling coefficient from the length of the symmetrical transverse slot in the common infinitely thin broad wall of two identical rectangular waveguides are in Figure 2. The dependences have been calculated by different methods. It is seen that the calculations made by means of the averaging, variational [4] and moments methods [6] give the values of the slot resonance length (slot "shortening") of $2L \cong 0.47\lambda$. The results obtained by using the quasi-static [3] and equivalent circuits (the "reaction" method [12]) methods lead to the resonance value of $2L = 0.5\lambda$ that does not correspond the reality. We note that Figure 2 gives the results of solving the problem with the help of the moments method as a numerical experiment.

In Figure 3 there are the plots of the amplitude-and-phase distribution $J(s) = |J(s)|e^{i\arg J(s)}$ of the current along the longitudinal/transverse slot in the common infinitely thin broad wall of two mutually perpendicular waveguides. It is seen that if the slot for the H_{10} excitation wave is transverse ($W_t \rightarrow W_{lb}$), then the amplitude distribution of current is purely symmetrical and the current phase is constant along the slot length. For another case of the excitation ($W_{lb} \rightarrow W_t$), the amplitude distribution of the current is sufficiently asymmetrical and the current phase changes along the slot. The current distribution curves are of the same kind in the case of two waveguides coupling through the longitudinal slot in the common broad wall of the finite thickness of the rectangular

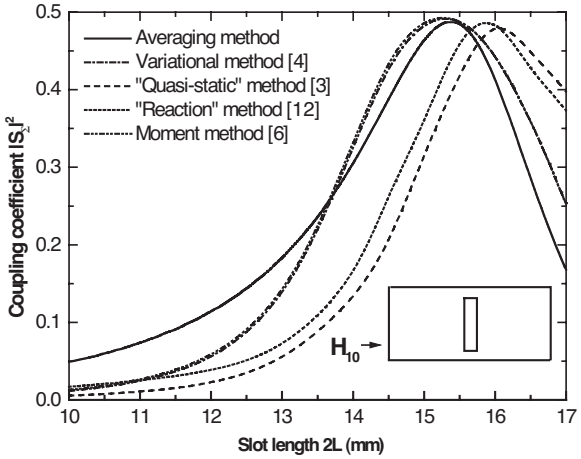

Figure 2. The coupling coefficient dependence from the symmetrical transverse slot length in the common broad wall of two rectangular waveguides at: $a = 22.86\,\text{mm}$, $b = 10.16\,\text{mm}$, $d = 1.5875\,\text{mm}$, $\lambda = 32.0\,\text{mm}$, $h = 0.0\,\text{mm}$.

waveguides in Figure 4. The calculations have been made according to the formula (38) (where there is the $W_t^{s,a} \to W_{lb}^{s,a}$ change) and by the Galerkin's method: $J(s) = \sum\limits_{n=1}^{N} J_n \sin\frac{n\pi(L+s)}{2L}$, taking into account 2, 6 and 12 basis functions. We can see that the change of the external volume sufficiently increases the contribution of the $J^a(s)$ current antisymmetrical component into the general distribution function.

Thus, the obtained asymptotic solution of the integral equation concerning the magnetic current in slot-hole coupling apertures allows us to obtain analytical expressions for the current to the first approximation which is valid for various ratios between the wavelength and a longitudinal size of the slot. The given numerical results demonstrate the efficiency and the effectiveness of such solution. However, there are some quantitative differences between the calculated values of electrodynamic characteristics of the slot coupling apertures, which have been obtained by using the above-mentioned asymptotic formulas and numerical methods. These differences may be removed by using the magnetic current expression obtained from asymptotic solution of the integral equation with the help of the averaging method in combination with other analytical methods, for example, with the induced magnetomotive forces method as it was proposed by the authors in [25–27].

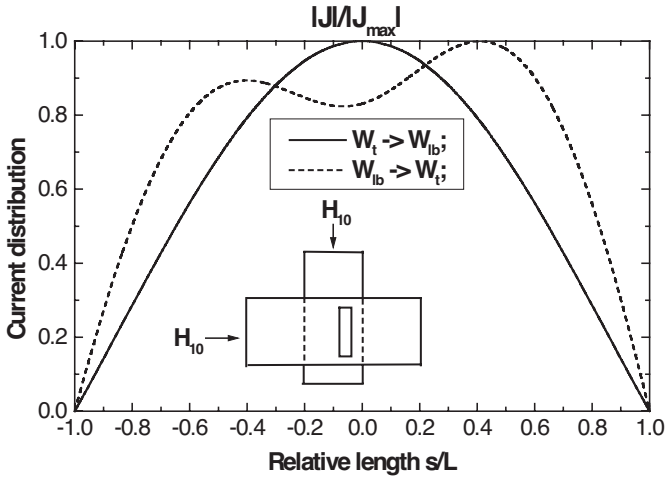

(a)

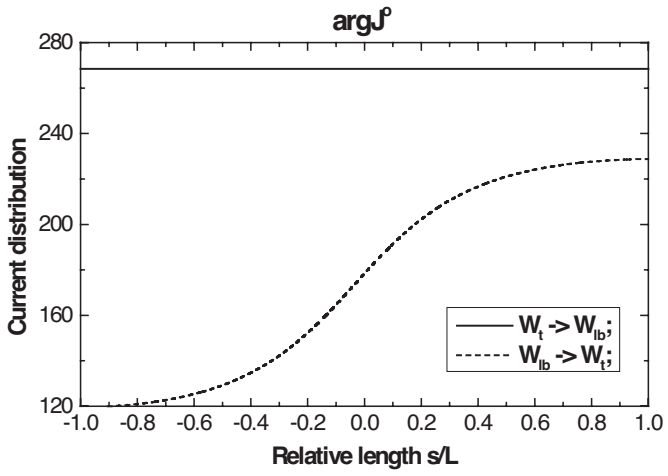

(b)

Figure 3. The current distribution along the longitudinal/transverse (W_{lb} and W_t, respectively) slots in the common broad wall of two mutually perpendicular waveguides at: $a = 22.86\,\text{mm}$, $b = 10.16\,\text{mm}$, $d = 1.5875\,\text{mm}$, $\lambda = 25.8\,\text{mm}$, $2L = 20.0\,\text{mm}$, $x_0 = 1.43\,\text{mm}$ is the slot axis position, $h = 0.0\,\text{mm}$.

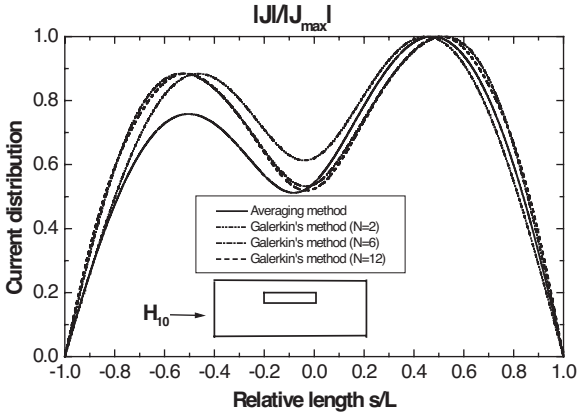

(a)

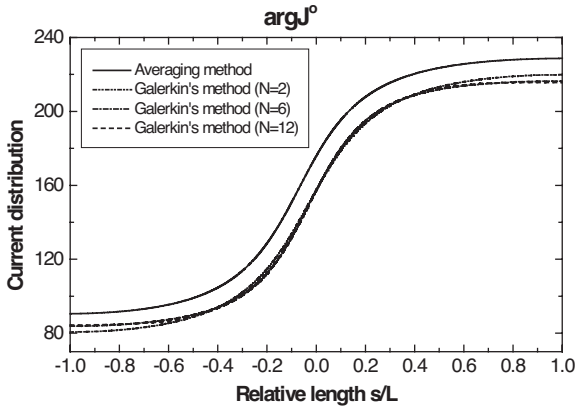

(b)

Figure 4. The current distribution along the longitudinal slot in the common broad wall of two rectangular waveguides at: $a = 22.86\,\text{mm}$, $b = 10.16\,\text{mm}$, $d = 1.5875\,\text{mm}$, $\lambda = 25.8\,\text{mm}$, $2L = 20.0\,\text{mm}$, $x_0 = 1.43\,\text{mm}$ is the slot axis position, $h = 2.0\,\text{mm}$.

3. INDUCED MAGNETOMOTIVE FORCES METHOD FOR ANALYSIS OF COUPLING SLOTS IN WAVEGUIDES

While applying the moments and Galerkin's methods to analyse single and multi-slot elements of the coupling of electrodynamic volumes, different basis and weight functions can be used: the piecewise [6], the piecewise linear and piecewise sinusoidal [28], the trigonometric

[7, 8, 29, 30] and Gegenbauer polynomials [31]. In these cases it is necessary to solve the system of linear algebraic equations (SLAE) of the N-order, where N is a number of linearly independent basis functions. The system matrix elements (N^2 in all) cannot always be obtained analytically, and calculation time increases proportionally to N^3 [32].

For slots system, the order of SLAE increases proportionally to the number of slots. Therefore it is necessary, to our minds, to approximate the distribution of the slot equivalent magnetic current by one or two functions (it depends on an excitation character) as it was done, for example, in [5, 12, 13]. When only one approximating function exists for every slot in a multi-slot system, the Galerkin's method gets the name the "induced magnetomotive forces method" (IMMFM). In this case the solution is more accurate when the approximating functions describing the slot magnetic current distribution are more accurate. In [5, 12, 13] the half-wave and wave sinusoidal functions were used for the slot with the $2L \leq \lambda$ length. For longer slots it is necessary to increase the number of approximating functions.

We suggest better functions of the current distribution for IMMFM that gives sufficiently satisfactory approximation of the current in longer longitudinal slots and in the transverse and longitudinal slots system. These functions have been obtained in Section 2 (formula (33) for transverse slots and formula (38) for longitudinal slots) when we solved the integral equation for the slot magnetic current by the asymptotic averaging method.

3.1. Electrically Long Longitudinal Slot in a Common Broad Wall of Waveguides

Generally, the projection of the $H_{0s}(s)$ impressed field on the slot axis and the $J(s)$ magnetic current in it can be represented with two components — symmetrical and antisymmetrical ones along the slot with the respect to its centre $-H_{0s}(s) = H^s_{0s}(s) + H^a_{0s}(s)$, $J(s) = J^s(s) + J^a(s)$. Owing to this, we can have the following integral-differential equation for the current (5) in a narrow linear slot:

$$\left(\frac{\mathrm{d}^2}{\mathrm{d}s^2} + k^2\right) \int_{-L}^{L} \left[J^s(s') + J^a(s')\right] \left[G^e_s(s, s') + G^i_s(s, s')\right] \mathrm{d}s' = -i\omega \left[H^s_{0s}(s) + H^a_{0s}(s)\right]. \quad (42)$$

Let us represent the current as unknown amplitudes and

distribution functions fixed:

$$J(s) = J_0^s f^s(s) + J_0^a f^a(s), \tag{43}$$

where the $f^s(s)$ and $f^a(s)$ functions must satisfy the following boundary conditions: $f^s(\pm L) = 0, f^a(\pm L) = 0$. From (43) we have only two unknown amplitudes J_0^s and J_0^a. They can be obtained from two independent equations with the respect of J_0^s and J_0^a that we have, using IMMFM:

$$\begin{aligned} J_0^s[Y_s^e(kd, kL) + Y_s^i(kd, kL)] &= -\frac{i\omega}{2k} M_s(kL), \\ J_0^a[Y_a^e(kd, kL) + Y_a^i(kd, kL)] &= -\frac{i\omega}{2k} M_a(kL), \end{aligned} \tag{44}$$

where

$$Y_{s,a}^{e,i}(kd, kL) = \frac{1}{2k} \int\limits_{-L}^{L} f^{s,a}(s) \left[\left(\frac{\mathrm{d}^2}{\mathrm{d}s^2} + k^2 \right) \int\limits_{-L}^{L} f^{s,a}(s') G_{s,a}^{e,i}(s, s') \mathrm{d}s' \right] \mathrm{d}s \tag{45}$$

are the external and inner partial slot admittances and

$$M_{s,a}(kd, kL) = \int\limits_{-L}^{L} f^{s,a}(s) H_{0s}^{s,a}(s) \mathrm{d}s \tag{46}$$

are the partial magnetomotive forces.

For the longitudinal slot in the broad wall of the rectangular waveguide due to (38) the $f^s(s)$ and $f^a(s)$ basis functions have the following forms:

$$\begin{aligned} f^s(s) &= \cos ks \cos \gamma L - \cos kL \cos \gamma s, \\ f^a(s) &= \sin ks \sin \gamma L - \sin kL \sin \gamma s. \end{aligned} \tag{47}$$

Using (47) we can obtain unknown amplitudes J_0^s, J_0^a from (44). It gives us the opportunity to obtain energy characteristics of the coupling slot elements. For the longitudinal slot in the common broad wall of rectangular waveguides, we have:

$$\begin{aligned} |S_{11}| &= |S_{13}| = \left| \frac{2\pi^3 \cos^2 \frac{\pi x_0}{a}}{a^3 b \gamma k^3} \left[\tilde{J}_0^s F^s(kL) + \tilde{J}_0^a F^a(kL) \right] \right|, \\ |S_{12}| &= \left| 1 - \frac{2\pi^3 \cos^2 \frac{\pi x_0}{a}}{i a^3 b \gamma k^3} \left[\tilde{J}_0^s F^s(kL) - \tilde{J}_0^a F^a(kL) \right] \right|, \\ |S_{14}| &= |S_{12} - 1|, \end{aligned} \tag{48}$$

where

$$\tilde{J}_0^s = \frac{F^s(kL)}{Y_s^e(kd,kL)+Y_s^i(kd,kL)},\ \tilde{J}_0^a = -\frac{F^a(kL)}{Y_a^e(kd,kL)+Y_a^i(kd,kL)}, \quad (49)$$

$$\begin{aligned} F^s(kL) &= 2\cos\gamma L\frac{\sin kL\cos\gamma L-(\gamma/k)\cos kL\sin\gamma L}{(\pi/ka)^2} \\ &\quad -\cos kL\frac{\sin 2\gamma L+2\gamma L}{2(\gamma/k)}, \\ F^a(kL) &= 2\sin\gamma L\frac{\cos kL\sin\gamma L-(\gamma/k)\sin kL\cos\gamma L}{(\pi/ka)^2} \\ &\quad -\sin kL\frac{\sin 2\gamma L-2\gamma L}{2(\gamma/k)}. \end{aligned}$$

The expressions for the $Y_s^{i,e}(kd,kL)$, $Y_a^{i,e}(kd,kL)$ admittances are given in Appendix C.

Generally, the slot can be located at the φ angle to the longitudinal waveguide axis. Then according to the general solution of the integral Equation (31) for the current, the basis functions of IMMFM have the forms:

$$\begin{aligned} f^s(s) &= \frac{\cos ks\cos k_2L-\cos kL\cos k_2s}{(\sin\varphi+(k_c/\gamma)\cos\varphi)^2}e^{ik_cx_0} \\ &\quad -\frac{\cos ks\cos k_1L-\cos kL\cos k_1s}{(\sin\varphi-(k_c/\gamma)\cos\varphi)^2}e^{-ik_cx_0}, \\ f^a(s) &= \frac{\sin ks\sin k_2L-\sin kL\sin k_2s}{(\sin\varphi+(k_c/\gamma)\cos\varphi)^2}e^{ik_cx_0} \\ &\quad +\frac{\sin ks\sin k_1L-\sin kL\sin k_1s}{(\sin\varphi-(k_c/\gamma)\cos\varphi)^2}e^{-ik_cx_0}, \end{aligned} \quad (50)$$

where: $k_1 = k_c\sin\varphi+\gamma\cos\varphi, k_2 = k_c\sin\varphi-\gamma\cos\varphi$, x_0 is the distance between the narrow waveguide wall and the slot center. Let us note that at $\varphi = 0$ formulas (70) are transformed into (47).

The current distribution curves in the case of two rectangular waveguides coupled through the longitudinal slot in the common broad wall of the finite thickness are given in Figure 5. The calculations have been made according to the formulas (43), (47) and by the Galerkin's method taking into account 6 basis functions. In the Figure 6, the plots of the $|S_\Sigma|^2 = |S_{13}|^2+|S_{14}|^2$ coupling coefficients dependences of the longitudinal slot in the broad waveguide wall due to its electrical length are represented. The calculations have been made with the

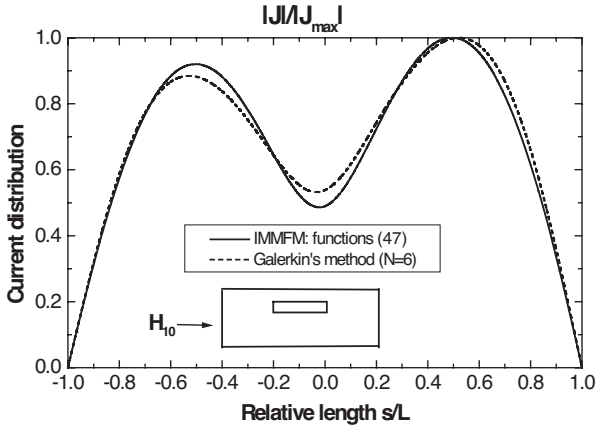

(a)

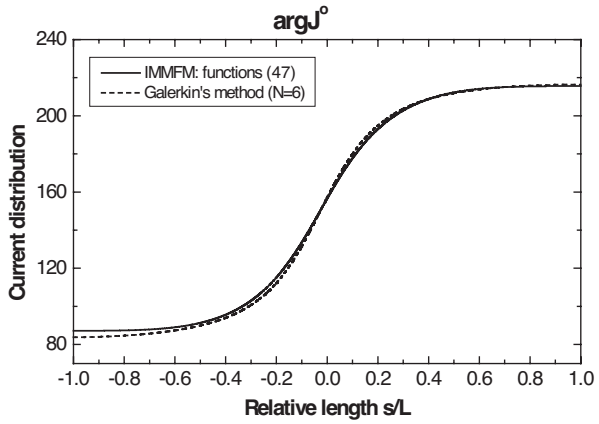

(b)

Figure 5. The current distribution along the longitudinal slot in the common broad wall of two rectangular waveguides at: $a = 22.86\,\text{mm}$, $b = 10.16\,\text{mm}$, $d = 1.5875\,\text{mm}$, $\lambda = 25.8\,\text{mm}$, $2L = 20.0\,\text{mm}$, $x_0 = 1.43\,\text{mm}$ is the slot axis position, $h = 2.0\,\text{mm}$.

following representations of the magnetic current: a) in the form of $J(s) = \sum\limits_{n=1}^{N} J_n \sin\frac{n\pi(L+s)}{2L}$ (the Galerkin's method) b) with the use of the functions (3.6), c) using the following approximation [5]:

$$J(s) = J_0^s \cos\left(\frac{\pi s}{2L}\right) + J_0^a \sin\left(\frac{\pi s}{L}\right). \tag{51}$$

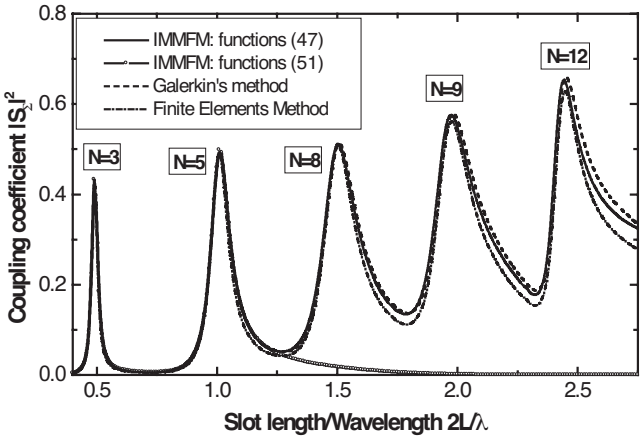

Figure 6. The coupling coefficient dependence from the relative length of the longitudinal slot in the common broad wall of two rectangular waveguides at: $a = 23.0\,\text{mm}$, $b = 10.0\,\text{mm}$, $d = a/15$, $x_0 = a/6$, $\lambda/\lambda_c = 0.625$, $h = 2.0\,\text{mm}$.

The Figure 6 also gives the calculated values obtained by using the finite elements method (FEM) due to the program "CST Microwave Studio".

Hence, the approximation (47), when only two basis functions are used, gives good match with the results obtained by using the Galerkin's and the finite elements methods for the longitudinal slots with the electrical length up to $2L/\lambda \leq 2.75$ (when it is necessary to use 12 basis functions for the Galerkin's method), meanwhile the (51) approximation is satisfactory for only up to $2L/\lambda \leq 1.25$. We think that (51) functions describe the slot current distribution less accurately than the (47) functions because they do not have the λ, λ_c (cut-off H_{10} wavelength) and λ_g (wavelength in the waveguide) values in the distribution, the ratios of which between each other, and slot length supposes the formation of the magnetic current amplitude-phase distribution and energy characteristics of the coupling slot holes.

The latter is proved by the plots given in the Figure 7 where the curves of the coupling coefficient dependences of two identical waveguides through the longitudinal slot in their common broad wall from $2L/\lambda$ are represented at different values of λ/λ_c. It is clear if the λ/λ_c ratio increases, then the Q-factor of the $|S_\Sigma|^2 = f(2L/\lambda)$ resonance curves decreases. At definite ratio between $2L/\lambda$ and λ/λ_c, practically, the full power of the initial wave from one waveguide to the other one can be transmitted.

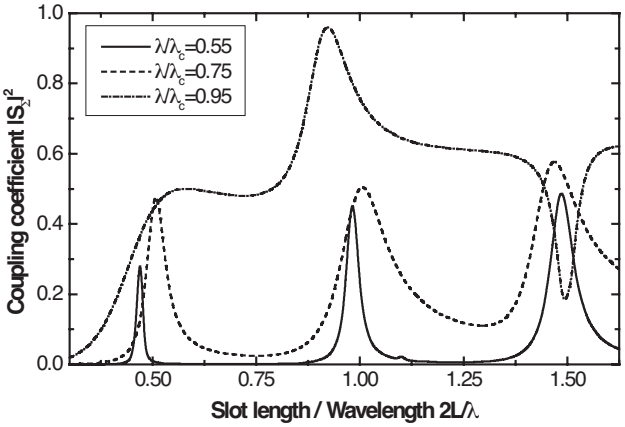

Figure 7. The coupling coefficient dependence from the relative length of the longitudinal slot in the common broad wall of two rectangular waveguides at: $a = 23.0\,\text{mm}$, $b = 10.0\,\text{mm}$, $d = a/15$, $x_0 = a/4$, $h = 2.0\,\text{mm}$.

3.2. Two Symmetrical Transverse Slots in a Common Broad Wall of Waveguides

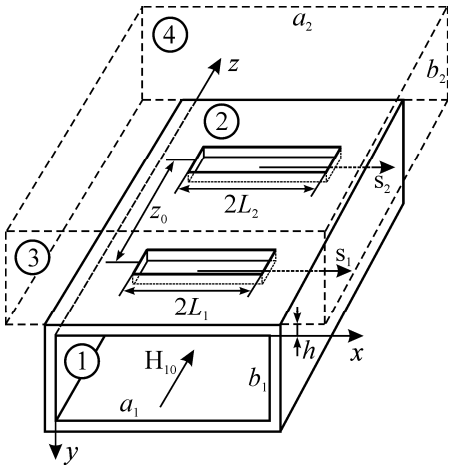

Figure 8. The two symmetrical transverse slots system in the waveguides common wall.

For the two slots in a waveguide wall (Figure 8), one can obtain the system of two coupled integral-differential equations for the $J_1(s_1)$

and $J_2(s_2)$ magnetic currents in the first and the second slots:

$$\begin{cases} \left(\frac{d^2}{ds_1^2}+k^2\right)\left[\int\limits_{-L_1}^{L_1} J_1(s_1')G_{s_1}^{\Sigma}(s_1,s_1')ds_1' + \int\limits_{-L_2}^{L_2} J_2(s_2')G_{s_1}^{\Sigma}(s_1,s_2')ds_2'\right] \\ \quad = -i\omega H_{0s_1}(s_1), \\ \left(\frac{d^2}{ds_2^2}+k^2\right)\left[\int\limits_{-L_2}^{L_2} J_2(s_2')G_{s_2}^{\Sigma}(s_2,s_2')ds_2' + \int\limits_{-L_1}^{L_1} J_1(s_1')G_{s_2}^{\Sigma}(s_2,s_1')ds_1'\right] \\ \quad = -i\omega H_{0s_2}(s_2), \end{cases} \tag{52}$$

where $G_{s_{1,2}}^{\Sigma}(s_{1,2},s_{1,2}') = G_{s_{1,2}}^{e}(s_{1,2},s_{1,2}') + G_{s_{1,2}}^{i}(s_{1,2},s_{1,2}')$, $H_{0s_1}(s_1)$ and $H_{0s_2}(s_2)$ are the projections of the field of the impressed sources to the slot axes.

As in a previous case (in Section 3.1) the currents in every slot can be written in the following way:

$$J_1(s_1) = J_{01}f_1(s_1),\ J_2(s_2) = J_{02}f_2(s_2); \quad f_1(\pm L_1) = 0,\ f_2(\pm L_2) = 0. \tag{53}$$

Due to the induced magnetomotive forces method used for two slots system, we transform (52) into the following algebraic equations system relative to J_{01} and J_{02} unknown amplitudes:

$$\begin{cases} J_{01}Y_{11}^{\Sigma}(kL_1,kL_1) + J_{02}Y_{12}^{\Sigma}(kL_1,kL_2) = -\frac{i\omega}{2k}M_1(kL_1), \\ J_{01}Y_{21}^{\Sigma}(kL_2,kL_1) + J_{02}Y_{22}^{\Sigma}(kL_2,kL_2) = -\frac{i\omega}{2k}M_2(kL_2). \end{cases} \tag{54}$$

Here

$$Y_{mn}^{\Sigma}(kL_m,kL_n) = \frac{1}{2k}\int\limits_{-L_m}^{L_m} f_m(s_m)\left[\left(\frac{\mathrm{d}^2}{\mathrm{d}s_m^2}+k^2\right)\int\limits_{-L_n}^{L_n} f_n(s_n')G_{s_m}^{\Sigma}(s_m,s_n')\mathrm{d}s_n'\right]\mathrm{d}s_m, \quad (m,n=1,2) \tag{55}$$

are the eigen ($m = n$) and mutual ($m \neq n$) slots admittances, respectively;

$$M_m(kL_m) = \int\limits_{-L_m}^{L_m} f_m(s_m)H_{0sm}(s_m)\mathrm{d}s_m, \quad (m=1,2) \tag{56}$$

are the magnetomotive forces.

In the case of two symmetrical transverse slots, the currents in them are also symmetrical. They can be represented as ($k_c = 2\pi/\lambda_c$, λ_c is the cut-off H_{10} wavelength) due to (33):

$$f_m(s_m) = \cos ks_m \cos k_cL_m - \cos kL_m \cos k_cs_m, \quad (m=1,2). \tag{57}$$

Using (57) we can obtain unknown amplitudes J_{01}, J_{02} from (54). It gives us the opportunity to obtain energy characteristics of the coupling slots elements:

$$\begin{aligned} |S_{11}| &= |S_{13}| = \left| \frac{2\pi\gamma}{abk^3} \left[\tilde{J}_1 F(kL_1) + e^{-i\gamma z_0} \tilde{J}_2 F(kL_2) \right] \right|, \\ |S_{12}| &= \left| 1 - \frac{2\pi\gamma}{iabk^3} \left[\tilde{J}_1 F(kL_1) + e^{i\gamma z_0} \tilde{J}_2 F(kL_2) \right] \right|, \\ |S_{14}| &= |S_{12} - 1\|, \end{aligned} \tag{58}$$

where

$$\begin{aligned} \tilde{J}_1 &= \frac{F(kL_1) Y_{22}^{\Sigma}(kd_2, kL_2) - e^{-i\gamma z_0} F(kL_2) Y_{12}^{\Sigma}(kL_1, kL_2)}{Y_{11}^{\Sigma}(kd_1, kL_1) Y_{22}^{\Sigma}(kd_2, kL_2) - [Y_{12}^{\Sigma}(kL_1, kL_2)]^2}, \\ \tilde{J}_2 &= \frac{e^{-i\gamma z_0} F(kL_2) Y_{11}^{\Sigma}(kd_1, kL_1) - F(kL_1) Y_{12}^{\Sigma}(kL_1, kL_2)}{Y_{11}^{\Sigma}(kd_1, kL_1) Y_{22}^{\Sigma}(kd_2, kL_2) - [Y_{12}^{\Sigma}(kL_1, kL_2)]^2}, \end{aligned} \tag{59}$$

$$\begin{aligned} F(kL_m) &= 2\cos k_c L_m \frac{\sin kL_m \cos k_c L_m - (k_c/k) \cos kL_m \sin k_c L_m}{1 - (k_c/k)^2} \\ &\quad - \cos kL_m \frac{\sin 2k_c L_m + 2k_c L_m}{(2k_c/k)}. \end{aligned}$$

The expressions for the $Y_{mm}(kd_m, kL_m)$, $Y_{mn}(kL_m, kL_n)$ admittances are given in Appendix C.

In the Figures 9, 10 the coupling coefficients dependences are given for the system of two identical, rectangular symmetrical transverse slots where the distance between them equals z_0. The calculations have been made with the following representations of the magnetic current: a) in the form of $J_m(s) = \sum\limits_{n=1}^{N} J_{mn} \sin \frac{n\pi(L+s)}{2L}$ (the Galerkin's method); b) with the use of the functions (57); c) using the following approximation:

$$J_m(s) = J_{0m} \cos\left(\frac{\pi s_m}{2L_m}\right), \quad m = 1, 2. \tag{60}$$

It is seen that in the case of two transverse slots, the (57) approximation is good. It gives satisfactory coincidence with the results of the Galerkin's method and the experimental data in different parts of the band of the operating length of the H_{10}-wave, especially at the resonance points. The (60) basis functions change the resonance frequency values.

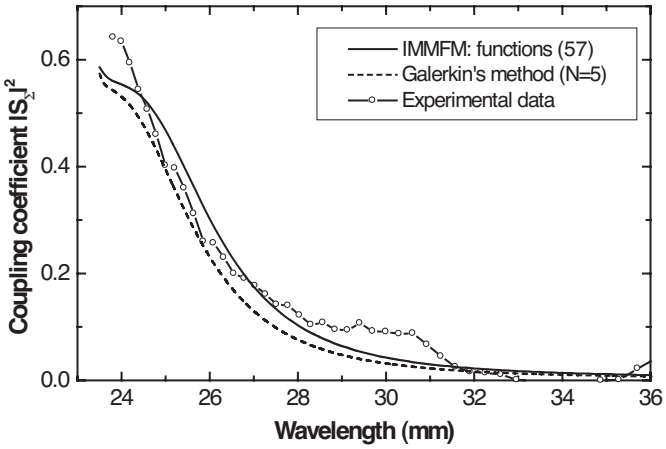

Figure 9. The coupling coefficient dependence from the wavelength for a pair of transverse slots in the common broad wall between a pair of rectangular waveguides at: $a = 23.0\,\text{mm}$, $b = 10.0\,\text{mm}$, $d_1 = d_2 = 2.0\,\text{mm}$, $2L_1 = 2L_2 = 10.6\,\text{mm}$, $z_0 = 10.0\,\text{mm}$, $h = 1.0\,\text{mm}$.

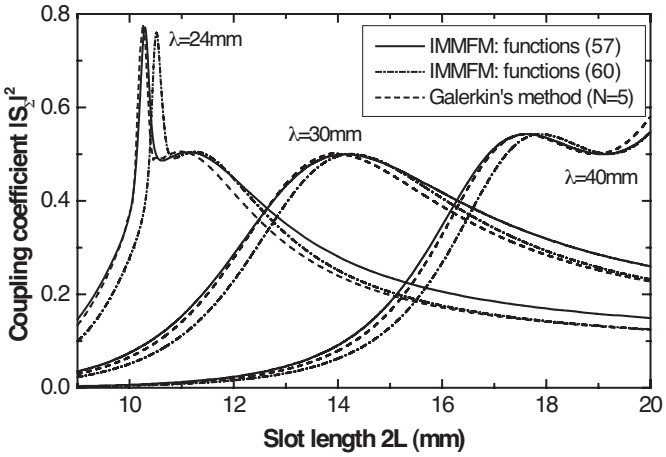

Figure 10. The coupling coefficient dependence from the slot length for a pair of transverse slots in the common broad wall between a pair of rectangular waveguides at: $a = 23.0\,\text{mm}$, $b = 10.0\,\text{mm}$, $d_1 = d_2 = 1.6\,\text{mm}$, $2L_1 = 2L_2 = 2L$, $z_0 = 2\lambda/3$, $h = 0.0\,\text{mm}$.

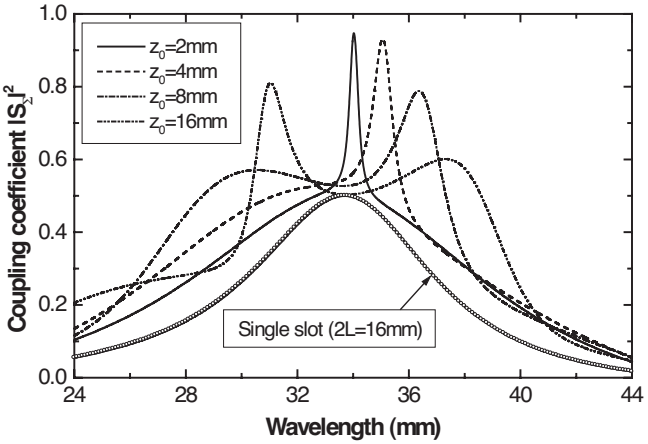

Figure 11. The coupling coefficient dependence from the wavelength for a pair of transverse slots in the common broad wall between a pair of rectangular waveguides at: $a = 23.0\,\text{mm}$, $b = 10.0\,\text{mm}$, $d_1 = d_2 = 1.6\,\text{mm}$, $2L_1 = 2L_2 = 16.0\,\text{mm}$, $h = 0.0\,\text{mm}$.

The energetic characteristics of the slots system are represented in Figures 11–14 in dependence from their mutual locations and the wavelength. To be more certain let us consider that $\lambda_{av} = 32.53\,\text{mm}$ is the average wavelength of a single-mode range of the waveguide at $\lambda_g = \lambda_c$.

The analysis of the plots and expressions (58) and (59) for the currents and energetic characteristics of slots system allows us to make the following conclusions.

- A sufficient increase of the $|S_\Sigma|^2$ coupling coefficient in the narrow range of frequencies (Figure 11) is observed at the distances $z_0 < (\lambda_{av}/2)$ because of strong coupling between the slots along the higher oscillation modes. We note, that if $z_0 \ll (\lambda_{av}/2)$, then $\text{Re}\tilde{J}_1 = -\text{Re}\tilde{J}_2$, $\text{Im}\tilde{J}_1 = \text{Im}\tilde{J}_2$ (more over $\text{Im}\tilde{J} \ll \text{Re}\tilde{J}$) and due to (58) $|S_{11}| = |S_{12}| = |S_{13}| \cong 0, |S_{14}| \cong 1$, that is, practically, the full-power of the incident wave enter to the region 4 ($z_0 = 2\,\text{mm}$ in Figure 11).
- If the distance between the slots $z_0 \geq (\lambda_{av}/2)$ and $2L_1 = 2L_2$, then $|S_\Sigma|^2$ does not depend on z_0 at the resonance wavelength λ_{res} of a single slot (Figure 12, the curve for $\lambda = 33.7\,\text{mm}$).
- At $z_0 = (n\lambda_g^{res}/2)(n = 1, 2, 3 \ldots, \lambda_g^{res}$ is the wavelength in the waveguide, corresponding to the resonance wavelength of a single

slot) it follows from (58) that in the case $2L_1 = 2L_2$ the radiation coefficient $|S_\Sigma|^2$=0.5, and it does not depend on the wavelength in the neighbourhood of the resonance of a single slot (Figure 12).

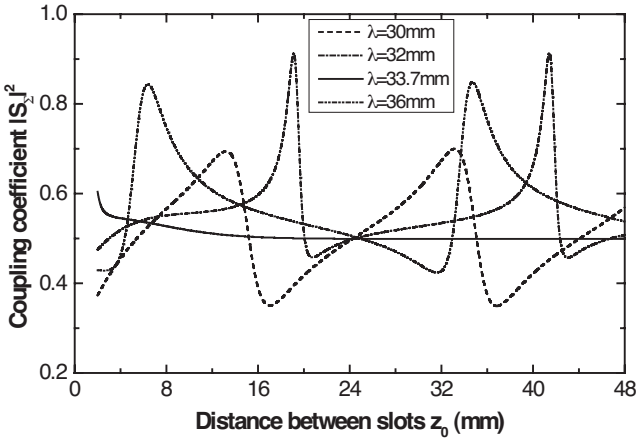

Figure 12. The coupling coefficient dependence from the distance between the slots for a pair of transverse slots in the common broad wall between a pair of rectangular waveguides at: $a = 23.0\,\text{mm}$, $b = 10.0\,\text{mm}$, $d_1 = d_2 = 1.6\,\text{mm}$, $2L_1 = 2L_2 = 16.0\,\text{mm}$, $h = 0.0\,\text{mm}$.

- Because of strong mutual influence of the slots on each other the minimal value of the reflection coefficient $|S_{11}|^2$ is reached at $z_0 = 0.4\lambda_g$ and not for $z_0 = 0.25\lambda_g$, as it was when the interaction was absent (Figure 13). In this case $|S_{12}|^2 = |S_{14}|^2 = 0.5$, that is, full incident power is divided equally between the regions 2 and 4.
- If $z_0 = \lambda_g^{res}/2 = 24.8\,\text{mm}$ ($\lambda_{res} = 33.7\,\text{mm}$ for $2L = 2L_1 = 2L_2 = 16\,\text{mm}$), then power entering the region 1 of the main waveguide, is divided into four equal parts in the wide range of the wavelengths: $|S_{11}|^2 = |S_{12}|^2 = |S_{13}|^2 = |S_{14}|^2 = 0.25$ (Figure 14).

3.3. Two Longitudinal Slots in a Common Broad Wall of Waveguides

For the two longitudinal slots in the broad wall of a waveguide (Figure 15) the system of coupled integral-differential equations has

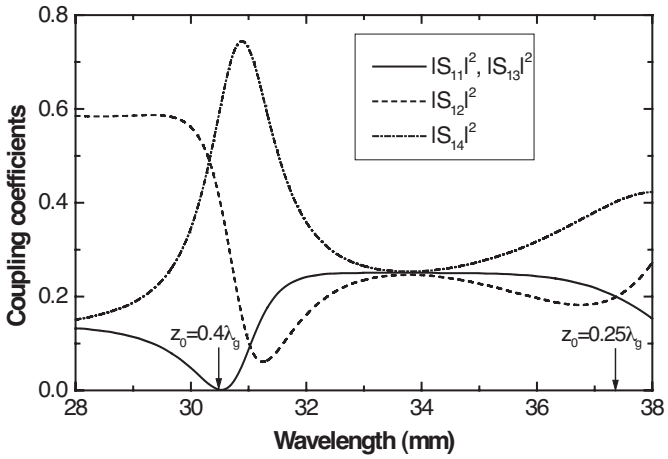

Figure 13. The coupling coefficients dependence from the wavelength for a pair of transverse slots in the common broad wall between a pair of rectangular waveguides at: $a = 23.0\,\text{mm}$, $b = 10.0\,\text{mm}$, $d_1 = d_2 = 1.6\,\text{mm}$, $2L_1 = 2L_2 = 16.0\,\text{mm}$, $z_0 = 16.0\,\text{mm}$, $h = 0.0\,\text{mm}$.

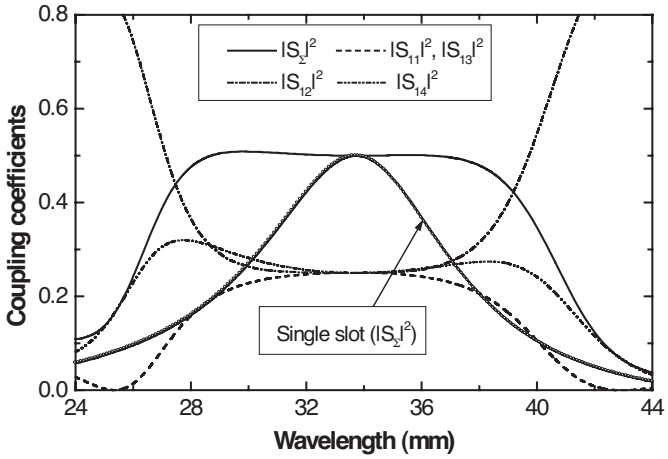

Figure 14. The coupling coefficients dependence from the wavelength for a pair of transverse slots in the common broad wall between a pair of rectangular waveguides at: $a = 23.0\,\text{mm}$, $b = 10.0\,\text{mm}$, $d_1 = d_2 = 1.6\,\text{mm}$, $2L_1 = 2L_2 = 16.0\,\text{mm}$, $z_0 = 24.8\,\text{mm}$, $h = 0.0\,\text{mm}$.

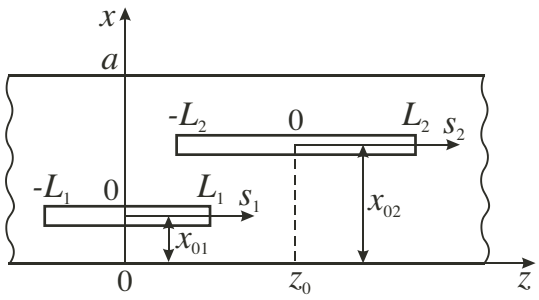

Figure 15. The two longitudinal slots system in the waveguides common wall.

the following form concerning the magnetic currents $J_1(s_1)$ and $J_2(s_2)$:

$$\begin{cases} \left(\frac{\mathrm{d}^2}{\mathrm{d}s_1^2}+k^2\right)\left[\int\limits_{-L_1}^{L_1} J_1(s_1')G_{s_1}^{\Sigma}(s_1,s_1')\mathrm{d}s_1'+\int\limits_{-L_2}^{L_2} J_2(s_2')G_{s_1}^{\Sigma}(s_1,s_2')\mathrm{d}s_2'\right] \\ \qquad\qquad = -i\omega[H_{0s_1}^{s}(s_1)+H_{0s_1}^{a}(s_1)], \\ \left(\frac{\mathrm{d}^2}{\mathrm{d}s_2^2}+k^2\right)\left[\int\limits_{-L_2}^{L_2} J_2(s_2')G_{s_2}^{\Sigma}(s_2,s_2')\mathrm{d}s_2'+\int\limits_{-L_1}^{L_1} J_1(s_1')G_{s_2}^{\Sigma}(s_2,s_1')\mathrm{d}s_1'\right] \\ \qquad\qquad = -i\omega[H_{0s_2}^{s}(s_2)+H_{0s_2}^{a}(s_2)]. \end{cases} \tag{61}$$

Here $G_{s_m}^{\Sigma}(s_m,s_n')=G_{s_m}^{i}(s_m,s_n')+G_{s_m}^{e}(s_m,s_n')(m,n=1,2)$, $H_{0s_m}^{s,a}$ are the projections of symmetrical (index "s") and antisymmetrical (index "a") components of the magnetic field of impressed sources to the slot axes.

As in the case of a single longitudinal slot (Section 3.1) slot currents can be represented in the form of unknown amplitudes and fixed distribution functions:

$$J_1(s_1)=J_{01}^{s}f_1^{s}(s_1)+J_{01}^{a}f_1^{a}(s_1),\ J_2(s_2)=J_{02}^{s}f_2^{s}(s_2)+J_{02}^{a}f_2^{a}(s_2)\,, \tag{62}$$

and the functions $f_m^{s,a}(s_m)$ must also satisfy the edge conditions $f_m^{s,a}(\pm L_m)=0$.

Substituting (62) in the Equations (61) we obtain the system of linear algebraic equations concerning the unknown amplitudes of the

currents $J_{0m}^{s,a}$:

$$\begin{cases} J_{01}^{s}Y_{11}^{\Sigma ss}(kL_1,kL_1)+J_{02}^{s}Y_{12}^{\Sigma ss}(kL_1,kL_2)+J_{02}^{a}Y_{12}^{\Sigma sa}(kL_1,kL_2)=-\frac{i\omega}{2k}M_1^s(kL_1), \\ J_{01}^{a}Y_{11}^{\Sigma aa}(kL_1,kL_1)+J_{02}^{s}Y_{12}^{\Sigma as}(kL_1,kL_2)+J_{02}^{a}Y_{12}^{\Sigma aa}(kL_1,kL_2)=-\frac{i\omega}{2k}M_1^a(kL_1), \\ J_{02}^{s}Y_{22}^{\Sigma ss}(kL_2,kL_2)+J_{01}^{s}Y_{21}^{\Sigma ss}(kL_2,kL_1)+J_{01}^{a}Y_{21}^{\Sigma sa}(kL_2,kL_1)=-\frac{i\omega}{2k}M_2^s(kL_2), \\ J_{02}^{s}Y_{22}^{\Sigma aa}(kL_2,kL_2)+J_{01}^{s}Y_{21}^{\Sigma as}(kL_2,kL_1)+J_{01}^{a}Y_{21}^{\Sigma aa}(kL_2,kL_1)=-\frac{i\omega}{2k}M_2^a(kL_2). \end{cases} \tag{63}$$

Here

$$\begin{aligned} &{}^{\Sigma}\begin{Bmatrix} ss\,sa \\ as\,aa \end{Bmatrix} Y_{mn}(kL_m,kL_n) \\ &= \frac{1}{2k}\int\limits_{-L_m}^{L_m} f_m^{s,a}(s_m)\left[\left(\frac{\mathrm{d}^2}{\mathrm{d}s_m^2}+k^2\right)\int\limits_{-L_n}^{L_n} f_n^{s,a}(s_n')G_{s_n}^{\Sigma}(s_m,s_n')\mathrm{d}s_n'\right]\mathrm{d}s_m \end{aligned} \tag{64}$$

are the eigen ($m=n$) and mutual ($m\neq n$) admittances of the slots;

$$M_m^{s,a}(kL_m)=\int\limits_{-L_m}^{L_m} f_m^{s,a}(s_m)H_{0s_m}^{s,a}(s_m)\mathrm{d}s_m \tag{65}$$

are the partial magnetomotive forces. Due to (38) the functions $f_m^{s,a}(s_m)$ equal to:

$$\begin{aligned} f_m^s(s_m)&=\cos ks_m\cos\gamma L_m-\cos kL_m\cos\gamma s_m, \\ f_m^a(s_m)&=\sin ks_m\sin\gamma L_m-\sin kL_m\sin\gamma s_m. \end{aligned} \tag{66}$$

For two longitudinal slots in the common broad wall of rectangular waveguides the S_{11} reflection and S_{12} transmission coefficients, the S_{13} and S_{14} transfer ones along the field and the $|S_\Sigma|^2$ power transfer coefficient have the form:

$$S_{11}=-\frac{4\pi k_c^2}{\omega ab\gamma H_0}\left\{\begin{array}{l} \cos\frac{\pi x_{01}}{a}\int\limits_{-L_1}^{L_1}J_1(s_1)e^{-i\gamma s_1}\mathrm{d}s_1 \\ +e^{-i\gamma z_0}\cos\frac{\pi x_{02}}{a}\int\limits_{-L_2}^{L_2}J_2(s_2)e^{-i\gamma s_2}\mathrm{d}s_2 \end{array}\right\}e^{2i\gamma z},$$

$$S_{12} = 1 - \frac{4\pi k_c^2}{\omega ab\gamma H_0} \left\{ \begin{array}{l} \cos\frac{\pi x_{01}}{a} \int\limits_{-L_1}^{L_1} J_1(s_1) e^{i\gamma s_1} \mathrm{d}s_1 \\ + e^{i\gamma z_0} \cos\frac{\pi x_{02}}{a} \int\limits_{-L_2}^{L_2} J_2(s_2) e^{i\gamma s_2} \mathrm{d}s_2 \end{array} \right\},$$

$$S_{13} = S_{11},\ S_{14} = S_{12} - 1,\ |S_\Sigma|^2 = |S_{13}|^2 + |S_{14}|^2 = 1 - |S_{11}|^2 - |S_{12}|^2. \quad (67)$$

In the case of electromagnetic coupling of two identical rectangular waveguides via couple of longitudinal slots of the same lengths ($2L_1 = 2L_2 = 2L$) and widths ($d_1 = d_2 = d$), located at $z_0 = 0$, we obtain $Y_{mn}^{\Sigma sa,\Sigma as} = 0$ and solution of the equations system (63) is sufficiently simplified. As a result we have ($Y_{mn}^{\Sigma ss,\Sigma aa} \to Y_{mn}^{\Sigma s,\Sigma a} = 2Y_{mn}^{is,ia}$):

$$\begin{array}{l} J_{0m}^s = -\frac{i\omega}{2k^2} H_0 \tilde{J}_{0m}^s,\ J_{0m}^a = -\frac{i\omega}{2k^2} H_0 i \tilde{J}_{0m}^a, \left\{ \begin{array}{l} m = 1,\ n = 2 \\ m = 2,\ n = 1 \end{array} \right\}, \\ \tilde{J}_{0m}^{s,a} = f^{s,a}(kL) \frac{\cos\frac{\pi x_{0m}}{a} Y_{nn}^{\Sigma s,\Sigma a}(kL) - \cos\frac{\pi x_{0n}}{a} Y_{mn}^{\Sigma s,\Sigma a}(kL)}{Y_{mm}^{\Sigma s,\Sigma a}(kL) Y_{nn}^{\Sigma s,\Sigma a}(kL) - Y_{mn}^{\Sigma s,\Sigma a}(kL) Y_{nm}^{\Sigma s,\Sigma a}(kL)}. \end{array} \quad (68)$$

$$\begin{array}{l} S_{11} = -\frac{2\pi k_c^2}{iab\gamma k^3} \left\{ \begin{array}{l} \cos\frac{\pi x_{01}}{a} [\tilde{J}_{01}^s f^s(kL) + \tilde{J}_{01}^a f^a(kL)] \\ + \cos\frac{\pi x_{02}}{a} [\tilde{J}_{02}^s f^s(kL) + \tilde{J}_{02}^a f^a(kL)] \end{array} \right\} e^{2i\gamma z}, \\ S_{12} = 1 - \frac{2\pi k_c^2}{iab\gamma k^3} \left\{ \begin{array}{l} \cos\frac{\pi x_{01}}{a} [\tilde{J}_{01}^s f^s(kL) - \tilde{J}_{01}^a f^a(kL)] \\ + \cos\frac{\pi x_{02}}{a} [\tilde{J}_{02}^s f^s(kL) - \tilde{J}_{02}^a f^a(kL)] \end{array} \right\}, \end{array} \quad (69)$$

where

$$\begin{aligned} f^s(kL) &= 2\cos\gamma L \frac{\sin kL\cos\gamma L - (\gamma/k)\cos kL\sin\gamma L}{1 - (\gamma/k)^2} \\ &\quad - \cos kL \frac{\sin 2\gamma L + 2\gamma L}{2(\gamma/k)}, \\ f^a(kL) &= 2\sin\gamma L \frac{\cos kL\sin\gamma L - (\gamma/k)\sin kL\cos\gamma L}{1 - (\gamma/k)^2} \\ &\quad - \sin kL \frac{\sin 2\gamma L - 2\gamma L}{2(\gamma/k)}. \end{aligned}$$

The expressions for the $Y_{mn}^{\left\{ \begin{array}{l} ss\,sa \\ as\,aa \end{array} \right\}}(kL_m, kL_n)$, $Y_{mn}^{\{s,\,a\}}(kL)$ admittances are given in Appendix C.

Figures 16, 17 give the plots of the dependencies of the coupling coefficient $|S_\Sigma|^2 = |S_{13}|^2 + |S_{14}|^2$ from a slots electrical length at their

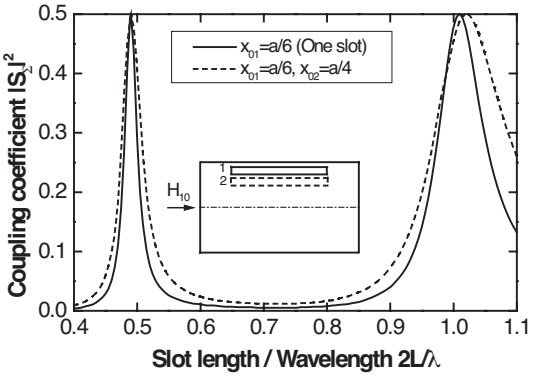

Figure 16. The coupling coefficient dependence from the relative length of the longitudinal slots in the common broad wall of two rectangular waveguides at: $a = 23.0\,\text{mm}$, $b = 10.0\,\text{mm}$, $d = a/15$, $\lambda/\lambda_c = 0.625$, $h = 2.0\,\text{mm}$.

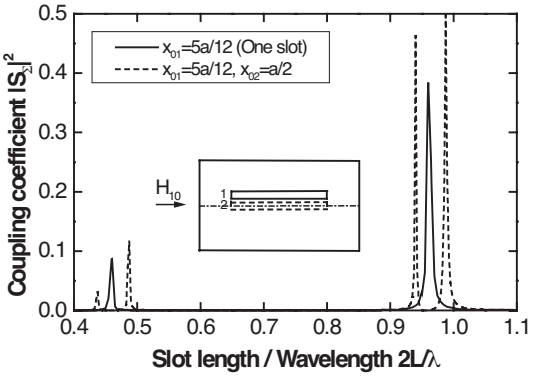

Figure 17. The coupling coefficient dependence from the relative length of the longitudinal slots in the common broad wall of two rectangular waveguides at: $a = 23.0\,\text{mm}$, $b = 10.0\,\text{mm}$, $d = a/15$, $\lambda/\lambda_c = 0.625$, $h = 2.0\,\text{mm}$.

different location relative to each other and wavegude walls. As one can see, two closely located slots have sufficiently differing characteristics $|S_\Sigma|^2 = f(2L/\lambda)$ in dependence from their locations in a waveguide wall, and what's more, if one of the slots is on the axis line of a waveguide, two resonances located on the sides of resonance peaks for a single slot take place (Figure 17). The explanation of this fact can be obtained with the help of the plots in Figure 18, where we give

the curves of change of the normalized values of current amplitudes and slots conductivities in the range of $0.4 \leq 2L/\lambda \leq 0.5$, when main contribution to the currents is made by symmetrical components. At $x_{02} = a/2$ it is resulted from the (69) that energetic characteristics of slots systems will be defined by the current in the first one of them, the amplitude of which equals (index "s" is omitted) due to (68):

$$\begin{aligned} \tilde{J}_{01} &= \frac{\frac{1}{2}\cos\frac{\pi x_{01}}{a} f(kL)}{[\mathrm{Re}Y_{11}^i(kL) - \mathrm{Re}Y_c^i(kL)] + i\mathrm{Im}Y_{11}^i(kL)}, \\ \mathrm{Re}Y_c^i(kL) &= \frac{\mathrm{Re}Y_{12}^i(kL)\mathrm{Re}Y_{21}^i(kL)}{\mathrm{Re}Y_{22}^i(kL)}, \end{aligned} \tag{70}$$

where we take into account that $Y_{mn}^i = \mathrm{Re}Y_{mn}^i + i\mathrm{Im}Y_{mn}^i$ and $\mathrm{Im}Y_{22}^i = \mathrm{Im}Y_{12}^i = \mathrm{Im}Y_{21}^i = 0$.

The analysis of the formula (70) shows that in the case the single slot ($Y_{12}^i = Y_{21}^i = 0$) a current amplitude reaches the maximum value if the $\mathrm{Re}Y_{11}^i(kL) = 0$ conditions are fulfilled, that is, when the reactive energy of all non-spreading modes of oscillations in the slot neighbourhood equals to null (resonance). If we have another slot, located on the waveguide axis line, a $\mathrm{Re}Y_c^i(kL)$ value, proportional to $1/\mathrm{Re}Y_{22}^i(kL)$ is added to the $\mathrm{Re}Y_{11}^i(kL)$ value, what's more, it occurs because of smallness of the $\Delta x = |x_{01} - x_{02}|$ value, as it is seen from the plots $\mathrm{Re}Y_{22}^i(kL) \cong \mathrm{Re}Y_{11}^i(kL)$, and $\mathrm{Re}Y_{12}^i(kL) = \mathrm{Re}Y_{21}^i(kL) \neq 0$. Thus, in this case the current amplitude is in inverse proportion to a function $F(x) = f(x) - \frac{C^2}{f(x)}$, the null equality of which, that is $\mathrm{Re}Y_{11}^i(kL) - \mathrm{Re}Y_c^i(kL) = 0$, is the resonance condition for the very slots couple. From the kind of the $F(x)$ function it follows that the current amplitude is minimal at $\mathrm{Re}Y_{11}^i(kL) = 0$ and it has two maximums at $\mathrm{Re}Y_{11}^i \cong \pm\mathrm{Re}Y_{12}^i$, as it is shown in Figure 18.

Let us note that in the following resonance ($0.9 \leq 2L/\lambda \leq 1.0$) all written above is valid, but the main contribution will be made into the current amplitude by the antisymmetrical component. From the plots in Figure 19 it is seen, that the transmission coefficients into the second wavegude are equal between each other $|S_{13}| = |S_{14}|$ for the slots system in question, that is, such a structure does not have directed qualities at the given slots lengths. Both for a single slot and in the case of two slots phase transition of the reflection coefficient via null ($\arg S_{11} = 0$) is the resonance condition at which the field amplitude, scattered by slots, sharply increases [33].

If a couple of slots is symmetrically located relatively to the waveguide axis line (Figure 20), then the decrease of the Δx distance between them leads to the goodness of resonance peaks (the interaction

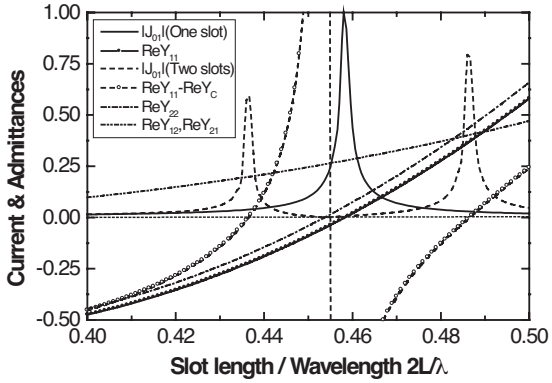

Figure 18. The current and admittances dependences from the relative length of the longitudinal slots in the common broad wall of two rectangular waveguides at: $a = 23.0\,\text{mm}$, $b = 10.0\,\text{mm}$, $d = a/15$, $\lambda/\lambda_c = 0.625$, $h = 2.0\,\text{mm}$.

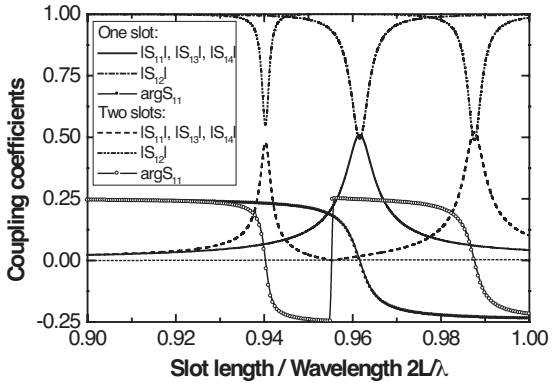

Figure 19. The coupling coefficients dependences from the relative length of the longitudinal slots in the common broad wall of two rectangular waveguides at: $a = 23.0\,\text{mm}$, $b = 10.0\,\text{mm}$, $d = a/15$, $\lambda/\lambda_c = 0.625$, $h = 2.0\,\text{mm}$.

level of the slots with the exciting field decreases) and a significant shift of the slots resonance line into the region of "shortening" (in comparison with the adjusted slot $2L = n\lambda/2$, $n = 1, 2, 3\ldots$), that corresponds to the character of change of the resonance line value of a single longitudinal slot in dependence of its location relatively to the axis line of the broad waveguide wall [33].

The comparison with the Galerkin's method (Figure 20, the curve

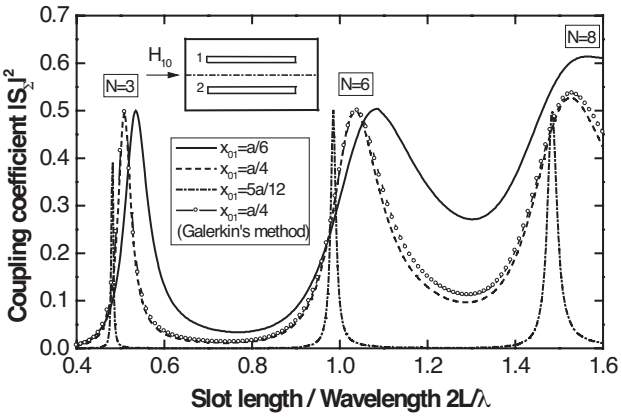

Figure 20. The coupling coefficient dependence from the relative length of the longitudinal slots in the common broad wall of two rectangular waveguides at: $a = 23.0\,\text{mm}$, $b = 10.0\,\text{mm}$, $d = a/15$, $x_{02} = a - x_{01}$, $\lambda/\lambda_c = 0.625$, $h = 2.0\,\text{mm}$.

—o—) proves adequacy of the proposed basic functions to physical process of this very considered waveguide-slotted structure.

3.4. Multi-slot Coupling Through Symmetrical Transverse Slots in a Common Broad Wall of Waveguides

The system, depicted in Figure 21, consists of N narrow ($\{d_n/(2L_n)\} \ll 1$, $\{d_n/\lambda\} \ll 1$, where $2L_n$ d_n are the length and width of the n-th slot) rectangular slots, located in the broad wall of thickness h of a rectangular waveguide with its cross section $\{a_1 \times b_1\}$ symmetrically about its longitudinal axis and radiating into the rectangular waveguide with cross section $\{a_2 \times b_2\}$.

After approximation of the current in the slots as

$$J_n^{i,e}(s_n) = J_{0n}^{i,e} f_n(s_n), \quad f_n(\pm L_n) = 0, \tag{71}$$

where $f_n(s_n)$ are some preset functions, and using the boundary conditions of continuity of tangential components of magnetic fields on both surfaces of each slot, we arrive at a SLAE in terms of unknown current amplitudes $J_{0n}^{i,e}$

$$\sum_{m=1}^{N}\sum_{n=1}^{N}(J_{0n}^{i} + J_{0n}^{e})Y_{mn}^{Wg^i,R,Wg^e}(kL_m, kL_n) = -\frac{i\omega}{2k}M_m^i(kL_m). \tag{72}$$

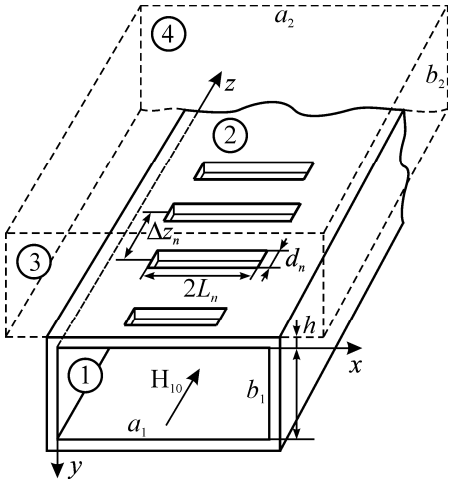

Figure 21. The multi-slot system in the waveguides common wall.

where

$$Y_{mn}^{Wg^i,R,Wg^e}(kL_m, kL_n) = \frac{1}{2k}\int\limits_{-L_m}^{L_m} f_m(s_m)\left[\left(\frac{\mathrm{d}^2}{\mathrm{d}s_m^2}+k^2\right)\int\limits_{-L_n}^{L_n} f_n(s'_n)G_{s_m}^{Wg^i,R,Wg^e}(s_m,s'_n)\mathrm{d}s'_n\right]\mathrm{d}s_m \quad (73)$$

are the eigen ($m = n$) and mutual ($m \neq n$) slots admittances, respectively,

$$M_m^i(kL_m) = \int\limits_{-L_m}^{L_m} f_m(s_m)H_{0s_m}(s_m)\mathrm{d}s_m \quad (74)$$

are the magnetomotive forces, $G_{s_m}^{Wg^i,R,Wg^e}$ are the quasi-onedimensional Green's magnetic functions of the infinite (semi-infinite) rectangular waveguide (Wg), rectangular resonator (R), formed by the slot cavity, respectively, and H_{0s_m} are projections of the magnetic field from impressed sources on the axes of the slots.

The calculations and the comparison with the results, obtained by other methods, showed that the formulas (40) and (41) to define the slot effective width d_e, taking into account the finite thickness of the waveguides walls, become less accurate as the slots number increases ($N > 2$). So, we consider one more electrodynamic volume, which is

a rectangular resonator, formed by the slot cavity. The $J_n^i(s_n)$ and $J_n^e(s_n)$ magnetic currents on the internal (index "i", region 1–2) and external (index "e", region 3–4) surfaces of the slots, correspondingly, will result at the SLAE (72) solution.

Provided that the system is excited by an H_{10}-type wave with amplitude H_0 propagating in the waveguide from the domain $z = -\infty$ let us take for $f_{m,n}(s_{m,n})$ the functions (57)

$$f_{m,n}(s_{m,n}) = \cos ks_{m,n} \cos k_c L_{m,n} - \cos kL_{m,n} \cos k_c s_{m,n}, \qquad (75)$$

Having substituted (75) into (73) and (74), we find all coefficients of SLAE (72). Resolving this system permits to find the energy characteristics of the waveguide-slotted structure under investigation.

The expressions for the S_{11} reflection and S_{12} transmission coefficients, the S_{13} and S_{14} transfer ones along the field and the $|S_\Sigma|^2$ power transfer coefficient of the structure under consideration can be written as

$$\begin{aligned}
S_{11} &= \frac{2\pi i\gamma_1}{a_1 b_1 k^3} \left\{ \sum_{n=1}^{N} J_{0n}^i F(kL_n) e^{-i\gamma_1 z_n} \right\} e^{2i\gamma_1 z}, \\
S_{12} &= 1 + \frac{2\pi i\gamma_1}{a_1 b_1 k^3} \left\{ \sum_{n=1}^{N} J_{0n}^i F(kL_n) e^{i\gamma_1 z_n} \right\}, \qquad (76) \\
S_{13} &= \frac{2\pi i\gamma_2}{a_2 b_2 k^3} \left\{ \sum_{n=1}^{N} J_{0n}^e F(kL_n) e^{-i\gamma_2 z_n} \right\} e^{2i\gamma_2 z}, \\
S_{14} &= \frac{2\pi i\gamma_2}{a_2 b_2 k^3} \left\{ \sum_{n=1}^{N} J_{0n}^e F(kL_n) e^{i\gamma_2 z_n} \right\}, \\
|S_\Sigma|^2 &= |S_{13}|^2 + |S_{14}|,
\end{aligned}$$

where

$$\begin{aligned}
F(kL_n) &= 2\cos k_c L_n \frac{\sin kL_n \cos k_c L_n - (k_c/k)\cos kL_n \sin k_c L_n}{1 - (k_c/k)^2} \\
&\quad - \cos kL_n \frac{\sin 2k_c L_n + 2k_c L_n}{2k_c/k}.
\end{aligned}$$

The expressions for the $Y_{mn}^{Wg}(kL_m, kL_n)$, $Y_{mn}^R(kL_{m,n})$ admittances are given in Appendix C.

The Figure 22 gives the dependences of the $|S_{11}|$, $|S_{12}|$, $|S_{13}|$, $|S_{14}|$ and $|S_\Sigma|^2$ coupling coefficients from the wavelength for the system consisting of 16 slots of equal length, the distance between

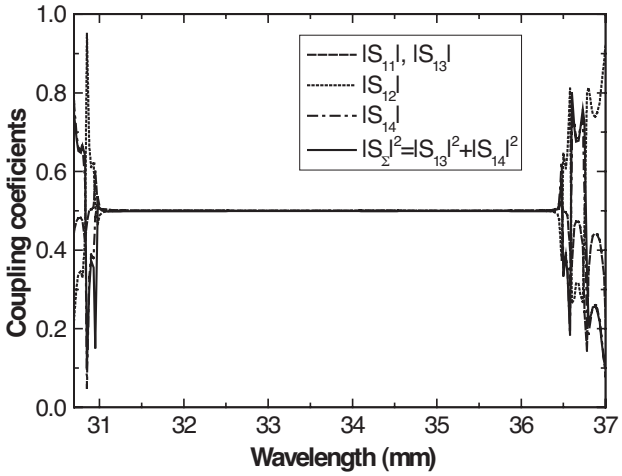

Figure 22. The coupling coefficients dependence from the wavelength for the system of 16 transverse slots in the common broad wall of two identical rectangular waveguides at: $a = 23.0\,\text{mm}$, $b = 10.0\,\text{mm}$, $d_n = 1.6\,\text{mm}$, $2L_n = 16.0\,\text{mm}$, $\Delta z_n = 12.4\,\text{mm}$, $h = 0.2\,\text{mm}$.

which equals $z_{0m} = \lambda_g^{res}/4$, where λ_g^{res} is the waveguide wavelength, which corresponds to the λ_{res} resonance wavelength of the single slot ($\lambda_{res} = 33.7\,\text{mm}$ for $2L = 16\,\text{mm}$). As it is seen from the plots, the power in this case, entering the first shoulder of the main waveguide (a region 1) is divided into 4 equal parts in sufficiently wide range of wavelengths ($\Delta\lambda/\lambda_{res} = 0.15$).

However, the quantitative ratios of the coupling coefficients relative to each other can be distributed differently in other parts of the H_{10}-wave band. Thus, for example, the region, where the whole power of the incident wave propagates along the main waveguide (from the region 1 to the region 2), and does not enter into the second waveguide (Figure 23), exists. On the contrary, the directional coupling takes place in definite parts of the one-mode band: from the region 1 into the region 4 (Figure 24); moreover the $|S_{14}|$ coefficient value can amount to the value 1.0 (Figure 24(b)).

Note, that here we take into account full interaction between all slots for a finite thickness of waveguides walls and the calculation time is far less then when the Galerkin's or the finite elements methods are used.

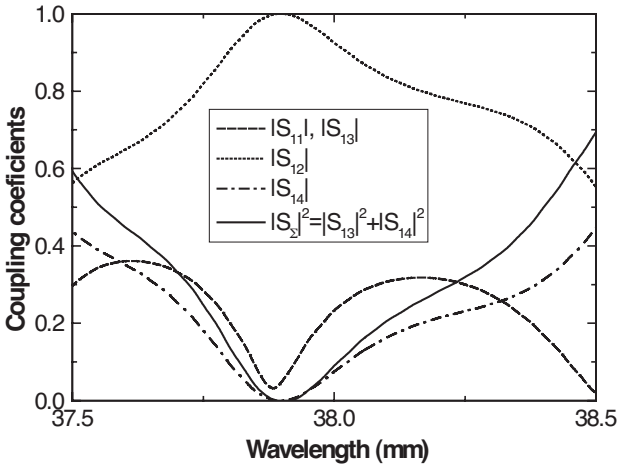

Figure 23. The coupling coefficients dependence from the wavelength for the system of 16 transverse slots in the common broad wall of two identical rectangular waveguides at: $a = 23.0\,\text{mm}$, $b = 10.0\,\text{mm}$, $d_n = 1.6\,\text{mm}$, $2L_n = 16.0\,\text{mm}$, $\Delta z_n = 12.4\,\text{mm}$, $h = 0.2\,\text{mm}$.

4. RESONANT IRIS WITH THE SLOT ARBITRARY ORIENTED IN A RECTANGULAR WAVEGUIDE

With the beginning of development of microwave technology the resonant irises, which have length and width less than the sizes of a waveguide cross section, are the integral part of elementary basis of different devices, for example, band-pass and band-rejection filters [34–36], transformers and diaphragmatic resonant joints of rectangular waveguides [37, 38] and so on. Starting with the classical monograph written by Levin L. [39], a considerable number of publications were devoted to the investigation of electrodynamic characteristics of a resonant iris directly as an elementary cell of complex waveguides units. In these papers the irises of infinite small and finite thicknesses, the slot axes of which are parallel to the broad walls of a rectangular waveguide (coordinate irises) were analyzed by different methods (both analytical and numerical ones). The investigation of the rectangular slot arbitrary located in the plane of a waveguide was evidently made in [40] by the numerical method of moments. However, the calculated and experimental values given in [40] correspond to the non-resonant apertures (the coordinate iris is an exception) and do not answer the question how angular deflection of the slot in the plane of the cross section of a waveguide influences the electrodynamic characteristics

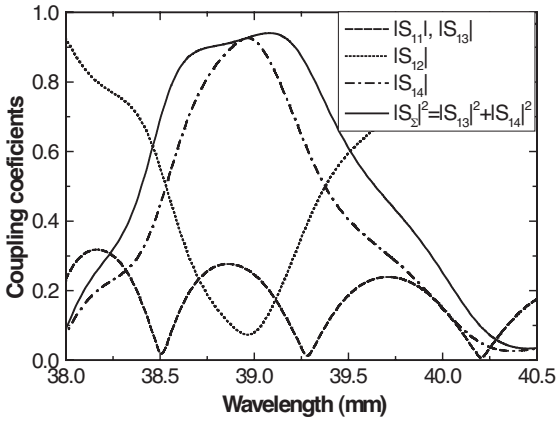

(a)

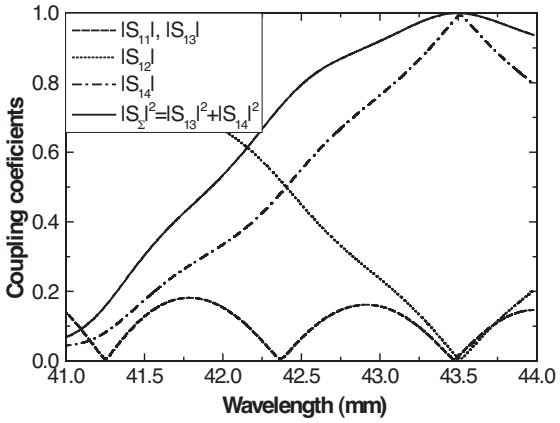

(b)

Figure 24. The coupling coefficients dependence from the wavelength for the system of 16 transverse slots in the common broad wall of two identical rectangular waveguides at: $a = 23.0\,\text{mm}$, $b = 10.0\,\text{mm}$, $d_n = 1.6\,\text{mm}$, $2L_n = 16.0\,\text{mm}$, $\Delta z_n = 12.4\,\text{mm}$, $h = 0.2\,\text{mm}$.

of a resonant iris. These investigations were made in [41], where the task of a oblique iris of the finite thickness in a rectangular waveguide has been solved by means of the rigorous method of the generalized matrices of scattering (matrix operators), and some calculated results are given for the reflection coefficient and goodness of hollow and filled by dielectric irises in a rectangular and square waveguides.

This Section represents the problem solution of electromagnetic waves scattering on the resonant iris of the finite thickness with the

arbitrary oriented slot in the plane of the cross section of a rectangular waveguide. The influence of geometric parameters of such a structure on its electrodynamic characteristics has been analyzed in details on basis of the obtained approximate analytical problem solution.

4.1. Problem Formulation

Let the resonant iris the slot of which is arbitrary oriented in the plane of the cross section of a waveguide (Figure 25) be located in the region $0 \leq z \leq h$ of an infinite rectangular waveguide by the section $\{a \times b\}$. The impressed sources of harmonic electromagnetic fields set by the magnetic intensities $\vec{H}_0^1(\vec{r})$ and $\vec{H}_0^2(\vec{r})$ (where $\vec{r}$ is the radius-vector in Cartesian coordinate system (x, y, z)) are situated in the volumes 1 and 2, representing semi-infinite rectangular waveguides. The volume 3 (a slot cavity) is limited by the surfaces S_1 and S_2 and is free from the impressed sources.

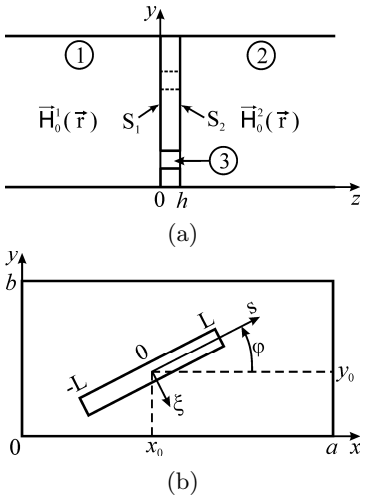

Figure 25. The problem formulation and the symbols used.

Let us formulate the boundary conditions of continuity of tangential components of full magnetic fields on the apertures S_1 and S_2 in order to solve the problem of electromagnetic waves scattering on the iris in question:

$$\begin{cases} \vec{H}_{0\tau}^1(\vec{r}) + \vec{H}_\tau^1[\vec{r}, \vec{J}_1(\vec{r})] = \vec{H}_\tau^3[\vec{r}, \vec{J}_1(\vec{r})] + \vec{H}_\tau^3[\vec{r}, \vec{J}_2(\vec{r})]\Big|_{\text{on } S_1}, \\ \vec{H}_\tau^3[\vec{r}, \vec{J}_1(\vec{r})] + \vec{H}_\tau^3[\vec{r}, \vec{J}_2(\vec{r})] = \vec{H}_{0\tau}^2(\vec{r}) + \vec{H}_\tau^2[\vec{r}, \vec{J}_2(\vec{r})]\Big|_{\text{on } S_2}, \end{cases} \tag{77}$$

where $\vec{J}_1(\vec{r})$ and $\vec{J}_2(\vec{r})$ — the unknown equivalent surface magnetic currents on the holes S_1 and S_2 at their conditional metallization; $\vec{H}^1_\tau$, $\vec{H}^2_\tau$, $\vec{H}^3_\tau$ — the tangential (respectively to the iris plane) components of the scattering magnetic fields in the volumes 1, 2 and 3, correspondingly.

Further we suppose that the slot of the iris is narrow, that is, its length $2L$ and its width d satisfy the inequathions

$$\frac{d}{2L} \ll 1, \quad \frac{d}{\lambda} \ll 1. \tag{78}$$

Then the surface magnetic fields on S_1 and S_2 can be represented in the following form:

$$\vec{J}_1(s_1,\xi_1) = \vec{e}_{s_1} J_1(s_1)\chi(\xi_1), \quad \vec{J}_2(s_2,\xi_2) = \vec{e}_{s_2} J_2(s_2)\chi(\xi_2), \tag{79a}$$

$$J_1(\pm L) = 0, \qquad J_2(\pm L) = 0. \tag{79b}$$

Here $\vec{e}_{s_1}$ and $\vec{e}_{s_2}$ are the single orts of the local coordinates (s,ξ) coupled with the slot (Figure 25(b)), and $\chi(\xi)$ is the function, taking account the electric field behaviour on the edges of the slot cavity [42].

Function $\chi(\xi)$, satisfying the normalization condition:

$$\int\limits_{-d/2}^{d/2} \chi(\xi)d\xi = 1. \tag{80}$$

Particularly, at $h = 0$ (the infinite thin iris) $\chi(\xi)$ has the form:

$$\chi(\xi) = \frac{1/\pi}{\sqrt{(d/2)^2 - \xi^2}}. \tag{81}$$

In the case when $h \neq 0$ (the iris of the finite thickness iris each of the edges of slot cavity represented an perfectly conductive rectangular wedge) $\chi(\xi)$ has the form:

$$\chi(\xi) = \frac{\Gamma(7/6)/\Gamma(2/3)}{\sqrt{\pi}(d/2)\sqrt[3]{1-(2\xi/d)^2}}, \tag{82}$$

where $\Gamma(x)$ is the Gamma-function.

It is shown in [22] that if $H^1_{0s_1}(s_1) + H^2_{0s_2}(s_2) \neq 0$ (where $H^1_{0s_1}(s_1)$ and $H^2_{0s_2}(s_2)$ are the projections of the magnetic fields of the impressed sources to the longitudinal slot axes) and $(h/\lambda) \ll 1$, one can suggest that $J_1(s_1) \approx J_2(s_2) = J(s)$ with the accuracy to the values of the

$\{(hd)/\lambda^2\}$ order under the condition, that the volume 3 is a rectangular resonator (the volumes 1 and 2 are arbitrary). Then the problem of the d slot width in the wall of the h finite thickness is reduced to the problem of the slot with "the equivalent" width d_e in the infinite thin wall after substitution (79a) into the equations system (77), taking into account (80)–(82):

$$H^1_{0s}(s) + H^1_s[s, J(s)] = H^2_{0s}(s) + H^2_s[s, J(s)]\big|_{z=0}. \tag{83}$$

For all that, d_e is coupled with d in the following way [22, 23]:

$$d_e = d\frac{\mathrm{K}}{\mathrm{E(K)}}, \tag{84}$$

where E(K) is the complete elliptic integral of the second kind, K is the integral modulus. We obtain suitable calculated ratios from (84) in the extreme cases as it is shown in Section 2.3 (formulas (40) and (41)).

Taking into account all, mentioned above, and supposing that the impressed field in the second volume equals null (index "1" is omitted), we get the integral-differential equation concerning the $J(s)$ magnetic current in the slot from (83):

$$\left(\frac{\mathrm{d}^2}{\mathrm{d}s^2} + k^2\right)\int_{-L}^{L} J(s')[G^1_s(d_e; s, s') + G^2_s(d_e; s, s')]\mathrm{d}s' = -i\omega H_{0s}(s). \tag{85}$$

Here functions $G^{1,2}_s(d_e; s, s')$ are the s-components of the quasi-onedimensional $|\xi - \xi'| \approx d_e/4$ magnetic dyadic Green's function $\hat{G}^m(\vec{r}, \vec{r}\,')$ for the Hertz's vector potentials of the first and second volumes, correspondingly (see Appendix A).

4.2. Solution of the Equation for a Magnetic Current

In Section 2 we have obtained the asymptotic solution of the integral-differential Equation (85) for the magnetic current in the narrow slot, coupling two arbitrary electrodynamic volumes with the help of the averaging method:

$$\begin{aligned} J^{s,a}(s) \;=\; & \overline{A}(-L)\cos ks + \overline{B}(-L)\sin ks \\ & + \alpha\int_{-L}^{s}\left\{\frac{i\omega}{k}H^{s,a}_{0s}(s') + \overline{F}^{s,a}_N[s', \overline{A}, \overline{B}]\right\}\sin k(s - s')\mathrm{d}s'. \end{aligned} \tag{86}$$

Here $\alpha = \frac{1}{8\ln(d_e/(8L))}$ is the natural small parameter of the problem.

Supposing that the wave of the main mode H_{10} with the H_0 amplitude propagates from region $z = -\infty$ in the first waveguide, we have:

$$H_{0s}(s) = 2H_0\cos\varphi\left[\sin\frac{\pi x_0}{a}\cos\frac{\pi(s\cos\varphi)}{a} + \cos\frac{\pi x_0}{a}\sin\frac{\pi(s\cos\varphi)}{a}\right]. \tag{87}$$

Then the current in the slot has the following form, taking into account its symmetrical and antisymmetrical components (relatively to the slot centre $s = 0$):

$$J(s) = J_0 f(s) = -\alpha 2H_0\cos\varphi\frac{2i\omega/k^2}{[1-(\tilde{k}/k)^2][\sin 2kL + \alpha 2W_0(kd_e, 2kL)]} \times \left\{ \begin{array}{l} \sin\frac{\pi x_0}{a}\sin kL(\cos ks\cos\tilde{k}L - \cos kL\cos\tilde{k}s) \\ +\cos\frac{\pi x_0}{a}\cos kL(\sin ks\sin\tilde{k}L - \sin kL\sin\tilde{k}s) \end{array} \right\}, \tag{88}$$

where J_0 is the amplitude, $f(s)$ is the current distribution function, $\tilde{k} = \frac{\pi}{a}\cos\varphi$, $W_0(kd_e, 2kL)$ is the slot own field function, defined by the corresponding components of the magnetic dyadic Green's function of a half-infinite rectangular waveguide.

It follows from the analysis of the current expression (88) that in the case of a resonance slot ($kL \approx \pi/2$) its antisymmetrical component is always small in comparison with a symmetrical one because $|\cos\frac{\pi x_0}{a}\cos kL| \ll |\sin\frac{\pi x_0}{a}\sin kL|$ in the frequencies range of the H_{10} wave mode of a standard rectangular waveguide. So, to investigate influence of the angle of rotation φ on the iris characteristics we assume in the formula (88) $x_0 = a/2$, $y_0 = b/2$. Then, taking into account that the ratio is performed,

$$W_0(kd_e, 2kL) = 2\sin kL W_\varphi(kd_e, kL), \tag{89}$$

the expressions for the current and the own field functions of the slot are considerably simplified:

$$J(s) = -\alpha H_0\cos\varphi\left(\frac{2i\omega}{k^2}\right) \frac{\left\{\cos ks\cos\frac{\pi}{a}(L\cos\varphi) - \cos kL\cos\frac{\pi}{a}(s\cos\varphi)\right\}}{\left[1-\left(\frac{\pi}{ka}\cos\varphi\right)^2\right][\cos kL + \alpha 2W_\varphi(kd_e, kL)]}. \tag{90}$$

We note, that if $x_0 = a/2$ and $y_0 \neq b/2$, and $\varphi \neq 0$, then the addendums, proportional to $\cos kL$, will be present in the

own field function of the slot $W_0(kd_e, 2kL)$; that is, the ratio (89) not will be performed. And for all that, both "symmetrical" and "antisymmetrical" components, are not defined by the slot excitation (in $H_{0s}(s)$ only a symmetrical component is present), but its location relatively to the waveguide walls, and they influence the near field of the iris.

The formula for the current (90) fully defines the S_{11} reflection coefficient and S_{12} transmission coefficient of the fundamental wave in the considered slot iris:

$$\begin{aligned} S_{11} &= (1 + S_{12})\, e^{2i\gamma z}, \\ S_{12} &= -\alpha \frac{16\pi\gamma \cos^2 \varphi f_\varphi(\tilde{k}L)}{iabk^3[1 - (\tilde{k}/k)^2][\cos kL + \alpha 2W_\varphi(kd_e, kL)]}. \end{aligned} \tag{91}$$

Here

$$\begin{aligned} f_\varphi(\tilde{k}L) \;=\; & 2\cos\tilde{k}L \frac{\sin kL \cos\tilde{k}L - (\tilde{k}/k)\cos kL \sin\tilde{k}L}{1 - (\tilde{k}/k)^2} \\ & - \cos kL \frac{\sin 2\tilde{k}L + 2\tilde{k}L}{2(\tilde{k}/k)}. \end{aligned}$$

The dispersive equation, defining its resonance frequencies, on which the equality of period average values of electrical and magnetic energies of the near fields takes place, follows from the null equality condition of the imaginary part of the reflection coefficient from the iris $\mathrm{Im}S_{11} = 0$:

$$\cos(kL)_{res} + \alpha 2ReW_\varphi\,(kd_e, (kL)_{res}) = 0, \tag{92}$$

at the same time the current distribution (90) has the maximum amplitude and null phase.

Let us define the approximate solution of the Equation (92), expanding the unknown value $(kL)_{res}$ into the series due to the small α parameter degrees:

$$(kL)_{res} = (kL)_0 + \alpha(kL)_1 + \alpha^2(kL)_2 + \ldots \tag{93}$$

If we substitute (93) into (92) and make equal the addendums at the same α degrees with the accuracy to the α^2 order terms, we get:

$$(kL)_{res} \approx \frac{\pi}{2} + \alpha 2\mathrm{Re}W_\varphi \left(\frac{\pi d_e}{2L}, \frac{\pi}{2}\right), \tag{94}$$

where $\mathrm{Re}W_\varphi$ is the real part of the W_φ.

If $x_0 = a/2$, $\varphi = 0$, and y_0 is arbitrary (the coordinate symmetrical iris), then the expressions for the current and reflection coefficient have the form:

$$J(s) = -\alpha H_0 \left(\frac{2i\omega}{\gamma^2}\right) \frac{\left(\cos ks \cos \frac{\pi}{a} L - \cos kL \cos \frac{\pi}{a} s\right)}{\cos kL + \alpha 2W(kd_e, kL)}, \qquad (95)$$

$$S_{11} = \left\{1 - \alpha \frac{16\pi\, f\left(kL, \frac{\pi L}{a}\right)}{iabk\gamma[\cos kL + \alpha 2W(kd_e, kL)]}\right\} e^{2i\gamma z}, \qquad (96)$$

$$f(kL, \frac{\pi L}{a}) = 2\cos\frac{\pi L}{a} \frac{\sin kL \cos \frac{\pi L}{a} - \left(\frac{\pi}{ka}\right) \cos kL \sin \frac{\pi L}{a}}{1 - (\pi/ka)^2} - \cos kL \frac{\sin \frac{2\pi L}{a} + \frac{2\pi L}{a}}{(2\pi/ka)}.$$

The own field function of the slot $W(kd_e, kL)$ equals at $kL = \pi/2$:

$$W\left(\frac{\pi d_e}{2L}, \frac{\pi}{2}\right) = \frac{\pi^2}{abL} \times \sum_{m=1,3\ldots}^{\infty} \sum_{n=0}^{\infty} \frac{\varepsilon_n \cos^2 k_x L}{k_z[(\pi/(2L))^2 - k_x^2]} \cos k_y y_0 \cos k_y \left(y_0 + \frac{d_e}{4}\right). \qquad (97)$$

Here $\varepsilon_n = 1$ at $n = 0$; $\varepsilon_n = 2$ at $n \neq 0$; $k_x = m\pi/a$, $k_y = n\pi/b$, $k_z = \sqrt{k_x^2 + k_y^2 - (\pi/(2L))^2}$ (m, n are integers).

The formula (97) can be resulted in expressions not containing double series (see Appendix D). Then we get the formula for the resonance wavelength λ_{res} of the symmetrical ($x_0 = a/2$) iris with the slot length $2L$, the width d and the thickness h at its arbitrary location relatively to the $y_0 = b/2$ line in the waveguide of the $\{a \times b\}$ crosssection from:

$$\frac{\lambda_{res}}{\lambda_c} = \frac{2L/a}{1 + \alpha\left(\frac{2}{\pi}\right) ReW\left(\frac{\pi d_e}{2L}, \frac{\pi}{2}\right)}, \qquad (98)$$

where λ_c is the cut-off H_{10} wavelength,

$$\mathrm{Re}W\left(\frac{\pi d_e}{2L}, \frac{\pi}{2}\right) \cong 2\pi \left\{\frac{4\cos^2 \frac{\pi L}{a}}{\gamma_{10}^2 aL} \left[\frac{2\pi \cos^2 \frac{\pi y_0}{b}}{k_{11} b} - 2\cos^2 \frac{\pi y_0}{b} + \left(\frac{\gamma_{10} b}{9}\right)^2 \cos^2 \frac{2\pi y_0}{b} - \ln\left(\frac{\pi d_e}{2b} \sin \frac{\pi y_0}{b}\right)\right]\right.$$

$$-\frac{4\cos^2\frac{3\pi L}{a}}{k_{30}^2 aL}\left[K_0\left(k_{30}\frac{d_e}{4}\right)+K_0(2k_{30}y_0)\right]+\left(\ln\frac{16L}{d_e}-1\right)$$
$$-\ln\frac{1-L/a}{1+L/a}+\ln\frac{1-2L/a}{1+2L/a}+\ln\frac{1-2L/(3a)}{1+2L/(3a)}$$
$$-\frac{a}{2L}\left[\ln\left(1-\left(\frac{2L}{a}\right)^2\right)-2\ln\left(1-\left(\frac{L}{a}\right)^2\right)+3\ln\left(1-\left(\frac{2L}{3a}\right)^2\right)-\left(\frac{L}{a}\right)^2\right]$$
$$-\frac{4a}{\pi^2 L}\left\{\begin{array}{l} K_0\left(\frac{\pi d_e}{4a}\right)\sin^2\frac{\pi L}{a}+\frac{1}{9}K_0\left(\frac{3\pi d_e}{4a}\right)\sin^2\frac{3\pi L}{a} \\ +\sum\limits_{m=5,7\ldots}^{\infty}K_0\left(\frac{m\pi d_e}{4a}\right)/m^2 \end{array}\right\}. \quad (99)$$

In (99) we have the symbols: $\gamma_{10}=\sqrt{(\pi/(2L))^2-(\pi/a)^2}$, $k_{11}=\sqrt{(\pi/a)^2+(\pi/b)^2-(\pi/(2L))^2}$, $k_{30}=\sqrt{(3\pi/a)^2-(\pi/(2L))^2}$, $d_e=d\exp(-\pi h/(2d))$, $K_0(x)$ is the McDonald's function. As $K_0(x)$ decreases rapidly at the x increase, then it is sufficient to take some first terms when summing up the rest series in (99).

We note, that in the case, when $\{d_e/(2L)\}\to 0$, the expression (98) transits into the classical Slatter's formula for the symmetrical resonant "window" in a rectangular waveguide, given, for example, in [32]. There we have obtained more accurate expression for the λ_{res} slot iris, however, it is just only when the conditions $y_0=b/2$ and $h=0$ are fulfilled.

The expressions for $W_0(kd_e,2kL)$, $W_\varphi(kd_e,kL)$, $W(kd_e,kL)$, functions are represented in Appendix B.

4.3. Numerical Results

Figure 26 represents the dependencies of the reflection coefficient $|S_{11}|^2$ from the wavelength λ of the H_{10}-wave mode, calculated due to the formula (91) (solid curves), for the iris which has the angle of 30° (Figure 26(a)) between the s slot axis and the $\{0x\}$ waveguide axis, and for the coordinate iris (Figure 26(b), $\varphi=0^o$). Here we also marked the experimental value (the circles) and the numerical results (the dotted curves) obtained with the use of the "CST Microwave Studio" programme. The comparison of the curves shows, that the calculations, made due to the approximate formula (91), give satisfactory results near the resonance λ_{res} wavelength of the iris (the $|S_{11}|^2$ minimal values region), and they qualitatively describe the characteristics change (the structure Q-factor increases at the slot turn) in other parts of the range. It is explained that the asymptotic solution (86) of the integral-differential Equation (85) was obtained in Section 2 by means of

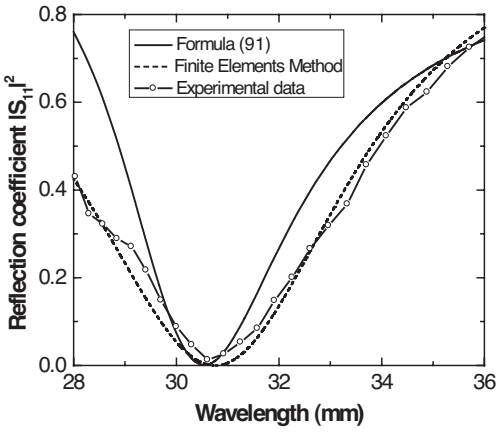

(a)

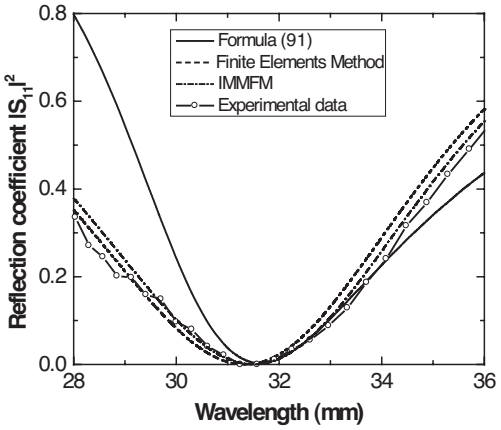

(b)

Figure 26. The reflection coefficient dependence from the wavelength for an iris in rectangular waveguide at: $a = 23.0\,\text{mm}$, $b = 10.0\,\text{mm}$, $d = 1.5\,\text{mm}$, $2L = 16.0\,\text{mm}$, $x_0 = a/2$, $y_0 = b/2$, $h = 2.0\,\text{mm}$, (a) $\varphi = 30°$, (b) $\varphi = 0°$.

the averaging method in the first approximation along the α small parameter; that is with the accuracy up to the terms of the α^2 order. To our minds, it is not worth while to define further approximations for the current by this method because of the inconvenience of the obtained expressions in the case of non-coordinate irises or some slots system. However, the obtained expressions for the $f(s)$ distribution functions of the magnetic current in the formulas (88), (90) and (95)

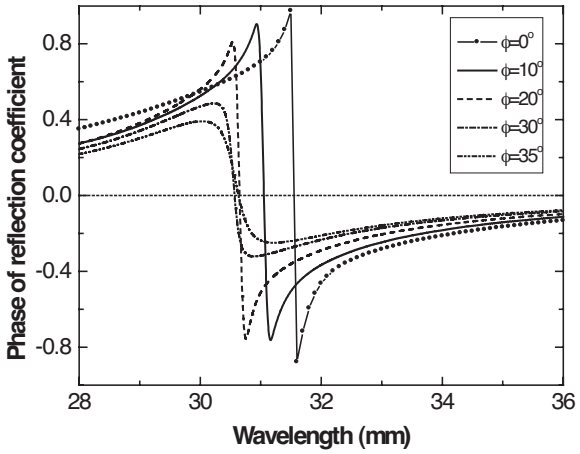

Figure 27. The phase of reflection coefficient (normalized on π) dependence from the wavelength for an iris in rectangular waveguide at: $a = 23.0\,\text{mm}$, $b = 10.0\,\text{mm}$, $d = 1.5\,\text{mm}$, $2L = 16.0\,\text{mm}$, $x_0 = a/2$, $y_0 = b/2$, $h = 2.0\,\text{mm}$.

can be used as basic ones to solve the Equation (85) by means of the induced magnetomotive forces method (IMMFM) (Section 3).

As example Figure 26(b) gives the $|S_{11}|^2$ calculated values, obtained by the IMMFM with the use of the approximating functions for the current in the coordinate slot of the type (95) (stroke-dotted curve).

Let us analyse influence of the angle of turn and the slot shift in the plane of the waveguide cross-section on a wave resonance length (frequency) of the considered iris. Figure 27 represents the dependencies of the $\arg S_{11}$ reflection coefficient phase (normalized on π) from the wavelength for different angles of inclination φ of the slot. As it is seen λ_{res} (the resonance is defined by the equality $\arg S_{11} = 0$) shifts firstly to the short-wave part of the H_{10} range of the wave (slot "lengthening" in comparison with "adjusted" one, when $2L = \lambda_{res}/2$, where $\lambda_{res} = 32\,\text{mm}$) at the angle φ increase. Then the resonance wavelength increases at some values of the angles ($\varphi \approx 30°$). This conformity is illustrated in Figure 28, where we give the values of resonance wavelength of the λ_{res}/λ_c angular irises (they are normalized on the λ_c) at different slots lengthes and for two values of the iris thickness: $h = 0.1\,\text{mm}$, $1.0\,\text{mm}$, calculated due to the formula (94).

The resonance wavelength increases in the case of the coordinate iris shift $\varphi = 0^o$ from the centre (y_0/b=0.5) of waveguide (the

calculations are made due to the formula (98) for Figure 29. In this case "lengthening" of the slot transits into its "shortening", reaching the $2L = \lambda_{res}/2$ value at different values of y_0/b for different slot lengths. We also note that influence of the h iris thickness on λ_{res} turns out to be more sufficient in the case of the slot inclination than at its shift to the waveguide broad wall.

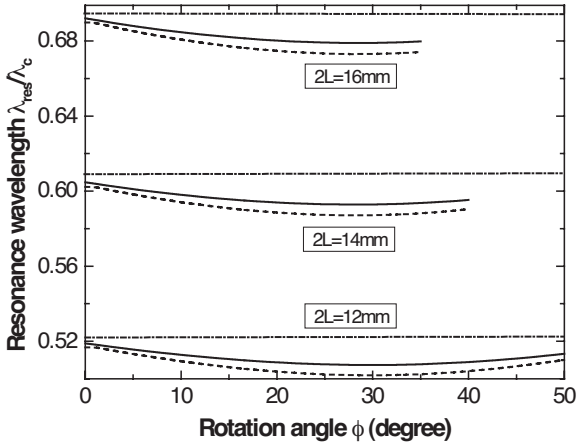

Figure 28. The relative resonance wavelength dependence from the rotation angle for an iris in rectangular waveguide at: $a = 23.0\,\text{mm}$, $b = 10.0\,\text{mm}$, $d = 1.5\,\text{mm}$, $x_0 = a/2$, $y_0 = b/2$; solid curves — $h = 1.0\,\text{mm}$, dotted curves — $h = 0.1\,\text{mm}$, stroke-dotted curves — $2L = \lambda_{res}/2$.

Different behavior of the resonant curves in Figure 28 and Figure 29 can be explained by the following way. The equality conditions of period average values of electrical and magnetic energies (resonance) of the iris near fields (defined by the functions W_0, W_φ and W of the own field of the slot) can be reached by two methods: slot geometrical sizes change relatively to the wavelength or its location change relatively to the waveguide walls at the fixed electrical sizes. So, additional oscillations of the E-mode ($E_{m,2n-1}$) appear in the near field (the own field function of the W_0 takes this into account) at the slot rotation to the narrow wall of a waveguide relatively to the normal and the H-mode ($H_{m,2n-1}$) oscillations appears at shift to the waveguide broad wall; and this is stipulated by the difference in redistribution of reactive energy and thus in the character of the resonant curves.

In order to estimate the accuracy of the obtained analytical formulas for $(kL)_{res}$ we have made the comparison with the numerical and experimental values due to the f_{res} frequencies of symmetrical

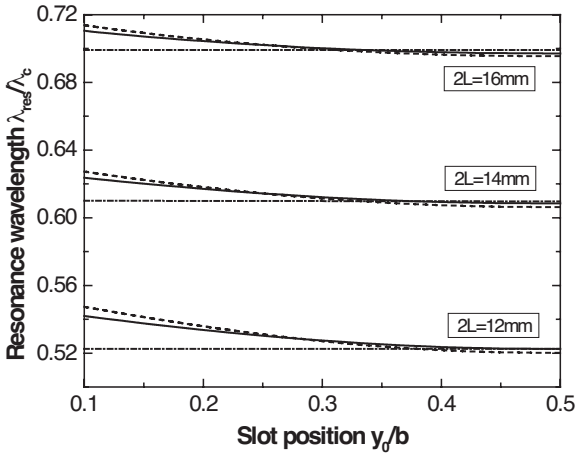

Figure 29. The relative resonance wavelength dependence from the slot position for an iris in rectangular waveguide at: $a = 23.0\,\text{mm}$, $b = 10.0\,\text{mm}$, $d = 1.5\,\text{mm}$, $x_0 = a/2$, $\varphi = 0°$; solid curves — $h = 1.0\,\text{mm}$, dotted curves — $h = 0.1\,\text{mm}$, stroke-dotted curves — $2L = \lambda_{res}/2$.

coordinate irises ($x_0 = a/2$, $y_0 = b/2$, $\varphi = 0°$) of different slot lengths and widths, given in [40] and Table 1.

Table 1. The resonance frequencies (in GHz) of a symmetrical coordinate irises in the rectangular waveguide at: $a = 22.86\,\text{mm}$, $b = 10.16\,\text{mm}$, $x_0 = a/2$, $y_0 = b/2$, $\varphi = 0°$, $h = 0.1\,\text{mm}$.

$2L \times d$, mm	Computation [40]	Experimental data [40]	Computation, formula (98)
16.9×0.9	8.87	8.84	8.84
14.8×0.5	10.22	10.20	10.13
12.9×0.9	11.62	11.65	11.66

5. STEPPED JUNCTION OF THE TWO RECTANGULAR WAVEGUIDES WITH THE IMPEDANCE SLOTTED IRIS

In the previous Section we have considered the problem of the resonance slot iris in the infinite rectangular waveguide in the case, when all surfaces of waveguide elements were supposed to be perfectly

conductive ones.

Thin-film coatings of materials with variable electrophysical properties can be used for expansion of functional capabilities of waveguide devices and realization of non-mechanical control of their characteristics by means of external field-effect or other actions. In particular, the coatings can be applied directly on iris surfaces.

Apparently, that experimental development of waveguide devices containing elements with thin-film coatings is very laborious process. In this connection evolution of the mathematical models of devices and elements of such kind is an important problem for practical applications. Here modeling is usually based on solutions of boundary-value problems in which statement the approximation of a distributed surface impedance is used [44, 45]. On the one hand this simplifies the problem solution, and on the other hand this allows one to generalize using of an obtained mathematical model.

The purpose of this Section is the development of an approximate analytical solution of the diffraction problem of H_{10}-wave by an impedance slot iris of finite thickness situated in the plane of stepped rectangular waveguide coupling which differ in dimensions of cross sections. In this case generally both surfaces of an iris will be assumed to be impedance.

5.1. Problem Formulation

Let impressed sources of the electromagnetic field $\vec{H}_0^{in}(\vec{r}_{in})$ (where $\vec{r}_{in}$ is the radius-vector in the local Cartesian system $(x_{in}, y_{in}, z_{in}$ related to a waveguide section in that way as is shown in Figure 30) be situated in internal region (denoted by the index "*in*") of a semi-infinite rectangular waveguide of cross section $\{a_{in} \times b_{in}\}$ with perfectly conductive side walls.

A narrow rectilinear slot of the length $2L$ and width d $((d/2L) \ll 1$, $(d/\lambda) \ll 1)$ is made in the end wall of the waveguide section of the thickness h $((h/\lambda) \ll 1)$. The long axis of the slot is parallel to the axis x_{in}, the center is at the point with coordinates $(x_{0in}, y_{0in}, 0_{in})$, and $x_{0in} = a_{in}/2$, i.e., the slot is situated symmetrically with respect to the axis line of the broad wall of the waveguide section. There are no impressed sources in the external region which is denoted by the index "*ext*". This region is semi-infinite rectangular waveguide of cross section $\{a_{ext} \times b_{ext}\}$ with perfectly conductive side walls. The center of coupling aperture with the waveguide section "*in*" will be determined by coordinates $x_{0ext}, y_{0ext}, 0_{ext}$ in the Cartesian system $x_{ext}, y_{ext}, z_{ext}$ which is local for the region "*ext*". The region formed with the slot cavity in the metal end wall of thickness h which is general

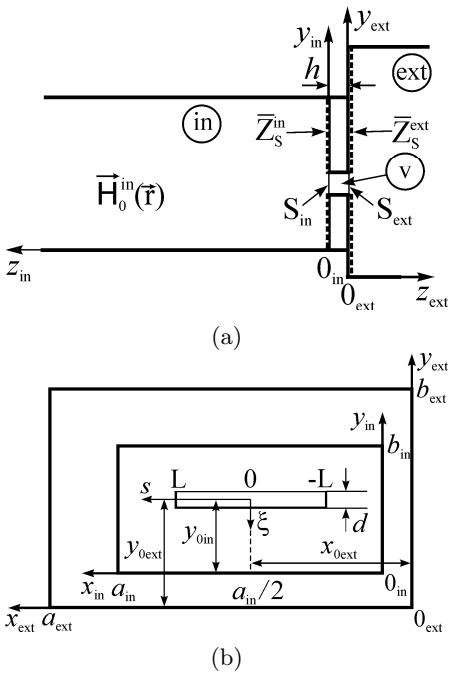

Figure 30. The problem formulation and the symbols used.

for the sections "*in*" and "*ext*" is denoted by the index "*v*". The local coordinate system x_v, y_v, z_v is introduced in this region.

Let surfaces of waveguide section ends ($z_{in,ext} = 0$) be generally characterized by different distributed impedances $\overline{Z}_s^{in,ext}$ of which complex values are considered to be constant. Here $\overline{Z}_s^{in,ext} = Z_s^{in,ext}/Z_0$ are the surface impedances normalized to the wave impedance of free space Z_0=120π [Ω].

Immediately we note that the solution of boundary-value problems with using of the Leontovich-Shchukin impedance boundary conditions [44], which will be used here, is approximate solution in nature. More precisely this solution is the first term of asymptotic expansion of the exact solution of the problem in power of the small parameter $|\overline{Z}_s|$ ($|\overline{Z}_s| \ll 1$). Therefore it should be specified that it is supposed that $|\overline{Z}_s^{in,ext}| \ll 1$ in the considered case. In this case the boundary conditions become extraneous, i.e., a value of the surface impedance does not depend on the pattern of an exciting field. Also it should be kept in mind that the impedance conditions are inapplicable near to edges of verges [45]. Really, the thickness of the skin-layer Δ^0

must be small both in comparison with the dimensions of the body in all directions and in comparison with curvature radii of its surface [44]. In this connection it is turned out to be impossible to require the fulfillment of impedance boundary conditions at the ends of waveguide sections in the neighborhood of edges of the slot of the width $(10\div100)\Delta^0$. Formally for the solution of a boundary-value problem it is necessary to exclude these boundary regions (the edge strip) from the total area of the impedance surface of the end. Using this approach in our case, we maintain accuracy of the approximate solution of the boundary-value problem and we can use the known methods developed for slots with perfectly conductive verges for studying fields of a slot aperture.

We note the continuity conditions of tangential components of a total magnetic field at the apertures of a coupling slot $S^{in}(z_{in}=0, z_v=0)$ and $S^{ext}(z_{ext}=0, z_v=-h)$:

$$\begin{cases} \vec{H}^{in}_{0\tau}\{\vec{r}_{in}\}+\vec{H}^{in}_{\tau}\{\vec{r}_{in},\vec{E}^{in}_{sl}\}=\vec{H}^{v}_{\tau}\{\vec{r}_{v},\vec{E}^{in}_{sl}\}+\vec{H}^{v}_{\tau}\{\vec{r}_{v},\vec{E}^{ext}_{sl}\}\Big|_{\text{on S}^{\text{in}},} \\ \vec{H}^{v}_{\tau}\{\vec{r}_{v},\vec{E}^{in}_{sl}\}+\vec{H}^{v}_{\tau}\{\vec{r}_{v},\vec{E}^{ext}_{sl}\}=\vec{H}^{ext}_{\tau}\{\vec{r}_{ext},\vec{E}^{ext}_{sl}\}\Big|_{\text{on S}^{\text{ext}}} \end{cases} \quad (100)$$

where $\vec{E}^{in}_{sl}$ and $\vec{E}^{ext}_{sl}$ are the electric fields at the corresponding apertures of the slot, $\vec{H}^{in}$, $\vec{H}^{v}$ and $\vec{H}^{ext}$ are the magnetic fields excited by the fields $\vec{E}^{in,ext}_{sl}$ in the space regions under consideration.

It is known [22] that $|E^{in,ext}_{sl_\xi}| \gg |E^{in,ext}_{sl_s}|$ (where s and ξ are the local coordinates related to the slot in the way shown in Figure 1(b)) is universally valid for narrow slots except of the small regions of $\{d/\lambda\}$ approximately on their ends. Therefore we suppose that the vectors $\vec{E}^{in,ext}_{sl}$ in set of Equations (100) have only ξ-components and the magnetic fields have only s-components. Then according to [22] the dependences of fields $E^{in,ext}_{sl_\xi}$ on coordinates $s_{in,ext}$ and $\xi_{in,ext}$ can be assumed to be equal to

$$\begin{aligned} &E^{in,ext}_{sl_\xi} = E^{in,ext}_0 f_{in,ext}(s_{in,ext})\chi_{in,ext}(\xi_{in,ext}), \\ &f_{in,ext}(-L) = f_{in,ext}(+L) = 0, \end{aligned} \quad (101)$$

where $E^{in,ext}_0$ are the amplitudes of the fields, $f_{in,ext}(s_{in,ext})$ are the functional dependences on longitudinal coordinates at the slot apertures, $\chi_{in,ext}(\xi_{in,ext})$ are the functions taking into account physically justified behavior of an electric field in verges of a slot cavity

and satisfying the normalization requirement

$$\int_{-d/2}^{d/2} \chi_{in,ext}(\xi_{in,ext})\, d\xi_{in,ext} = 1\,. \tag{102}$$

Using the results of study [22], in the considered boundary-value problem it is permissible that $E_0^{in} f_{in}(s_{in}) \approx E_0^{ext} f_{ext}(s_{ext}) = E_0 f(s) = E_{s_\xi}(s)$ to an accuracy of the terms of the order of $\{(hd)/\lambda^2\}$. Taking into account the normalization condition (102) after substitution of (101) in (100) the equation set can be reduced to one equation with "equivalent" slot width d_e:

$$H_{0s}^{in}\{s,\xi\} + H_s^{in}\{s,\xi;E_{sl_\xi}\} = H_s^{ext}\{s,\xi;E_{sl_\xi}\}\big|_{z_{in,ext}=0.} \tag{103}$$

In this case the region of the slot cavity v is eliminated from the consideration, and in Equation (103) d_e is related to real slot width d and wall thickness h by the approximate relationships (40) and (41).

To change the unknown electric field in the slot E_{sl_ξ} to equivalent currents distributed on its surface in Equation (103) it is formally necessary to close the slot aperture in such way that homogeneity of the surface in which the slot is made, should not be violated from the side of the considered region. So, to obtain a perfectly conductive plane it is necessary to metallize the slot aperture. In the considered case of impedance surfaces according to the Leontovich-Shchukin boundary conditions $[\vec{n}, \vec{E}^{in,ext}] = -\overline{Z}_s^{in,ext}[\vec{n}, [\vec{n}, \vec{H}^{in,ext}]]$ ($\vec{n}$ is the normal to the surface, this normal is directed into the interior of the impedance body) it is necessary to take also into account "one-way" electric currents $\vec{J}^E_{in,ext} = \frac{1}{Z_0}[\vec{n}, \vec{H}^{in,ext}_{sl}]$ at that $\vec{J}^M = -\overline{Z}_s^{in,ext}[\vec{n}, \vec{J}^E_{in,ext}]$ besides for the magnetic current $\vec{J}^M$ at the slot aperture. We emphasize that in each of the connected waveguide sections the equivalent electric current will have different value because it is determined through values of the surface impedances $\overline{Z}_s^{in,ext}$, which are generally assumed to be different. It must be said that "maintenance" of homogeneity of the boundary surfaces and introduction of the functionally related surface equivalent currents $\vec{J}^M$ and $\vec{J}^E_{in,ext}$ (where only $\vec{J}^M$ is unknown) does not contradict the requirements of assurance of uniqueness of the boundary-value problem solution. The "pair" assignment of equivalent currents on the impedance surface allows one to represent the electromagnetic field in semi-infinite waveguide sections simultaneously as superposition of waves of both magnetic and electric kinds using the corresponding

components of the tensor Green's functions for the Hertz vector potentials [46].

Thus, Equation (103) can be written in the following form

$$H_{0s}^{in}\{s,\xi\} + H_s^{in}\{s,\xi;J_s^M\} + H_s^{in}\{s,\xi;J_{\xi_{in}}^E\} = H_s^{ext}\{s,\xi;J_s^M\} + H_s^{ext}\{s,\xi;J_{\xi_{ext}}^E\}, \quad (104)$$

where $J_{\xi_{in,ext}}^E = \frac{1}{\overline{Z}_s^{in,ext}} J_s^M$.

At the solution of Equation (104) one can assume that $|\xi - \xi'| \cong \frac{d_e}{4}$ (quasi-onedimensional approximation) in the dependences of field components on transverse coordinates with sufficient degree of accuracy, as it is accepted in the theory of thin dipole antennas and can be rightfully used for narrow slot radiators [15]. Then after simple transformations we finally obtain the integral differential equation in the unknown magnetic slot current $J_s^M = J(s)$ in the following form

$$\left(\frac{\mathrm{d}^2}{\mathrm{d}s^2} + k^2\right) \int_{-L}^{L} J(s')[G_s^{in}(s,s') + G_s^{ext}(s,s')]\mathrm{d}s' + ik \int_{-L}^{L} J(s')[\overline{Z}_s^{in}\tilde{G}_s^{in}(s,s') + \overline{Z}_s^{ext}\tilde{G}_s^{ext}(s,s')]\mathrm{d}s' = -i\omega H_{0s}^{in}(s). \quad (105)$$

Here, $H_{0s}^{in}(s)$ is the projection of the field of impressed sources onto the slot axis, $G_s^{in,ext}(s,s')$ are the s-components of the quasi-onedimensional tensor magnetic Green's functions $\hat{G}^M(\vec{r}_{in,ext}, \vec{r}\,'_{in,ext})$ for vector potential of corresponding volumes (see the Appendix A), $\tilde{G}_s^{in,ext}(s,s') = \frac{\partial}{\partial z} G_s^{in,ext}\left(\begin{array}{c} x_{in,ext}(s), y_{0in,ext}, z_{in,ext}; \\ x'_{in,ext}(s'), y_{0in,ext} + \frac{d_e}{4}, 0 \end{array}\right)$ at substitution of $z_{in,ext} = 0$ after derivation. It is necessary to note that at derivation of Equation (105) it was taken into account that (in the case when the impressed sources are situated on the impedance surface of the end of a semi-infinite rectangular waveguide) the components of the tensor of the electric Green's function $\hat{G}^E(\vec{r}_{in,ext}, \vec{r}\,'_{in,ext})$ are related to the components $\hat{G}^M(\vec{r}_{in,ext}, \vec{r}\,'_{in,ext})$ in the following way [46]

$$G_x^E(\vec{r}_{in,ext}, \vec{r}\,'_{in,ext}) = (\overline{Z}_s^{in,ext})^2 G_y^M(\vec{r}_{in,ext}, \vec{r}\,'_{in,ext})$$

and

$$G_y^E(\vec{r}_{in,ext}, \vec{r}\,'_{in,ext}) = (\overline{Z}_s^{in,ext})^2 G_x^M(\vec{r}_{in,ext}, \vec{r}\,'_{in,ext}).$$

In the case when $\overline{Z}_s^{in,ext} = 0$ Equation (105) is transformed to the Equation (85) concerning the magnetic current in a slot coupling two semi-infinite rectangular waveguides.

5.2. Solution of the Equation for a Magnetic Current

We will apply the induced magnetomotive force method (IMMFM) [Section 3] for the approximate analytical solution of the Equation (105). As approximation for the magnetic current we will use the distribution (95) which has been obtained due to solution (by means of the averaging method) of the problem of diffraction of a fundamental mode by a narrow symmetrical slot which is made in the resonance iris of an infinite rectangular waveguide [Section 4]:

$$J(s) = J_0 f(s) = J_0 \left(\cos ks \cos \frac{\pi}{a_{in}} L - \cos kL \cos \frac{\pi}{a_{in}} s \right), \qquad (106)$$

where J_0 is the unknown complex amplitude.

Approximation (106) obeys boundary conditions (101) and is natural in the considered case of symmetrical arrangement of the slot with respect to the axial line of the broad wall of the waveguide section "*in*", where impressed sources of the electromagnetic field are placed.

Substituting (106) in Equation (105) and carrying out necessary transformations according to [Section 3], we obtain the solution for the sought current in the form

$$J(s) = -\left(\frac{i\omega}{2k}\right) \frac{\cos ks \cos \frac{\pi}{a_{in}} L - \cos kL \cos \frac{\pi}{a_{in}} s}{Y^{in}(kL, \overline{Z}_s^{in}) + Y^{ext}(kL, \overline{Z}_s^{ext})} \times \int_{-L}^{L} f(s) H_{0s}^{in}(s) \mathrm{d}s, \qquad (107)$$

where $Y^{in,ext}$ are the corresponding admittances of the slot in the volumes "*in*" and "*ext*" determined by means of the expressions

$$Y^{in,ext}(kL, \overline{Z}_s^{in,ext}) = \frac{1}{2k} \int_{-L}^{L} f(s) \left[\begin{array}{l} \left(\frac{\mathrm{d}^2}{\mathrm{d}s^2} + k^2 \right) \int_{-L}^{L} f(s') G_s^{in,ext}(s,s') \mathrm{d}s' \\ + ik \overline{Z}_s^{in,ext} \int_{-L}^{L} f(s') \tilde{G}_s^{in,ext}(s,s') ds' \end{array} \right] \mathrm{d}s. \qquad (108)$$

Using the expression (A4) for the Green's function $G_s^{in,ext}(s,s')$ from the Appendix A, we find explicit admittances of the slot in each of the coupled waveguide sections from relations (108) (see Appendix C).

Taking into account that in the case under consideration the slot is excited by the fundamental mode $H_{10}(x_{in}, z_{in}) = H_0 \sin \frac{\pi x_{in}}{a_{in}} e^{-i\gamma z_{in}}$,

where H_0 is its amplitude and $\gamma = \sqrt{k^2 - (\pi/a_{in})^2}$ is the propagation constant in the waveguide "*in*", it is valid $H_{0s}^{in}(s) = 2H_0 \cos\frac{\pi s}{a_{in}}$ in expression (107). After integration in (107) we obtain the final formula for determination of the magnetic current in the slot aperture

$$J(s) = -\frac{i\omega}{k^2} H_0 \frac{g(kL)}{Y^{in}(kL, \overline{Z}_s^{in}) + Y^{ext}(kL, \overline{Z}_s^{ext})} \times \left(\cos ks \cos\frac{\pi}{a_{in}} L - \cos kL \cos\frac{\pi}{a_{in}} s \right), \tag{109}$$

where

$$g(kL) = 2\cos\frac{\pi L}{a_{in}} \frac{\sin kL \cos\frac{\pi L}{a_{in}} - \left(\frac{\pi}{ka_{in}}\right) \cos kL \sin\frac{\pi L}{a_{in}}}{1 - [\pi/(ka_{in})]^2} - \cos kL \frac{\sin\frac{2\pi L}{a_{in}} + \frac{2\pi L}{a_{in}}}{[2\pi/(ka_{in})]}.$$

Thus we have realized the approximate analytical solution (109) of integral-differential Equation (105) for the magnetic current in the slot aperture. This enables us to determine coefficients of the scattering matrix of stepped rectangular waveguides coupling with an impedance slot iris.

The expression for power reflection coefficient $|S_{11}|^2$ at slot obstacle in a semi-infinite rectangular waveguide "*in*" with impedance end at single-mode operating has the following form:

$$|S_{11}|^2 = \left| \frac{1 - (\gamma/k)\overline{Z}_s^{in}}{1 + (\gamma/k)\overline{Z}_s^{in}} - \frac{8\pi\gamma g^2(kL)}{ia_{in}b_{in}k^3[Y^{in}(kL, \overline{Z}_s^{in}) + Y^{ext}(kL, \overline{Z}_s^{ext})]} \times \frac{1 + (\overline{Z}_s^{in})^2}{1 + (\gamma/k)\overline{Z}_s^{in}} \right|^2 \tag{110}$$

The second item in the formula (110) is determined by the field, which is excited in a waveguide section by proper magnetic current (109) of the slot. This item is found by means of the magnetic the Green's function (A4). The first addend is the coefficient of H_{10}-wave reflection at impedance end without a slot. This item is determined by means of Green's function of magnetic kind (A5) for a longitudinal current which excites the semi-infinite rectangular waveguide with impedance end assuming arrangement of a point source at $z' \to \infty$. Note that in the case of perfectly conductive end ($\overline{Z}_s^{in} = 0$) the first item becomes equal to unity (as it must be).

The number of propagated modes M in the waveguide section "*ext*", certainly, will depend on the dimensions of its cross section $\{a_{ext} \times b_{ext}\}$. In keeping with mentioned above the scattering matrix of a waveguide coupling will contain definite number of elements, which are power transmission coefficients of the propagated modes (or power transformation coefficients of the modes). They are determined as the ratio of the transmitted power P^{tr}_{mn} in the waveguide "*ext*" per each mode separately to the power P^{inc}_{10} of the incident H_{10}-wave in the waveguide "*in*", i.e.,

$$P_{mn} = \frac{P^{tr}_{mn}}{P^{inc}_{10}}, \tag{111}$$

where $P^{inc}_{10} = H^2_0 \left(\frac{a_{in} b_{in} k}{2\gamma}\right)$.

In expression (111) the quantity $P^{tr}_{mn} =$ is the power transferred in the waveguide section "*ext*" by the mode with the indexes (m, n). It is determined by means of the found equivalent currents in the slot aperture and the dyadic Green's functions. Since the particular case of H-plane coupling of waveguides considered as an example below in the study, here we will write down the explicit expressions for P_{m0} of waveguide modes of a magnetic type

$$\begin{aligned} P_{m0} \;=\; & \frac{a_{ext} b_{ext} \gamma}{a_{in} b_{in} \gamma_{m0}} \left| \frac{8\pi\gamma_{m0} \sin\frac{\pi x_{0ext}}{a_{ext}} g(kL) f_{m0}(kL)}{a_{ext} b_{ext} k^3} \right. \\ & \left. \times \frac{F(\gamma_{m0}, \overline{Z}^{ext}_s)}{[Y^{in}(kL, \overline{Z}^{in}_s) + Y^{ext}(kL, \overline{Z}^{ext}_s)]} \right|^2, \end{aligned} \tag{112}$$

where

$$\gamma_{m0} \;=\; \sqrt{k^2 - (m\pi/a_{ext})^2}, \quad F(\gamma_{m0}, \overline{Z}^{ext}_s) = \frac{1 + (\overline{Z}^{ext}_s)^2}{1 + (\gamma_{m0}/k)\overline{Z}^{ext}_s},$$

$$\begin{aligned} f_{m0}(kL) \;=\; & 2\cos\frac{\pi L}{a_{in}} \frac{\sin kL \cos\frac{m\pi L}{a_{ext}} - \left(\frac{m\pi}{ka_{ext}}\right) \cos kL \sin\frac{m\pi L}{a_{ext}}}{1 - [m\pi/(ka_{ext})]^2} \\ & -2\cos kL \frac{\left(\frac{\pi}{ka_{in}}\right) \sin\frac{\pi L}{a_{in}} \cos\frac{m\pi L}{a_{ext}} - \left(\frac{m\pi}{ka_{ext}}\right) \cos\frac{\pi L}{a_{in}} \sin\frac{m\pi L}{a_{ext}}}{[\pi/(ka_{in})]^2 - [m\pi/(ka_{ext})]^2}. \end{aligned}$$

In the case under consideration the complete scattering matrix of waveguide coupling, besides the coefficients $|S_{11}|^2$ and P_{m0}, will contain also the quantity P_σ. This is the loss power in impedance

coatings of ends of both coupled waveguide sections. The loss power can be determined from the condition of energy balance fulfillment:

$$|S_{11}|^2 + \sum_{m=1}^{M} P_{m0} + P_\sigma = 1. \tag{113}$$

In the case of absence of loss ($P_\sigma = 0$) it is necessary to use condition (113) for validation of algorithms of mathematical simulation.

The expressions for the $Y^{in,ext}(kL, \overline{Z}_s^{in,ext})$ admittances are given in Appendix C.

5.3. Surface Impedance of the Coating with the ε_1 and μ_1 Homogeneous Parameters

For some examples of physical realization of impedance surfaces, we give the formulas determining the quantity $\overline{Z}_s$ since they are necessary for numerical calculations. For this purpose, we consider the model problem of a plane electromagnetic wave normally incident on a dielectric layer of thickness h_d with complex dielectric permittivity ε_1 and magnetic permeability μ_1, and wave number $k_1 = k\sqrt{\varepsilon_1\mu_1}$. The layer separates two half-spaces. The upper half-space, from which the plane wave is incident, is free space ($\varepsilon = \mu = 1$), while the second half-space is described by the material parameters ε_2, μ_2.

Making use of the boundary conditions for the electric and magnetic field components on both surfaces of a dielectric layer it is easy to find the solution of the boundary-value problem. Comparing this solution with the requirements, that the Leontovich-Shchukin impedance boundary condition on the upper boundary of the dielectric layer must be fulfilled, we obtain a rigorous expression for the distributed surface impedance in the form:

$$\overline{Z}_s = \bar{Z}_1 \frac{i\overline{Z}_1 tg\,(k_1 h_d) + \overline{Z}_2}{\overline{Z}_1 + i\overline{Z}_2 tg(k_1 h_d)}, \tag{114}$$

where $\overline{Z}_1 = \sqrt{\mu_1/\varepsilon_1}$ and $\overline{Z}_2 = \sqrt{\mu_2/\varepsilon_2}$.

For a magnetodielectric layer of the thickness h_d on a metallic surface on substituting $\overline{Z}_2 = 0$ we obtain the formula, which is used to calculate of the value $\overline{Z}_s$ in [47]:

$$\overline{Z}_s = i\sqrt{\frac{\mu_1}{\varepsilon_1}} tg(\sqrt{\varepsilon_1\mu_1} k h_d). \tag{115}$$

We note, that in the case of the arbitrary incident field formula (115) is approximate and it becomes as more accurate as better the inequality $|\varepsilon_1\mu_1| \gg 1$ is fulfilled. So, for example, if the incident field is the wave of the H_{10} mode, propagating in a rectangular wavequide, then the formulas (114) and (115) have the form:

$$\overline{Z}_s = \overline{Z}_1 \frac{i\overline{Z}_1 tg\,(\gamma_1 h_d) + \overline{Z}_2}{\overline{Z}_1 + i\overline{Z}_2 tg\,(\gamma_1 h_d)}, \tag{116}$$

$$\overline{Z}_s = i\frac{k_1}{\gamma_1}\sqrt{\frac{\mu_1}{\varepsilon_1}} tg(\gamma_1 h_d), \quad \gamma_1 = \sqrt{k_1^2 - k_c^2}, \tag{117}$$

and when the condition $|\varepsilon_1\mu_1| \gg 1$ is performed, they transit into the expressions (114) and (115), correspondingly.

For the electrically thin layer ($|k_1 h_d| \ll 1$, the quasi-stationary approximation [45]) from (115) and (117) it follows that $\overline{Z}_s \approx ik\mu_1 h_d$ [45], that is, the normalized surface impedance does not depend on dielectric permittivity of material.

Supposing that in the expression (114) $\overline{Z}_2 = \overline{Z}_1$ under the condition $|\varepsilon_1| \gg 1$ and $\mu_1 = 1$, taking into account that $\varepsilon_1 = \mathrm{Re}\varepsilon_1 + \frac{4\pi\sigma_1}{i\omega}$, where σ_1 is the material conductivity, we can obtain a known formula to take into account the skin-effect of the conductor:

$$\overline{Z}_s = \frac{1+i}{Z_0\sigma_1\Delta^0}, \tag{118}$$

where $\Delta^0 = \frac{1}{30\sqrt{2\pi\sigma_1\omega}}$ is the depth of penetration of the electromagnetic field into a conductor.

In the case of a thin conductive film with the thickness h_R ($(h_R/\Delta^0) \ll 1$) which is covered on a magnetodielectric layer, located on a metallic plane, the surface impedance equals to due to (114):

$$\overline{Z}_{sR} = \frac{\overline{R}_{sR}}{1 + \overline{R}_{sR}/\overline{Z}_s}, \quad \overline{R}_{sR} = \frac{1}{Z_0\sigma_1 h_R}, \tag{119}$$

where $\overline{Z}_s$ is defined by the formulas (115) and (117).

Further we will use the representations (115) and (119) for $\overline{Z}_s$. However, if the analysis of other structures of impedance coverings is required, the expressions for $\overline{Z}_s$ can be obtained by different methods, as it is demonstrated in the following Section.

5.4. Surface Impedance of the Magnetodielectric Layer with Inhomogeneous Dielectric Permittivity on the Perfectly Conductive Surface

Modern technology of thin-film coverings allow to obtain both homogeneous (in the direction perpendicular to the completely conducting plane of the basis) and inhomogeneous structures [48]. In this Section we have obtained the approximate analytical expressions for distributed surface impedance of the magnetodielectric layer with inhomogeneous dielectric permittivity which is located on the infinite conductive plane, and they are just at rather small change of the value of dielectric permittivity within the range of this layer.

Let plane monochromatic electromagnetic wave, for which the component of the electric field equals to $E_x(z) = E_{0x}e^{-ikz}$ (E_{0x} is the amplitude) incident on the magnetodielectric layer with the thickness $2h_d$ ($-\infty < x, y < \infty$; $-h_d \leq z \leq h_d$, where $\{x, y, z\}$ is Cartesian coordinate system) and with magnetic permeability μ_1 and dielectric permittivity ε_1, located on the infinite conductive plane at $z = h_d$, perpendicular to the surface layer from the region $z = -\infty$ (half-space). Then for this layer the distributed surface impedance, normalized on a wave impedance of free space $Z_0 = 120\pi$ [Ω], will be defined by the expression [45]:

$$\overline{Z}_s = \frac{E_{0x}(-h_d)}{H_{0y}(-h_d)}. \tag{120}$$

To obtain $E_{0x}(-h_d)$ and $H_{0y}(-h_d)$ it is necessary to know the fields $E_x(z)$ and $H_y(z)$ inside the magnetodielectric layer, where they satisfy the following differential equations at $\mu_1 = const$ and $\varepsilon_1 = \varepsilon_1(z)$:

$$\frac{\mathrm{d}^2 E_x(z)}{\mathrm{d}z^2} + k^2\mu_1\varepsilon_1(z)E_x(z) = 0, \tag{121a}$$

$$H_y(z) = \frac{i}{k\mu_1}\frac{dE_x(z)}{dz}. \tag{121b}$$

The solution of the equations (121) together with boundary conditions on the surfaces of the layer at $z = \pm h_d$ gives opportunity to define the values $E_{0x}(-h_d)$, $H_{0y}(-h_d)$ and the value defined of the surface impedance $\bar{Z}_s$, correspondingly. We note, that the Equations (121) are just at the arbitrary functional dependence $\varepsilon_1(z)$ and ratio (120) is rigorous at a normal incident of a plane wave on a flat boundary of magnetodielectric.

For a limited number of laws of change $\varepsilon_1(z)$ we can obtain exact solutions of the Equations (121) [49]. However, they are very

complicated and in every concrete case are obtained through a definite class of special functions. At relatively small changes of the dielectric permittivity $\varepsilon_1(z)$ values within the layer we can obtain approximate solutions in the class of elementary functions, which have sufficient accuracy and simplicity. Let us consider some of them which allow to obtain expressions for the surface impedance $\overline{Z}_s$ in an analytical form.

5.4.1. Power Law of the $\varepsilon_1(z)$ Change

In this case it is possible to represent $\varepsilon_1(z)$ in the following form:

$$\varepsilon_1(z) = \varepsilon_1(0)[1 - \varepsilon_r f(z)], \tag{122}$$

where $\varepsilon_r = \frac{\varepsilon_1(0)-\varepsilon(-h_d)}{\varepsilon_1(0)}$ is the value of relative change of dielectric permittivity within the layer ($|\varepsilon_r| \ll 1$) and $f(z) = \left(-\frac{z}{h_d}\right)^n$, ($n = 1, 2, 3\ldots$) is the fixed function. Then the Equation (121a) transforms into the non-uniform differential equation with constant coefficients:

$$\frac{\mathrm{d}^2 E_x(z)}{\mathrm{d}z^2} + k_1^2 E_x(z) = \varepsilon_r k_1^2 f(z) E_x(z), \tag{123}$$

where $k_1^2 = k^2 \mu_1 \varepsilon_1(0)$.

Further, due to the method of variation of arbitrary constants we have, considering the right part of the Equation (123) fixed:

$$E_x(z) = C_1 e^{-ik_1 z} + C_2 e^{ik_1 z} + \varepsilon_r k_1 \int_{-h_d}^{z} f(z') E_x(z') \sin k_1(z - z')\mathrm{d}z'. \tag{124}$$

We will search the solution of the integral Equation (124) in the form of expansion $E_x(z)$ on the ε_r small parameter:

$$E_x(z) = E_{x0}(z) + \varepsilon_r E_{x1}(z) + \varepsilon_r^2 E_{x2}(z) + \ldots + \varepsilon_r^m E_{xm}(z) + \ldots \tag{125}$$

Then, substituting (125) into the Equation (124) and being limited by components of the null and first order of smallness, we obtain the following expressions for the electric and magnetic fields inside the layer:

$$\begin{aligned} E_x(z) &= C_1 e^{-ik_1 z}[1 + \varepsilon_r f_E(k_1 z)] + C_2 e^{ik_1 z}[1 + \varepsilon_r f_E^*(k_1 z)], \\ H_y(z) &= \frac{1}{\overline{Z}_1}\left\{C_1 e^{-ik_1 z}[1 + f_H(k_1 z)] - C_2 e^{ik_1 z}[1 + f_H^*(k_1 z)]\right\}. \end{aligned} \tag{126}$$

Here "$*$" is the sign of complex conjugation, $\overline{Z}_1 = \sqrt{\mu_1/\varepsilon_1(0)}$, and the functions $f_E(k_1 z)$ and $f_H(k_1 z)$ are defined by the law of change $\varepsilon_1(z)$. Particularly, they are equal for the linear and square laws, correspondingly:

a) the linear law: $\varepsilon_1(z) = \varepsilon_1(0)\left(1 + \varepsilon_r \frac{z}{h_d}\right)$;

$$\begin{aligned} f_E(k_1 z) &= -\frac{1}{4k_1 h_d}[(k_1 z) + i(k_1 z)^2 - i/2], \\ f_H(k_1 z) &= -\frac{1}{4k_1 h_d}[-(k_1 z) + i(k_1 z)^2 + i/2]. \end{aligned} \tag{127}$$

b) the square law: $\varepsilon_1(z) = \varepsilon_1(0)\left(1 - \varepsilon_r \frac{z^2}{h_d^2}\right)$;

$$\begin{aligned} f_E(k_1 z) &= \frac{1}{(2k_1 h_d)^2}\left[(k_1 z)^2 - \frac{1}{2} + i\frac{2(k_1 z)^3}{3} - i(k_1 z)\right], \\ f_H(k_1 z) &= \frac{1}{(2k_1 h_d)^2}\left[-(k_1 z)^2 + \frac{1}{2} + i\frac{2(k_1 z)^3}{3} + i(k_1 z)\right]. \end{aligned} \tag{128}$$

We obtain searched expressions for the surface impedance defining unknown constants C_1 and C_2 from the boundary conditions of the components continuity at $z = -h_d$ and the null equality of the electrical component at $z = h_d$ in (126):

$$\overline{Z}_s = \overline{Z}_1 \frac{\left\{ \begin{array}{l} [1 + \varepsilon_r f_E(-k_1 h_d)][1 + \varepsilon_r f_E^*(k_1 h_d)] e^{i4k_1 h_d} \\ -[1 + \varepsilon_r f_E^*(-k_1 h_d)][1 + \varepsilon_r f_E(k_1 h_d)] \end{array} \right\}}{\left\{ \begin{array}{l} [1 + \varepsilon_r f_H^*(-k_1 h_d)][1 + \varepsilon_r f_E(k_1 h_d)] \\ +[1 + \varepsilon_r f_H(-k_1 h_d)][1 + \varepsilon_r f_E^*(k_1 h_d)] e^{i4k_1 h_d} \end{array} \right\}}. \tag{129}$$

At $\varepsilon_r = 0$ and the change $2h_d \to h_d$ the formula (129) transits into the ratio (115) obtained before, for impedance of the homogeneous magnetodielectric layer of the thickness h_d on the perfectly conductive surface.

Neglecting the components of the ε_r^2-order in the formula (129) and making change $2h_d \to h_d$, finally, we have:

a) for the linear law of change $\varepsilon_1(z)$:

$$\begin{aligned} \overline{Z}_s &= i\overline{Z}_1 \frac{tg(k_1 h_d)}{1 + \varepsilon_r f_{Lin}(k_1 h_d) tg(k_1 h_d)}, \\ f_{Lin}(k_1 h_d) &= \left(\frac{1}{2k_1 h_d} + \frac{i}{2}\right). \end{aligned} \tag{130}$$

b) for the square law of change $\varepsilon_1(z)$:

$$\begin{aligned} &\overline{Z}_s = i\overline{Z}_1 \frac{tg(k_1 h_d) + \varepsilon_r f_{Sq1}(k_1 h_d)}{1 + \varepsilon_r f_{Sq2}(k_1 h_d) tg(k_1 h_d)}, \\ &f_{Sq1}(k_1 h_d) = \frac{1}{k_1 h_d} - \frac{tg(k_1 h_d)}{(k_1 h_d)^2}, \quad f_{Sq2}(k_1 h_d) = \frac{k_1 h_d}{6}. \end{aligned} \tag{131}$$

One must note, that the obtained approximate solution (126) of the Equation (123) (and the expression for impedance (129), correspondingly), is just not only for the power law of change $\varepsilon_1(z)$, because representation of dielectric permittivity in the form (122) is possible for another functions $f(z)$, e.g., trigonometric ones: $f(z) = \left(1 - \cos\frac{\pi z}{2h_d}\right)$, $f(z) = -\sin\frac{\pi z}{2h_d}$.

5.4.2. Exponential Law of the $\varepsilon_1(z)$ Change

Let us consider that dielectric permittivity of magnetodielectric layer of the h_d $(0 \le z \le h_d)$ thickness varies due to the exponential law

$$\varepsilon_1(z) = \varepsilon_1(0) e^{kz}. \tag{132}$$

In this case transformation (122), made in order to separate the ε_r small parameter, does not already take place, though some other representations $\varepsilon_1(z)$ are possible, which allow to reduce the initial Equation (121a) to the integral equation with a small parameter and to apply the method, described above, for its solution. To our minds, at this functional dependence $\varepsilon_1(z)$ it is more convenient to use the approximate solution of the Equation (121a) in a form of the so-called WKB-approach [49, 50]:

$$E_x(z) = \frac{1}{\sqrt[4]{\varepsilon_1(z)}} \left\{ C_1 e^{-ik\sqrt{\mu_1}\int\limits_0^z \sqrt{\varepsilon_1(z)}\mathrm{d}z} + C_2 e^{ik\sqrt{\mu_1}\int\limits_0^z \sqrt{\varepsilon_1(z)}\mathrm{d}z} \right\}. \tag{133}$$

Let us note, that the expression (133) is just if the $\varepsilon_1(z)$ function does not have nulls or poles on the $[0, z]$ interval. The criteria to apply the WKB-approach is the following inequality [50]:

$$\left| \frac{\mathrm{d}\varepsilon_1(z)/\mathrm{d}z}{k\sqrt{\mu_1}[\varepsilon_1(z)]^{3/2}} \right|_{\max} \ll 1, \tag{134}$$

which has form $\left| \frac{1}{\sqrt{\mu_1 \varepsilon_1(0)}} \right| \ll 1$ in our case.

Substituting (132) into (133) and impose a restriction $(h_d/\lambda)^2 \ll 1$ after transformations we get:

$$\begin{aligned} E_x(z) &= \tfrac{e^{-kz/4}}{\sqrt[4]{\varepsilon_1(0)}} \left(C_1 e^{-ik_1 z} + C_2 e^{ik_1 z}\right), \\ H_y(z) &= \tfrac{1}{\overline{Z}_1} \tfrac{e^{-kz/4}}{\sqrt[4]{\varepsilon_1(0)}} \left\{C_1 e^{-ik_1 z} f_H[\varepsilon_1(0)\mu_1] - C_2 e^{ik_1 z} f_H^*[\varepsilon_1(0)\mu_1]\right\}, \end{aligned} \tag{135}$$

where $f_H[\varepsilon_1(0)\mu_1] = 1 - \frac{i}{4\sqrt{\varepsilon_1(0)\mu_1}}$. Due to the requirements of boundary conditions performance at $z = 0$ and $z = h_d$ we define the arbitrary constants C_1 and C_2 and later on the expression for the normalized surface impedance at the exponential law of change of dielectric permittivity inside the magnetodielectric layer:

$$\begin{aligned} \overline{Z}_s &= i\overline{Z_1} \frac{tg(k_1 h_d)}{1 + f_{Exp}[\varepsilon_1(0)\mu_1] tg(k_1 h_d)}, \\ f_{Exp}[\varepsilon_1(0)\mu_1] &= \tfrac{1}{4\sqrt{\varepsilon_1(0)\mu_1}}, \end{aligned} \tag{136}$$

transiting to the already known ratio $\bar{Z}_s \approx ik\mu_1 h_d$ at $|k_1 h_d| \ll 1$.

We must emphasize the fact, that the formulas (130), (131) and (136) for the distributed surface impedance of the magnetodielectric layer with inhomogeneous dielectric permittivity, located on infinite conductive plane, are just at different laws of change of dielectric permeability inside the layer and obtained by different methods, have similar structure and are reduced to the same ratios in the restricted case $\varepsilon_1 = const$ and $|k_1 h_d| \ll 1$. Using this methods, the obtained results permit to generalize them for the case, when a metallic film of the thickness less than skin-layer thickness, is covered on the magnetodielectric layer located on the metallic surface. Then the surface impedance of such a structure will be defined by the expression (119), and $\overline{Z}_s$ is calculated due to the formulas (130), (131), and (136) according to the law of distribution of dielectric permittivity of the layer.

5.4.3. Numerical Examples

We give some results of numerical calculations of the value of the distributed surface impedance, which illustrate effect of that or other law of dielectric permittivity change, on the values of active and reactive parts of the impedance of the magnetodielectric layer located on the infinite metallic plane. Because of dependence of magnetodielectric parameters from the frequency we limit ourselves by the corresponding single-mode standard rectangular waveguide of a centimetre band to define waves lengths.

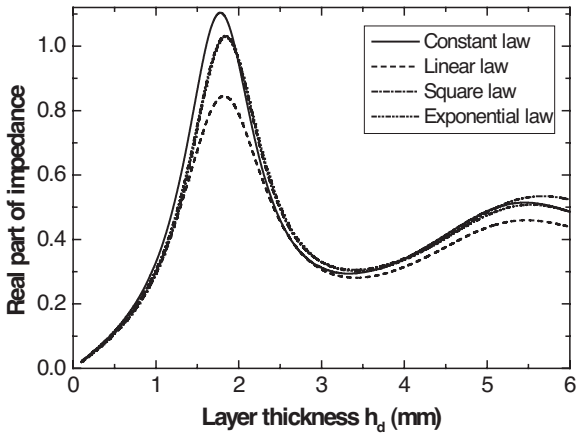

(a)

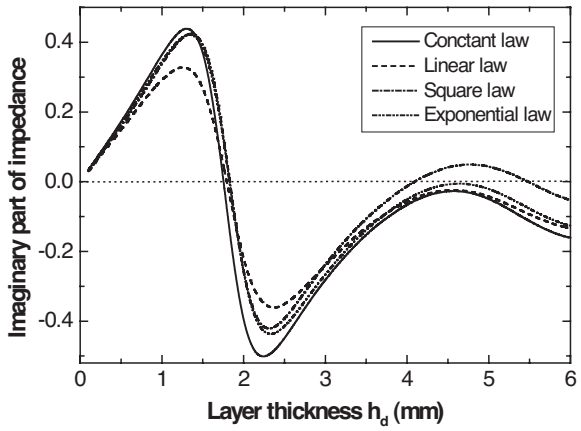

(b)

Figure 31. The real and imaginary parts of surface impedance dependence from the layer thickness for a magnetodielectric layer on a metallic plane at $\lambda = 30.0\,\text{mm}$.

Figure 31 represents the curves of a real and imaginary parts of the complex surface impedance $\bar{Z}_s = \bar{R}_s + i\bar{X}_s$ depending from the thickness of the magnetodielectric layer made from the TDK IR-E110 material, for which due to [47] $\varepsilon_1 = 8.84 - i0.084$ and $\mu_1 = 2,42 - 0.0825f - i0.994$, where f is the frequency [GHz] corresponding to the band of the H_{10}-mode of the rectangular waveguide by cross-section $22.86 \times 10.16\,\text{mm}^2$. As it is seen, a real impedance $\bar{R}_s$ has explicitly marked maximum for all considered laws of change $\varepsilon_1(z)$

(here and further $\varepsilon_r^2 = 0.04$ for the linear and square laws) at a definite layer thickness which is equal to a quarter of wavelength in the magnetodielectric ($h_d \approx 1.8\,\text{mm}$ for $\lambda = 30\,\text{mm}$), and it aspires to a constant value, which equals $Re\overline{Z}_1$ at losses presence, when the layer thickness increases further. At the same time the dependence of the imaginary part $\bar{X}_s$ of the impedance from the layer thickness has alternating-sign character, more over, for the fixed ε_1, μ_1 and λ at $h_d \approx 1.8\,\text{mm}$ for all dependences $\varepsilon_1(z)$ they have $\overline{X}_s = 0$, and $\overline{R}_s = \overline{R}_{s_{\max}}$, and coefficient of plane wave reflection from such a structure will be minimal: the layer becomes the so-called "anti-reflecting coating". We note that the largest difference of the $\bar{Z}_s$ value from the case of a homogeneous magnetodielectric takes place at the linear law of distribution $\varepsilon_1(z)$.

Figure 32 gives the curves of the dependences of the surface impedance from a wavelength due to different laws of change of dielectric permittivity of a magnetodielectric TDK IR-E110 and the layer thickness $h_d \approx 1.6\,\text{mm}$, that corresponds to the value in [47], where the problem of radiation from a longitudinal slot in the broad wall of a rectangular waveguide ($a = 22.86\,\text{mm}$; $b = 10.16\,\text{mm}$) into half-space over the impedance plane has been solved. From the plots it follows that inhomogeneous layer leads to the $\bar{R}_s$ decrease in a whole band of the H_{10}-mode of a waveguide, meanwhile, the imaginary part of impedance can be of both larger and smaller values, corresponding to the case of a homogeneous material. Let us note, that the values of the surface impedance $\bar{Z}_s$, practically coincide for the square and exponential laws of change $\varepsilon_1(z)$ at the given layer thickness.

When solving the problem of an impedance slotted iris we used the Leontovich-Shchukin approximate impedance boundary condition which assumes performance of the inequality $|\overline{Z}_s| \ll 1$. Such values of impedance take place for small thicknesses of the layer, as it is shown, for example, in Figure 33 (the same material, $h_d = 0.3\,\text{mm}$). In this case both the real and imaginary parts of impedance independent from the law of change of dielectric permittivity decrease monotonously at a wave length increase, more over, the $\overline{X}_s$ value is always positive, that is, it has an inductive character.

At it is seen in Figure 34 if a resistive film of a definite thickness with low conductivity (e.g., Nichrome) is covered on the magnetodielectric surface, then the real part $\text{Re}\overline{Z}_{sR}$ of the surface impedance of such a structure has the same value and changes, practically, as in the previous case (Figure 33(a)). The imaginary part of the $\text{Im}\overline{Z}_{sR}$ impedance becomes sufficiently less, and it has maximum in a short wave part of waveguide single-mode band.

The made analysis shows that effect of inhomogeneity of

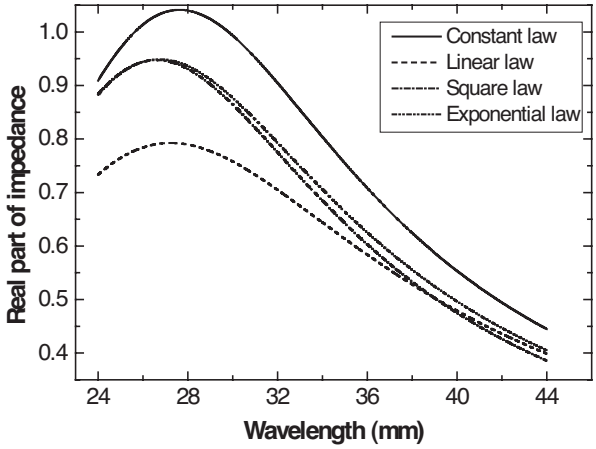

(a)

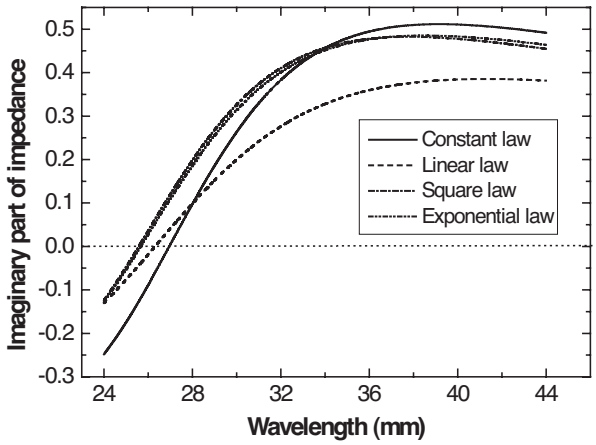

(b)

Figure 32. The real and imaginary parts of surface impedance dependence from the wavelength for a magnetodielectric layer on a metallic plane at $h_d = 1.6\,\text{mm}$.

magnetodielectric in the considered cases is relatively small — not more than 25% in comparison with a homogeneous layer, and it is sufficient for the linear law of distribution (in comparison with the square and exponential laws). The layer inhomogeneity characterized by one or another law of change of dielectric permittivity is an additional method to range extension of conducting of management of electrodynamic parameters of microwave wave-slotted devices.

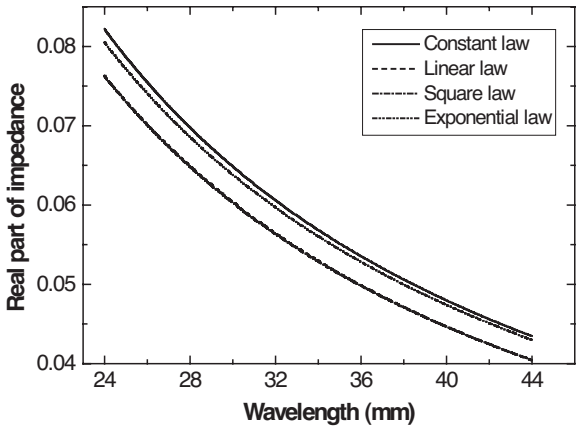

(a)

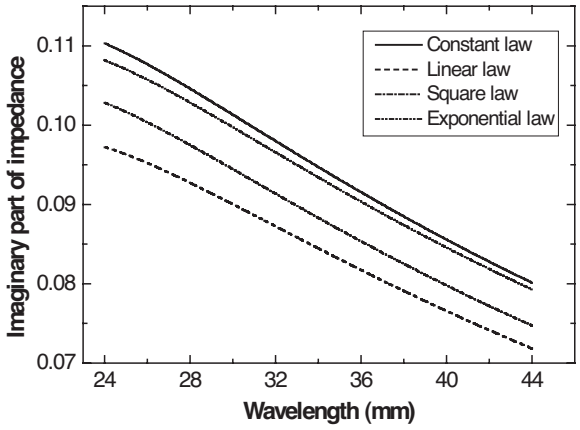

(b)

Figure 33. The real and imaginary parts of surface impedance dependence from the wavelength for a magnetodielectric layer on a metallic plane at $h_d = 0.3\,\text{mm}$.

5.5. Numerical Results

Based on the obtained problem solution the numerical analysis of coefficients of the scattering matrix of an impedance slot iris for a number of cases of realization of stepped joint of two rectangular waveguides are carried out. All calculations are carried out under the assumption that the excited region "*in*" is a hollow semi-infinite rectangular waveguide of standard cross section $a_{in} \times b_{in}$=23×10 mm^2 with thickness of end wall $h = 2\,\text{mm}$ and geometrical parameters of

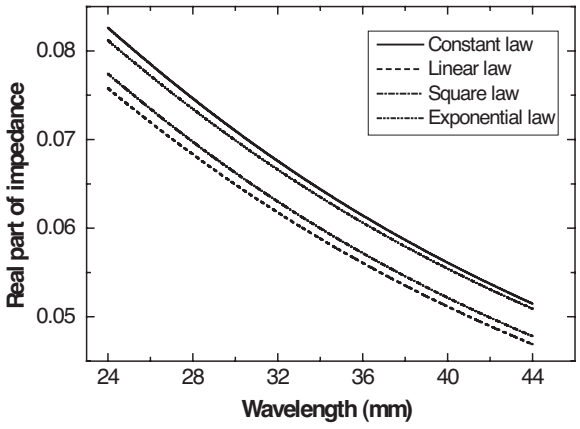

(a)

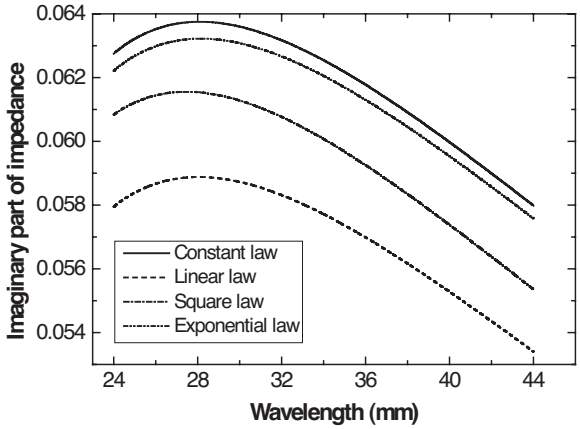

(b)

Figure 34. The real and imaginary parts of surface impedance dependence from the wavelength for a magnetodielectric layer on a metallic plane covered by resistive film at: $\overline{R}_{sR} = 0.3$, $h_d = 0.3\,\text{mm}$.

a slot: $d = 1.5\,\text{mm}$, $x_{0in} = a_{in}/2$ and $y_{0in} = b_{in}/4$; the waveguide is used in single-mode operating. The other parameters of the diffraction problem are varied during calculations.

Figures 35 and 36 represents the range dependences of coefficients of the scattering matrix and loss power of a slot iris in a regular rectangular waveguide ($a_{ext} = a_{in} = 23\,\text{mm}$, $b_{ext} = b_{in} = 10\,\text{mm}$) for $2L = 16\,\text{mm}$ as the matter for convenience and completeness of the analysis of the numerical results. Curves 1 show the results of

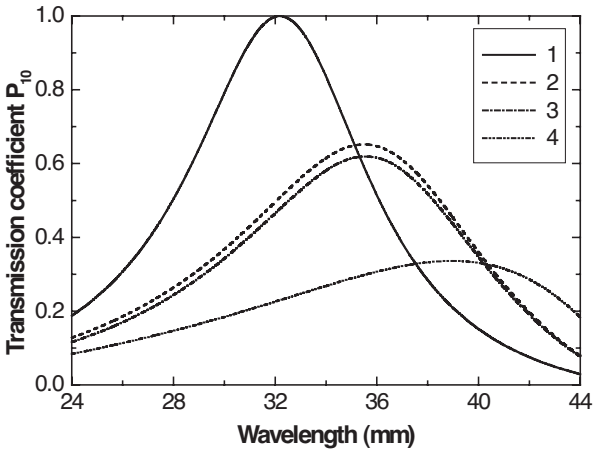

(a)

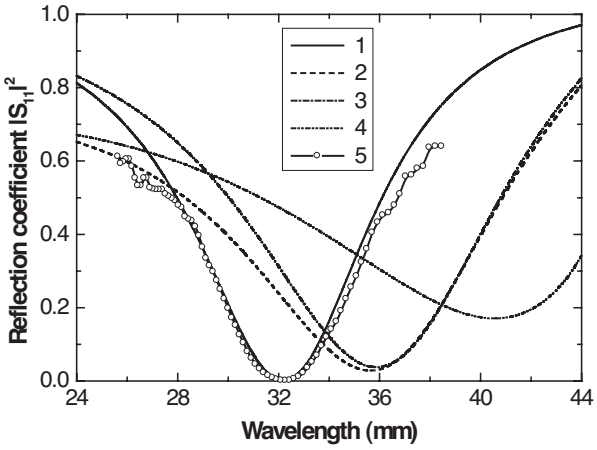

(b)

Figure 35. The coefficients of the scattering matrix dependence from the wavelength for a slot impedance iris in a regular waveguide at: $a_{in} = a_{ext} = 23.0\,\text{mm}$, $b_{in} = b_{ext} = 10.0\,\text{mm}$, $d = 1.5\,\text{mm}$, $2L = 16.0\,\text{mm}$, $x_{0in} = a_{in}/2$, $y_{0in} = b_{in}/4$.

calculation of the characteristics at $\overline{Z}_s^{in,ext} = 0$. Certainly there is no curve 1 in Figure 36 because the loss power is $P_\sigma = 0$ in the case of a perfectly conductive iris. As one can see from Figure 35(b) the satisfactory agreement of theoretical (curve 1) and experimental (curve 5) results confirms both validity of the used procedure and the accepted approximations and validity of construction of algorithms of

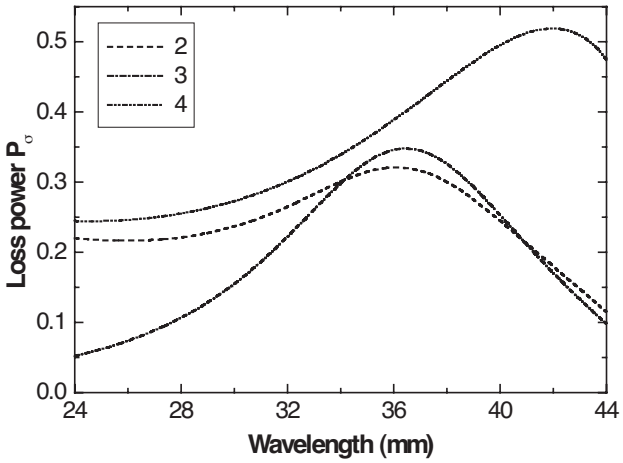

Figure 36. The loss power dependence from the wavelength for a slot impedance iris in a regular waveguide at: $a_{in} = a_{ext} = 23.0\,\text{mm}$, $b_{in} = b_{ext} = 10.0\,\text{mm}$, $d = 1.5\,\text{mm}$, $2L = 16.0\,\text{mm}$, $x_{0in} = a_{in}/2$, $y_{0in} = b_{in}/4$.

mathematical simulation.

Figure 35 also represents the calculation dependences of energy characteristics of a slot iris over working range of wavelengths of a rectangular waveguide at various values of complex impedances $\overline{Z}_s^{in,ext}$ with imaginary part of inductive type for a layer situated on metal of the magnetodielectric TDK IR-E110. In this case the values $\overline{Z}_s^{in,ext}$ are determined by the formula (115). In Figure 35 curves 2 correspond to the case of coating of iris surface from the side of the region "*in*" with the material TDK (in this case $\overline{Z}_s^{ext} = 0$), curves 3 correspond to the case of coating of the iris surface from the side of the region "*ext*" with the material TDK ($\overline{Z}_s^{in} = 0$), curves 4 correspond to the case of two-sided coating of the iris. Here it is assumed that the thickness of layers of the material TDK is $h_d = 0.2\,\text{mm}$ everywhere.

Naturally that the two-sided impedance iris exerts more essential influence upon behavior of the energy dependences than one-sided ones. Also is observed nonequivalence of the cases of one-sided impedance coating of an iris ($\overline{Z}_s^{in} \to (115)$, $\overline{Z}_s^{ext} = 0$) and ($\overline{Z}_s^{in} = 0, \overline{Z}_s^{ext} \to (115)$). It follows from formula (110) which is asymmetrical with respect to the parameters $\overline{Z}_s^{in}$ and $\overline{Z}_s^{ext}$. Note that in the cases under consideration the displacement of the resonance wavelength of the iris λ_{res} (corresponds to minimum in dependences of power

reflection coefficient $|S_{11}|^2$ in Figure 35(b)) in the long-wave region of the working band of the waveguide is characterized by considerable level of the loss power P_σ in impedance surfaces (Figure 36). Thus for $\lambda_{res} = 41\,\text{mm}$ (curve 4 in Figure 35(b)) $P_\sigma \approx 0.52$ (curve 4 in Figure 36). We emphasize that though the dependences $P_\sigma(\lambda)$ (Figure 36) have resonant character, in no way it can be treated as resonance absorption by an impedance surface of a waveguide iris. It is bound up first of all with range change of emissivity of a slot element, namely the more active a slot excites diffraction fields in jointed electrodynamic volumes the greater amplitudes of these fields and accordingly the greater amplitude of currents induced on boundary surfaces. Therefore the curves $P_\sigma(\lambda)$ "iterate" resonant features of the range dependences of the power transmission coefficient P_{10} (Figures 35(a) and 36)).

The similar physical regularities are also observed for joint of semi-infinite rectangular waveguides different in dimensions of cross sections. For substantiation of such assertion Figures 37 and 38 represents as an example the results of calculations of range characteristics of asymmetrical H-plane waveguide coupling for which $a_{ext} = 46\,\text{mm}$, $b_{ext} = b_{in} = 10\,\text{mm}$ and $x_{0ext} = a_{ext}/4$, $y_{0ext} = b_{ext}/4$. The other parameters of the problem and numeration of the curves are chosen in the same way as for the previous series of calculations. The waveguide device geometry under consideration determines possibility of propagation of two modes, namely, H_{10} and H_{20} (the onset of the H_{30}-wave is excluded by requirements of the excitation) in the waveguide section "*ext*". As one can see from Figures 37 and 38, the two-mode operation of the waveguide section "*ext*" really has not effect inherently upon the regularities mentioned above.

A thin layer of a concrete magnetodielectric applied in practice in radiating devices for special purposes [47] has been used in the considered examples as realization of an impedance surface at the iris. The analysis of these examples confirms the evident assumption that other materials in which there is no, practically, microwave loss should be used for control functions in waveguide devices under investigation. In this connection it is expedient to analyze possibility of influence of a surface impedance of an iris upon redistribution of transmitted power between propagated modes in a waveguide "*ext*" in the case of hypothetically pure imaginary value of an inductive impedance.

Figure 39 represents the results of calculations of asymmetrical H-plane of waveguide coupling of the same geometry (Figure 37) in the similar form for various values of inductive impedances $\overline{Z}_s^{in}$ and $\overline{Z}_s^{ext}$. In the given example curves 1 correspond to values of impedances $\overline{Z}_s^{in,ext} = 0$, curves 2 correspond to $\overline{Z}_s^{in} = 0$ and $\overline{Z}_s^{ext} = i0.05$, curves 3 correspond to $\overline{Z}_s^{in} = i0.02$ and $\overline{Z}_s^{ext} = i0.05$, curves 4 correspond

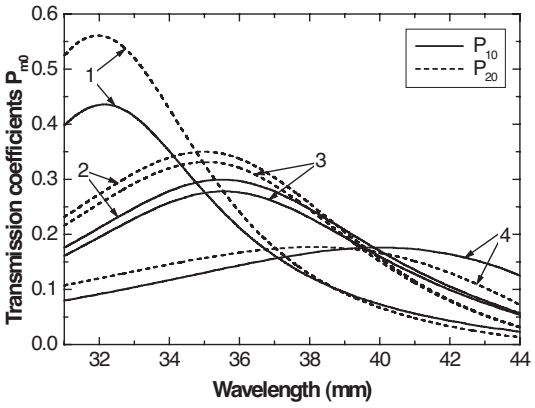

(a)

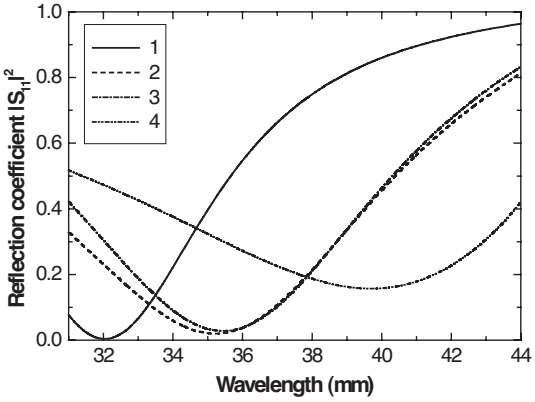

(b)

Figure 37. The coefficients of the scattering matrix dependence from the wavelength for an asymmetrical H-plane waveguide coupling at: $a_{in} = 23.0\,\text{mm}$, $a_{ext} = 46.0\,\text{mm}$, $b_{in} = b_{ext} = 10.0\,\text{mm}$, $d = 1.5\,\text{mm}$, $2L = 16.0\,\text{mm}$, $x_{0in} = a_{in}/2$, $x_{0ext} = a_{ext}/4$, $y_{0in} = b_{in}/4$, $y_{0ext} = b_{ext}/4$.

to equal values of impedances $\overline{Z}_s^{in,ext} = i0.05$. As can be seen from Figure 39 that by means of variation of corresponding values of $\overline{Z}_s^{in,ext}$ it is possible to ensure wide-band equal of division of the power transmitted in a waveguide section "*ext*" between the H_{10}- and H_{20}-modes being in it.

As a number of propagated modes in the waveguide "*ext*" grows, the analysis of division of transmitted power between them becomes

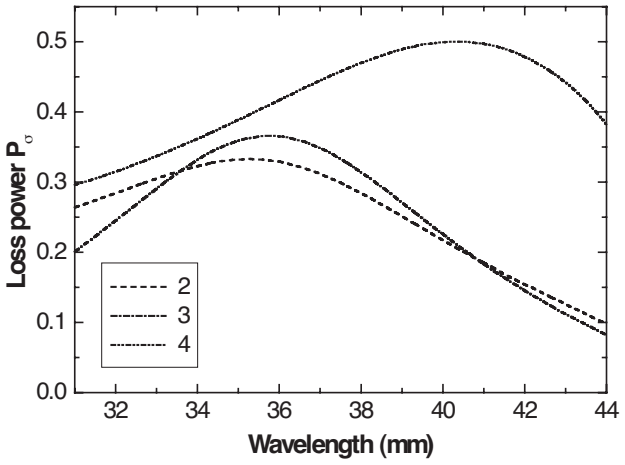

Figure 38. The loss power dependence from the wavelength for an asymmetrical H-plane waveguide coupling at: $a_{in} = 23.0\,\text{mm}$, $a_{ext} = 46.0\,\text{mm}$, $b_{in} = b_{ext} = 10.0\,\text{mm}$, $d = 1.5\,\text{mm}$, $2L = 16.0\,\text{mm}$, $x_{0in} = a_{in}/2$, $x_{0ext} = a_{ext}/4$, $y_{0in} = b_{in}/4$, $y_{0ext} = b_{ext}/4$.

rather complicated. However, one can show, that in these cases it is possible also to realize wide-band retuning of a resonance frequency of the waveguide device by means of variation of values of the impedances $\overline{Z}_s^{in,ext}$. Figure 40 represents the dependences of the scattering matrix coefficients $P_{m0}(\lambda)$ (Figure 40(a)) and $|S_{11}|^2(\lambda)$ (Figure 40(b)) of asymmetrical H-plane waveguide coupling for which $x_{0ext} = a_{ext}/6$ and $2L = 12\,\text{mm}$ (the other geometrical parameters are chosen as well as for the previous series of the calculations). Curves 1 in Figure 40 correspond to the case of perfectly conductive iris surfaces $\overline{Z}_s^{in,ext} = 0$, curves 2 correspond to the surface impedance values $\overline{Z}_s^{in} = 0$ and $\overline{Z}_s^{ext} = i0.05$, curves 3 correspond to the equal values of the impedances $\overline{Z}_s^{in,ext} = i0.05$. One can see from Figure 40 that at change in the corresponding values of surface impedances it is possible to maintain amplitude relations between the modes which are propagated in the waveguide "*ext*" and between which the transmitted power is divided. This maintenance is possible over wide range of wavelengths.

Thus, based on the numerical investigations of characteristics of asymmetrical H-plane waveguide coupling (the particular cases of realization of a stepped joint) the regularities of diffraction excitation of a slot element which is made in an impedance iris has been analyzed. The possibility of essential change of a operating (resonance)

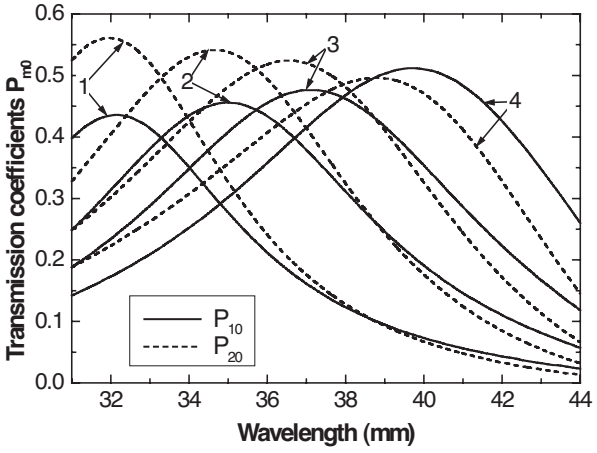

(a)

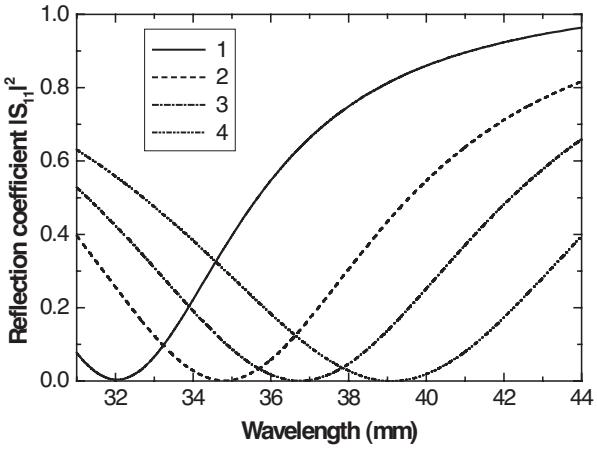

(b)

Figure 39. The coefficients of the scattering matrix dependence from the wavelength for an asymmetrical H-plane waveguide coupling at: $a_{in} = 23.0\,\text{mm}$, $a_{ext} = 46.0\,\text{mm}$, $b_{in} = b_{ext} = 10.0\,\text{mm}$, $d = 1.5\,\text{mm}$, $2L = 16.0\,\text{mm}$, $x_{0in} = a_{in}/2$, $x_{0ext} = a_{ext}/4$, $y_{0in} = b_{in}/4$, $y_{0ext} = b_{ext}/4$.

wavelength of the waveguide device under consideration at variation of the corresponding values of the distributed impedances on iris surfaces has been shown.

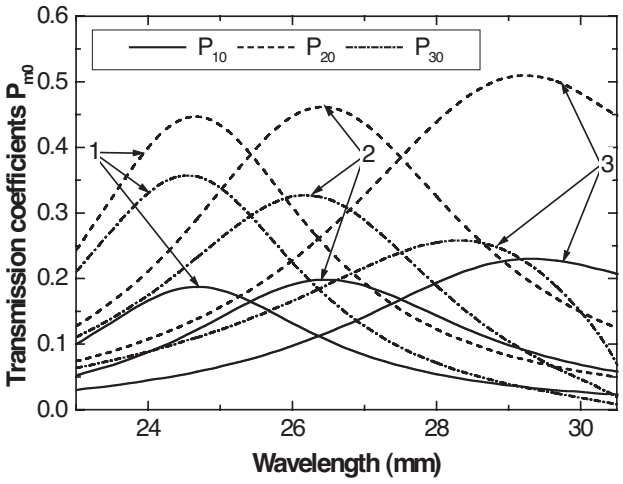

(a)

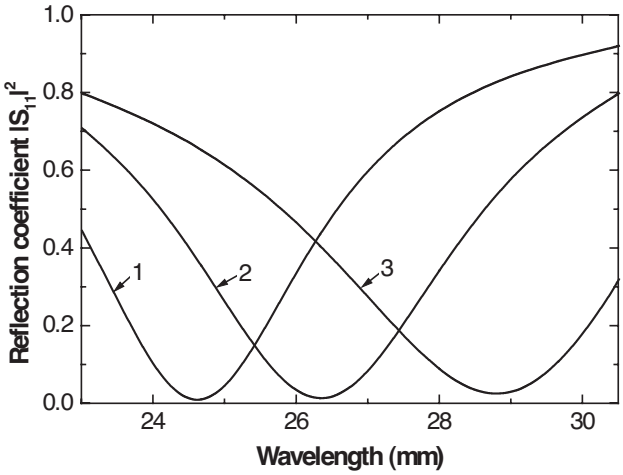

(b)

Figure 40. The coefficients of the scattering matrix dependence from the wavelength for an asymmetrical H-plane waveguide coupling at: $a_{in} = 23.0\,\text{mm}$, $a_{ext} = 46.0\,\text{mm}$, $b_{in} = b_{ext} = 10.0\,\text{mm}$, $d = 1.5\,\text{mm}$, $2L = 12.0\,\text{mm}$, $x_{0in} = a_{in}/2$, $x_{0ext} = a_{ext}/6$, $y_{0in} = b_{in}/4$, $y_{0ext} = b_{ext}/4$.

6. CONCLUSION

Impetuous development of technical opportunities of PC for the last twenty years and a powerful set of numerical methods available in arsenal of investigators somehow forced out the working-outs connected with search of analytical solutions of radiophysical problems backward. However, at present the fact is left evident, that optimal use of computer calculations should be based on application of analytical methods of boundary problems solution. These methods allow to increase PC use efficiency and also expand their calculation abilities to solve complex electrodynamic problems. Hence the results in the development of analytical methods to solve the problems of diffraction of waveguide electromagnetic waves on slot coupling holes, represented in this paper, will be useful for the investigators, interested both in the field of theoretical electrodynamics and in the field of practical working-outs of multi-functional waveguide devices and the systems with slot coupling elements.

APPENDIX A. MAGNETIC DYADIC GREEN'S FUNCTIONS OF THE CONSIDERED ELECTRODYNAMIC VOLUMES

1. Infinite rectangular waveguide with perfectly conducting walls:

$$\begin{aligned}\hat{G}^m(\vec{r},\vec{r}\,') = \frac{2\pi}{ab}\sum_{m,n}\frac{\varepsilon_m\varepsilon_n}{k_z}\Big\{&(\vec{e}_x\otimes\vec{e}_x')\Phi_x^m(x,y;x',y')\,e^{-k_z|z-z'|}\\ &+(\vec{e}_y\otimes\vec{e}_y')\Phi_y^m(x,y;x',y')\,e^{-k_z|z-z'|}\\ &+(\vec{e}_z\otimes\vec{e}_z')\Phi_z^m(x,y;x',y')\,e^{-k_z|z-z'|}\Big\}.\end{aligned} \tag{A1}$$

2. Semi-infinite rectangular waveguide with perfectly conducting walls:

$$\begin{aligned}\hat{G}^m(\vec{r},\vec{r}\,') = \frac{2\pi}{ab}\sum_{m,n}&\frac{\varepsilon_m\varepsilon_n}{k_z}\\ &\times\Big\{(\vec{e}_x\otimes\vec{e}_x')\Phi_x^m(x,y;x',y')\left[e^{-k_z|z-z'|}+e^{-k_z(z+z')}\right]\\ &+(\vec{e}_y\otimes\vec{e}_y')\Phi_y^m(x,y;x',y')\left[e^{-k_z|z-z'|}+e^{-k_z(z+z')}\right]\\ &+(\vec{e}_z\otimes\vec{e}_z')\Phi_z^m(x,y;x',y')\left[e^{-k_z|z-z'|}-e^{-k_z(z+z')}\right]\Big\}.\end{aligned} \tag{A2}$$

3. Rectangular resonator with perfectly conducting walls:

$$\hat{G}^m(\vec{r},\vec{r}\,') = \frac{2\pi}{a_R b_R}\sum_{m,n}\frac{\varepsilon_m\varepsilon_n}{k_z} \times\left\{(\vec{e}_x\otimes\vec{e}\,'_x)\Phi_x^m(x,y;x',y')\left[\frac{chk_z(h-|z-z'|)+chk_z(h-|z+z'|)}{shk_zh}\right] +(\vec{e}_y\otimes\vec{e}\,'_y)\Phi_y^m(x,y;x',y')\left[\frac{chk_z(h-|z-z'|)+chk_z(h-|z+z'|)}{shk_zh}\right] + (\vec{e}_z\otimes\vec{e}\,'_z)\Phi_z^m(x,y;x',y')\left[\frac{chk_z(h-|zv-z'|)-chk_z(h-|z+z'|)}{shk_zh}\right]\right\}. \tag{A3}$$

4. Semi-infinite rectangular waveguide with impedance end in the case where impressed sources are located on the end-wall surface:

$$\hat{G}^M(\vec{r},\vec{r}\,') = \frac{2\pi}{ab}\sum_{m,n}\frac{\varepsilon_m\varepsilon_n}{k_z} \times\left\{(\vec{e}_x\otimes\vec{e}\,'_x)\Phi_x^m(x,y;x',y')f_{\rm II}(k_z,\overline{Z}_s)2e^{-k_zz} +(\vec{e}_y\otimes\vec{e}\,'_y)\Phi_y^m(x,y;x',y')f_{\rm II}(k_z,\overline{Z}_s)2e^{-k_zz}\right\}, \tag{A4}$$

where

$$f_{\rm II}(k_z,\overline{Z}_s) = \frac{kk_z(1+\overline{Z}_s^2)}{(ik+k_z\overline{Z}_s)(k\overline{Z}_s-ik)}.$$

5. Semi-infinite rectangular waveguide with impedance end excited by longitudinal impressed currents:

$$\hat{G}^M(\vec{r},\vec{r}\,') = \frac{2\pi}{ab}\sum_{m,n}\frac{\varepsilon_m\varepsilon_n}{k_z} \times\left\{(\vec{e}_z\otimes\vec{e}\,'_z)\Phi_z^m(x,y;x',y')\begin{bmatrix} e^{-k_z|z-z'|} \\ -f_\perp(k_z,\overline{Z}_s)e^{-k_z(z+z')}\end{bmatrix}\right\}, \tag{A5}$$

where

$$f_\perp(k_z,\overline{Z}_s) = \frac{ik-k_z\overline{Z}_s}{ik+k_z\overline{Z}_s}.$$

The following notations are adopted in the expressions (A1)–(A5):

$$\Phi_x^m(x,y;x',y') = \sin k_xx\sin k_xx'\cos k_yy\cos k_yy',$$
$$\Phi_y^m(x,y;x',y') = \cos k_xx\cos k_xx'\sin k_yy\sin k_yy',$$
$$\Phi_z^m(x,y;x',y') = \cos k_xx\cos k_xx'\cos k_yy\cos k_yy',$$

$$\varepsilon_{m,n} = \begin{cases} 1, m, n = 0 \\ 2, , n \neq 0 \end{cases},$$

$$k_x = \frac{m\pi}{a(a_R)},\ k_y = \frac{n\pi}{b(b_R)},\ k_z = \sqrt{k_x^2 + k_y^2 - k^2},$$

m and n are the integers, $\overline{Z}_s$ is the normalized surface impedance, $\vec{e}_x$, $\vec{e}_y$, and $\vec{e}_z$ are the unit vectors of the Cartesian coordinate system fixed to the waveguide, and "$\otimes$" stands for dyadic product.

APPENDIX B. FUNCTIONS OF THE OWN FIELD OF SINGLE SLOTS

The functions of the slot own field for the case of coupling of two infinite rectangular waveguides are given below:

$$W_t^s(kd, kL) = \frac{8\pi}{ab} \sum_{m,n} \frac{\varepsilon_n e^{-k_z d/4}}{k_z(k^2 - k_x^2)} \sin^2 \frac{m\pi}{2} \times \cos k_x L(k \sin kL \cos k_x L - k_x \cos kL \sin k_x L) \quad \text{(B1)}$$

$$W_t^a(kd, kL) = -\frac{8\pi}{ab} \sum_{m,n} \frac{\varepsilon_n e^{-k_z d/4}}{k_z(k^2 - k_x^2)} \cos^2 \frac{m\pi}{2} \times \sin k_x L(k \cos kL \sin k_x L - k_x \sin kL \cos k_x L) \quad \text{(B2)}$$

$$W_{lb}^s(kd, kL) = \frac{4\pi}{ab} \sum_{m,n} \frac{\varepsilon_m \varepsilon_n \cos k_x x_0 \cos k_x (x_0 + d/4)}{k_z(k_x^2 + k_y^2)} \times e^{-k_z L} [k_z \cos kL sh k_z L + k \sin kL ch k_z L] \quad \text{(B3)}$$

$$W_{lb}^a(kd, kL) = \frac{4\pi}{ab} \sum_{m,n} \frac{\varepsilon_m \varepsilon_n \cos k_x x_0 \cos k_x (x_0 + d/4)}{k_z(k_x^2 + k_y^2)} \times e^{-k_z L} [k_z \sin kL ch k_z L - k \cos kL sh k_z L] \quad \text{(B4)}$$

$$W_{ln}^s(kd, kL) = \frac{4\pi}{ab} \sum_{m,n} \frac{\varepsilon_m \varepsilon_n \cos k_y y_0 \cos k_y (y_0 + d/4)}{k_z \left(k_x^2 + k_y^2\right)} \times e^{-k_z L} [k_z \cos kL sh k_z L + k \sin kL ch k_z L] \quad \text{(B5)}$$

$$W_{ln}^a(kd, kL) = \frac{4\pi}{ab} \sum_{m,n} \frac{\varepsilon_m \varepsilon_n \cos k_y y_0 \cos k_y (y_0 + d/4)}{k_z(k_x^2 + k_y^2)} \times e^{-k_z L} [k_z \sin kL ch k_z L - k \cos kL sh k_z L] \quad \text{(B6)}$$

In the (B1)–(B6) expressions there are the following symbols: $k_x = \frac{m\pi}{a}$, $k_y = \frac{n\pi}{b}$, $k_z = \sqrt{k_x^2 + k_y^2 - k^2}$, $(m, n = 0, 1, 2\dots)$; $\varepsilon_{m,n} = 1$ at $m, n = 0$, $\varepsilon_{m,n} = 2$ at $m, n \neq 0$; x_0 and y_0 are the slots axes coordinates.

The functions of the slot own field for the case of resonant iris with the slot arbitrary oriented in a rectangular waveguide are given below:

$$
\begin{aligned}
W_0(kd_e, 2kL) &= \frac{4\pi}{ab}\sum_{m=0}^{\infty}\sum_{n=0}^{\infty}\frac{\varepsilon_m\varepsilon_n}{k_z}\\
&\times\langle\cos^2\varphi\{\sin kL[\Phi_s(k_x x_0)\Phi_c(k_y y_0)(\cos k_1 L + \cos k_2 L)I_1^+(k_{1,2}L)\\
&+\Phi_c(k_x x_0)\Phi_s(k_y y_0)(\cos k_1 L - \cos k_2 L)I_1^-(k_{1,2}L)]\\
&+\frac{1}{2}\cos kL\sin 2k_x x_0[\Phi_s(k_y y_0)(\cos k_1 L - \cos k_2 L)I_2^-(k_{1,2}L)\\
&-\Phi_c(k_y y_0)(\cos k_1 L + \cos k_2 L)I_2^+(k_{1,2}L)]\\
&+\frac{1}{2}\cos kL\sin 2k_y y_0[\Phi_s(k_x x_0)(\cos k_1 L + \cos k_2 L)I_2^-(k_{1,2}L)\\
&-\Phi_c(k_x x_0)(\cos k_1 L - \cos k_2 L)I_2^+(k_{1,2}L)]\}\\
&+\sin^2\varphi\{\sin kL[\Phi_s(k_x x_0)\Phi_c(k_y y_0)(\cos k_1 L - \cos k_2 L)I_1^-(k_{1,2}L)\\
&+\Phi_c(k_x x_0)\Phi_s(k_y y_0)(\cos k_1 L + \cos k_2 L)I_1^+(k_{1,2}L)]\\
&+\frac{1}{2}\cos kL\sin 2k_x x_0[\Phi_s(k_y y_0)(\cos k_1 L + \cos k_2 L)I_2^+(k_{1,2}L)\\
&-\Phi_c(k_y y_0)(\cos k_1 L - \cos k_2 L)I_2^-(k_{1,2}L)]\\
&+\frac{1}{2}\cos kL\sin 2k_y y_0[\Phi_s(k_x x_0)(\cos k_1 L - \cos k_2 L)I_2^+(k_{1,2}L)\\
&-\Phi_c(k_x x_0)(\cos k_1 L + \cos k_2 L)I_2^-(k_{1,2}L)]\}\\
&+\frac{1}{2}\sin kL\sin 2k_x x_0\sin 2k_y y_0[\cos k_1 L I_1(k_1 L) - \cos k_2 L I_1(k_2 L)]\rangle, \qquad \text{(B7)}
\end{aligned}
$$

$$
\begin{aligned}
W_\varphi(kd_e, kL) &= \frac{2\pi}{ab}\sum_{m=0}^{\infty}\sum_{n=0}^{\infty}\frac{\varepsilon_m\varepsilon_n}{k_z}\\
&\times\{[\Phi_s(k_x x_0)\Phi_c(k_y y_0)[(\cos k_1 L + \cos 2\varphi\cos k_2 L)I_1(k_1 L)\\
&+(\cos k_2 L + \cos 2\varphi\cos k_1 L)I_1(k_2 L)]\\
&-\Phi_c(k_x x_0)\Phi_s(k_y y_0)[(\cos k_1 L - \cos 2\varphi\cos k_2 L)I_1(k_1 L)\\
&+(\cos k_2 L - \cos 2\varphi\cos k_1 L)I_1(k_2 L)]\}, \qquad \text{(B8)}
\end{aligned}
$$

$$W(kd_e, kL) = \frac{16\pi}{ab} \sum_{m=1,3\ldots}^{\infty} \sum_{n=0}^{\infty} \frac{\varepsilon_n}{k_z} \cos k_y y_0 \cos k_y \left(y_0 + \frac{d_e}{4} \right) \cos k_x L \times \left[\frac{k \sin kL \cos k_x L - k_x \cos kL \sin k_x L}{k^2 - k_x^2} \right]. \quad \text{(B9)}$$

In the (B7)–(B9) expressions there are the following symbols:

$$I_1(k_{1,2}L) = \frac{k \sin kL \cos k_{1,2}L - k_{1,2} \cos kL \sin k_{1,2}L}{k^2 - k_{1,2}^2},$$
$$I_2(k_{1,2}L) = \frac{k_{1,2} \sin kL \cos k_{1,2}L - k \cos kL \sin k_{1,2}L}{k^2 - k_{1,2}^2},$$

$$\Phi_s(k_x x_0) = \sin(k_x x_0^{\varphi}) \sin(k_x x_0),\ \Phi_c(k_x x_0) = \cos(k_x x_0^{\varphi}) \cos(k_x x_0),$$
$$\Phi_s(k_y y_0) = \sin(k_y y_0^{\varphi}) \sin(k_y y_0),\ \Phi_c\ (k_y y_0) = \cos(k_y y_0^{\varphi}) \cos(k_y y_0),$$

$$k_{1,2} = k_x \cos\varphi \pm k_y \sin\varphi, \quad x_0^{\varphi} = x_0 - \frac{d_e}{4} \sin\varphi, \quad y_0^{\varphi} = y_0 + \frac{d_e}{4} \cos\varphi,$$

$$I_{1,2}^{\pm}(k_{1,2}L) = I_{1,2}(k_1 L) \pm I_{1,2}(k_2 L).$$

The rest symbols are the same as in the (B1)–(B6) formulas.

APPENDIX C. EIGEN AND MUTUAL SLOT ADMITTANCES

The eigen longitudinal slots admittances:

$$Y^s(kd, kL) = \frac{2\pi}{ab} \sum_{m=0}^{\infty} \sum_{n=0}^{\infty} \frac{\varepsilon_m \varepsilon_n}{k} \cos k_x x_0 \cos k_x \left(x_0 + \frac{d}{4} \right) \times \left\{ \left[\cos\gamma L \left(\frac{k}{k_z} \sin kL - \cos kL \right) \right] F^s(k_z L) - \frac{\cos kL}{k_z^2 + \gamma^2} \left[(k_z^2 + k^2) \left(\frac{\gamma}{k_z} \sin\gamma L - \cos\gamma L \right) F^s(k_z L) + \left(\frac{\pi}{a} \right)^2 F^s(kL) \right] \right\}, \quad \text{(C1)}$$

$$F^s(kL) = 2\cos\gamma L \frac{k \sin kL \cos\gamma L - \gamma \cos kL \sin\gamma L}{(\pi/a)^2} - \cos kL \frac{\sin 2\gamma L + 2\gamma L}{2\gamma}, \quad \text{(C2)}$$

$$F^s(k_zL)=\frac{\cos\gamma L}{k_z^2+k^2}\left[k_z\cos kL\left(1-e^{-2k_zL}\right)+k\sin kL\left(1+e^{-2k_zL}\right)\right]$$
$$-\frac{\cos kL}{k_z^2+\gamma^2}\left[k_z\cos\gamma L\left(1-e^{-2k_zL}\right)+\gamma\sin\gamma L\left(1+e^{-2k_zL}\right)\right]. \quad \text{(C3)}$$

$$Y^a(kd,kL)=\frac{2\pi}{ab}\sum_{m=0}^{\infty}\sum_{n=0}^{\infty}\frac{\varepsilon_m\varepsilon_n}{k}\cos k_xx_0\cos k_x\left(x_0+\frac{d}{4}\right)$$
$$\times\left\{\left[-\sin\gamma L\left(\frac{k}{k_z}\cos kL+\sin kL\right)\right]F^a(k_zL)+\frac{\sin kL}{k_z^2+\gamma^2}\right.$$
$$\left.\left[(k_z^2+k^2)\left(\frac{\gamma}{k_z}\cos\gamma L+\sin\gamma L\right)F^a(k_zL)+\left(\frac{\pi}{a}\right)^2F^a(kL)\right]\right\}, \quad \text{(C4)}$$

$$F^a(kL) \;=\; 2\sin\gamma L\frac{k\cos kL\sin\gamma L-\gamma\sin kL\cos\gamma L}{(\pi/a)^2}$$
$$-\sin kL\frac{\sin 2\gamma L-2\gamma L}{2\gamma}, \quad \text{(C5)}$$

$$F^a(k_zL)=\frac{\sin k_gL}{k_z^2+k^2}\left[k_z\sin kL\left(1+e^{-2k_zL}\right)-k\cos kL\left(1-e^{-2k_zL}\right)\right]$$
$$-\frac{\sin kL}{k_z^2+\gamma^2}\left[k_z\sin\gamma L\left(1+e^{-2k_zL}\right)-\gamma\cos\gamma L\left(1-e^{-2k_zL}\right)\right] \quad \text{(C6)}$$

The mutual longitudinal slots admittances:

$$Y^{ss}_{\left\{\begin{smallmatrix}12\\21\end{smallmatrix}\right\}}(kL_m,kL_n)=$$
$$\frac{2\pi}{ab}\sum_{m=0}^{\infty}\sum_{n=0}^{\infty}\frac{\varepsilon_m\varepsilon_n}{kk_z}chk_zz_0\cos k_xx_{0m}\cos k_x\left(x_{0n}+\frac{d_n}{4}\right)$$
$$\times\{\cos\gamma L_n(k\sin kL_n-k_z\cos kL_n)F^s(k_zL_m)$$
$$-\frac{\cos kL_n}{k_z^2+\gamma^2}[k_zk_c^2F^s(kL_m)\left\{\begin{array}{c}1\\ \frac{\cos\gamma z_0}{chk_zz_0}\end{array}\right\}$$
$$+(k_z^2+k^2)(\gamma\sin\gamma L_n-k_z\cos\gamma L_n)F^s(k_zL_m)]\}, \quad \text{(C7)}$$

$$Y^{as}_{\left\{\begin{smallmatrix}12\\21\end{smallmatrix}\right\}}(kL_m, kL_n) =$$

$$\frac{2\pi}{ab}\sum_{m=0}^{\infty}\sum_{n=0}^{\infty}\frac{\varepsilon_m\varepsilon_n}{kk_z}shk_z z_0\cos k_x x_{0m}\cos k_x\left(x_{0n}+\frac{d_n}{4}\right)$$
$$\times\{\mp\cos\gamma L_n(k\sin kL_n - k_z\cos kL_n)F^a(k_zL_m)$$
$$+\frac{\cos kL_n}{k_z^2+\gamma^2}[k_zk_c^2F^a(kL_m)\left\{\begin{array}{c}\gamma/k_z\\ -\frac{\sin\gamma z_0}{shk_z z_0}\end{array}\right\}$$
$$\pm(k_z^2+k^2)(\gamma\sin\gamma L_n - k_z\cos\gamma L_n)F^a(k_zL_m)]\}, \tag{C8}$$

$$Y^{aa}_{\left\{\begin{smallmatrix}12\\21\end{smallmatrix}\right\}}(kL_m, kL_n) =$$

$$\frac{2\pi}{ab}\sum_{m=0}^{\infty}\sum_{n=0}^{\infty}\frac{\varepsilon_m\varepsilon_n}{kk_z}chk_z z_0\cos k_x x_{0m}\cos k_x\left(x_{0n}+\frac{d_n}{4}\right)$$
$$\times\{-\sin\gamma L_n(k\cos kL_n + k_z\sin kL_n)F^a(k_zL_m)$$
$$+\frac{\sin kL_n}{k_z^2+\gamma^2}[k_zk_c^2F^a(kL_m)\left\{\begin{array}{c}1\\ \frac{\cos\gamma z_0}{chk_z z_0}\end{array}\right\}$$
$$+(k_z^2+k^2)(\gamma\cos\gamma L_n + k_z\sin\gamma L_n)F^a(k_zL_m)]\}, \tag{C9}$$

$$Y^{sa}_{\left\{\begin{smallmatrix}12\\21\end{smallmatrix}\right\}}(kL_m, kL_n) =$$

$$\frac{2\pi}{ab}\sum_{m=0}^{\infty}\sum_{n=0}^{\infty}\frac{\varepsilon_m\varepsilon_n}{kk_z}shk_z z_0\cos k_x x_{0m}\cos k_x\left(x_{0n}+\frac{d_n}{4}\right)$$
$$\times\{\pm\sin\gamma L_n(k\cos kL_n + k_z\sin kL_n)F^s(k_zL_m)$$
$$-\frac{\sin kL_n}{k_z^2+\gamma^2}[k_zk_c^2F^s(kL_m)\left\{\begin{array}{c}-\gamma/k_z\\ \frac{\sin\gamma z_0}{shk_z z_0}\end{array}\right\}$$
$$\pm(k_z^2+k^2)(\gamma\cos\gamma L_n + k_z\sin\gamma L_n)F^s(k_zL_m)]\}, \tag{C10}$$

$$Y^s_{mn}(kL) = \frac{2\pi}{ab}\sum_{m=0}^{\infty}\sum_{n=0}^{\infty}\frac{\varepsilon_m\varepsilon_n}{kk_z}\cos k_x x_{0m}\cos k_x\left(x_{0n}+\frac{d_n}{4}\right)$$
$$\times\{\cos\gamma L(k\sin kL - k_z\cos kL)F^s(k_zL) - \frac{\cos kL}{k_z^2+\gamma^2}$$
$$[(k_z/k)k_c^2f^s(kL)+(k_z^2+k^2)(\gamma\sin\gamma L - k_z\cos\gamma L)F^s(k_zL)]\}, \tag{C11}$$

$$Y^a_{mn}(kL) = \frac{2\pi}{ab}\sum_{m=0}^{\infty}\sum_{n=0}^{\infty}\frac{\varepsilon_m\varepsilon_n}{kk_z}\cos k_x x_{0m}\cos k_x\left(x_{0n}+\frac{d_n}{4}\right)$$
$$\times\{-\sin\gamma L(k\cos kL + k_z\sin kL)F^a(k_zL)$$
$$+\frac{\sin kL}{k_z^2+\gamma^2}[(k_z/k)k_c^2 f^a(kL)$$
$$-(k_z^2+k^2)(\gamma\cos\gamma L + k_z\sin\gamma L)F^a(k_zL)]\}, \quad \text{(C12)}$$

$$f^s(kL_m) = 2\cos\gamma L_m\frac{\sin kL_m\cos\gamma L_m - (\gamma/k)\cos kL_m\sin\gamma L_m}{1-(\gamma/k)^2}$$
$$-\cos kL_m\frac{\sin 2\gamma L_m + 2\gamma L_m}{2(\gamma/k)}, \quad \text{(C13)}$$

$$f^a(kL_m) = 2\sin\gamma L_m\frac{\cos kL_m\sin\gamma L_m - (\gamma/k)\sin kL_m\cos\gamma L_m}{1-(\gamma/k)^2}$$
$$-\sin kL_m\frac{\sin 2\gamma L_m - 2\gamma L_m}{2(\gamma/k)}. \quad \text{(C14)}$$

The eigen ($m = n$) and mutual ($m \neq n$) slot admittances of the transverse slots system:

$$Y^{Wg}_{mm}(kL_m, kL_m) = \frac{2\pi}{ab}\sum_{m=1,3\ldots}^{\infty}\sum_{n=0}^{\infty}\frac{\varepsilon_n(k^2-k_x^2)}{kk_z}e^{-k_z\frac{d_m}{4}}I^2_{Wg}(kL_m), \quad \text{(C15)}$$

$$Y^{Wg}_{mn}(kL_m, kL_n) =$$
$$\frac{2\pi}{ab}\sum_{m=1,3\ldots}^{\infty}\sum_{n=0}^{\infty}\frac{\varepsilon_n(k^2-k_x^2)}{kk_z}e^{-k_z|z_m-z_n|}I_{Wg}(kL_m)I_{Wg}(kL_n), \quad \text{(C16)}$$

$$Y^R_{\left\{\begin{smallmatrix}mm\\mn\end{smallmatrix}\right\}}(kL_m) = \frac{2\pi}{L_m d_m}\sum_{m=1,3\ldots}^{\infty}\sum_{n=0}^{\infty}\frac{\varepsilon_n(k^2-k_{xR}^2)}{kk_{zR}}\left\{\begin{smallmatrix}\coth(k_{zR}h)\\1/\mathrm{sh}(k_{zR}h)\end{smallmatrix}\right\}$$
$$\times\cos\frac{n\pi}{2}\cos\left(k_{yR}\frac{3d_m}{4}\right)I_R^2(kL_m), \quad \text{(C17)}$$

$$I_{Wg(R)}(kL_m) =$$
$$2\left\{\frac{k\sin kL_m\cos k_{x(xR)}L_m - k_{x(xR)}\cos kL_m\sin k_{x(xR)}L_m}{k^2-k^2_{x(xR)}}\cos k_cL_m\right.$$
$$\left.-\frac{k_c\sin k_cL_m\cos k_{x(xR)}L_m - k_{x(xR)}\cos k_cL_m\sin k_{x(xR)}L_m}{k_c^2-k^2_{x(xR)}}\cos kL_m\right\}. \quad \text{(C18)}$$

In the (C1)–(C18) expressions are the following symbols: $k_{xR} = \frac{m\pi}{2L_m}$, $k_{yR} = \frac{n\pi}{d_m}$, $k_{zR} = \sqrt{k_{xR}^2 + k_{yR}^2 - k^2}$. The rest symbols are the same as in the (B1)–(B6) formulas.

The slot admittances for the case of impedance slotted iris:

$$Y^{in,ext}(kL, \overline{Z}_s^{in,ext}) = \frac{4\pi}{a_{in,ext} b_{in,ext}} \times \sum_{m=1}^{\infty} \sum_{n=0}^{\infty} \frac{\varepsilon_n (k^2 - k_{x_{in,ext}}^2)}{k k_{z_{in,ext}}} \sin^2(k_{x_{in,ext}} x_{0in,ext}) \times \cos(k_{y_{in,ext}} y_{0in,ext}) \cos\left(k_{y_{in,ext}} (y_{0in,ext} + \frac{d_e}{4})\right) F(k_{z_{in,ext}} \overline{Z}_s^{in,ext}) \times \left[I_{in,ext}(kL) \cos\frac{\pi L}{a_{in}} - I_{in,ext}\left(\frac{\pi L}{a_{in}}\right) \cos kL \right]^2, \quad \text{(C19)}$$

$$F(k_{z_{in,ext}}, \overline{Z}_s^{in,ext}) = \frac{k k_{z_{in,ext}} (1 + (\overline{Z}_s^{in,ext})^2)}{(ik + k_{z_{in,ext}} \overline{Z}_s^{in,ext})(k \overline{Z}_s^{in,ext} - i k_{z_{in,ext}})} \times \left(1 - i \frac{k k_{z_{in,ext}} \overline{Z}_s^{in,ext}}{k^2 - k_{x_{in,ext}}^2}\right), \quad \text{(C20)}$$

$$I_{in,ext}(kL) = 2 \frac{k \sin kL \cos k_{x_{in,ext}} L - k_{x_{in,ext}} \cos kL \sin k_{x_{in,ext}} L}{k^2 - k_{x_{in,ext}}^2}, \quad \text{(C21)}$$

$$I_{in,ext}\left(\frac{\pi L}{a_{in}}\right) = 2 \frac{\frac{\pi}{a_{in}} \sin\frac{\pi L}{a_{in}} \cos k_{x_{in,ext}} L - k_{x_{in,ext}} \cos\frac{\pi L}{a_{in}} \sin k_{x_{in,ext}} L}{(\pi/a_{in})^2 - k_{x_{in,ext}}^2}. \quad \text{(C22)}$$

In the (C19)–(C22) expressions there are the following symbols: $k_{x_{in,ext}} = \frac{m\pi}{a_{in,ext}}$, $k_{y_{in,ext}} = \frac{n\pi}{b_{in,ext}}$, $k_{z_{in,ext}} = \sqrt{k_x^2 + k_y^2 - k^2}$, $(m, n = 0, 1, 2 \ldots)$; $\varepsilon_n = 1$ at $n = 0$, $\varepsilon_n = 2$ at $n \neq 0$; $x_{0in,ext}$ and $y_{0in,ext}$ are the slots axes coordinates.

APPENDIX D. SERIES SUMMING UP IN THE FUNCTION OF THE IRIS OWN FIELD

The real part of the own field function $W\left(\frac{\pi d_e}{2L}, \frac{\pi}{2}\right)$of the slot has the form:

$$\mathrm{Re}W\left(\frac{\pi d_e}{2L}, \frac{\pi}{2}\right) = \frac{4\pi^2}{abL}\left\{\sum_{m=3,5\ldots}^{\infty} \frac{1+\cos 2k_x L}{k_z^{m0}[(\pi/(2L))^2 - k_x^2]}\right.$$
$$+\frac{2\cos^2(\pi L/a)}{\gamma_{10}^2}\sum_{n=1}^{\infty}\frac{\cos(k_y d_e/4)+\cos 2k_y y_0}{\sqrt{k_y^2-\gamma_{10}^2}}$$
$$\left.+\sum_{m=3,5\ldots}^{\infty}\frac{1+\cos 2k_x L}{(\pi/(2L))^2-k_x^2}\sum_{n=1}^{\infty}\frac{\cos(k_y d_e/4)+\cos 2k_y y_0}{k_z^{mn}}\right\}. \quad \text{(D1)}$$

The following symbols are accepted in (D1): $k_z^{m0} = \sqrt{k_x^2-(\pi/(2L))^2}$; $k_z^{mn} = \sqrt{k_x^2+k_y^2-(\pi/(2L))^2}$; $\gamma_{10}^2 = (\pi/(2L))^2 - (\pi/a)^2$; $k_x = m\pi/a$; $k_y = n\pi/b$.

The second series over n in (D1) can be summed up with the help of the relation reduced in [39]:

$$\sum_{n=1}^{\infty}\frac{\cos(k_y d_e/4)+\cos 2k_y y_0}{k_z^{mn}} \cong -\frac{1}{k_z^{m0}}$$
$$+\frac{b}{\pi}\left[K_0(k_z^{m0}\frac{d_e}{4}) + K_0(2k_z^{m0}y_0)\right], \quad \text{(D2)}$$

where $K_0(x)$ is the McDonald's function. Then (D1) grades into the expression which does not contain double series:

$$\mathrm{Re}W\left(\frac{\pi d_e}{2L}, \frac{\pi}{2}\right) \cong \frac{4\pi^2}{abL}\left\{\frac{2\cos^2(\pi L/a)}{\gamma_{10}^2}\sum_{n=1}^{\infty}\frac{\cos\frac{n\pi d_e}{4b}+\cos\frac{2n\pi y_0}{b}}{\sqrt{(n\pi/b)^2-\gamma_{10}^2}}\right.$$
$$\left.-\frac{b}{\pi}\left[\begin{array}{c}\frac{2\cos^2\frac{3\pi L}{a}}{k_{30}^2}\left[K_0\left(k_{30}\frac{d_e}{4}\right)+K_0\left(2k_{30}y_0\right)\right]\\ +\left(\frac{a}{\pi}\right)^2\sum\limits_{m=5}^{\infty}[1-(-1)^m]\frac{1+\cos\frac{2m\pi L}{a}}{m^2}K_0\left(\frac{m\pi d_e}{4a}\right)\end{array}\right]\right\}. \quad \text{(D3)}$$

The term series (D3) is separated out in the explicit form ($k_{30} = \sqrt{(3\pi/a)^2-(\pi/(2L))^2}$) at $m = 3$ in (D3), and in the rest sum along m we take into account, that while increases, the $K_0(x)$ function decreases rapidly.

Let us sum up the first series in (D3), expanded the square root into series $\left(\sqrt{(n\pi/b)^2-\gamma_{10}^2}\right)^{-1} \approx \frac{b}{\pi}\left[\frac{1}{n}+\left(\frac{\gamma_{10}b}{\sqrt{2}\pi}\right)^2\frac{1}{n^3}\right]$ and using the formula 1.441.2 from [43]: $\sum\limits_{n=1}^{\infty}\frac{\cos nx}{n} = -\ln\left(2\sin\frac{x}{2}\right)$, valid under condition of $0<x<2\pi$, and which in our case ($x=\frac{\pi d_e}{4b}$, $x=\frac{2\pi y_0}{b}$) is performed. As the result after some transformations we get:

$$\sum_{n=1}^{\infty}\frac{\cos n\frac{\pi d_e}{4b}+\cos n\frac{2\pi y_0}{b}}{\sqrt{(n\pi/b)^2-\gamma_{10}^2}} \cong \frac{2\cos^2\frac{\pi y_0}{b}}{k_{11}} - \frac{b}{\pi}\left[2\cos^2\frac{\pi y_0}{b}-\left(\frac{\gamma_{10}b}{9}\right)^2\cos^2\frac{2\pi y_0}{b}+\ln\left(\frac{\pi d_e}{2b}\sin\frac{\pi y_0}{b}\right)\right], \quad \text{(D4)}$$

where $k_{11}=\sqrt{(\pi/a)^2+(\pi/b)^2-(\pi/(2L))^2}$.

We can sum up the rest series along m in (D3) with the help of the expressions 8.526.1,2 from [43]:

$$\sum_{m=1}^{\infty}\left[1-(-1)^m\right]K_0(mx)\cos mxt \cong \frac{\pi}{2x\sqrt{1+t^2}} + \frac{1}{2}\left[\frac{1}{1-(xt/(2\pi))^2}-\frac{2}{1-(xt/\pi)^2}-\frac{2/3}{1-(xt/(3\pi))^2}+\frac{1}{2}\right], \quad \text{(D5)}$$

which are valid while performing the following conditions: $x>0$, $\{x/\pi\} \ll 1$, $\{xt/\pi\}<1$ (here and further x and t — are non-dimensional parameters, m is the integers). Making double integration along t in (D5), we have:

$$\begin{aligned}\sum_{m=1}^{\infty}&\left[1-(-1)^m\right]K_0(mx)\frac{1+\cos mxt}{m^2}\\ &\cong -\frac{\pi x}{2}\left\{t\ln(t+\sqrt{1+t^2})-\sqrt{1+t^2}+1+t\ln\frac{\pi-xt}{\pi+xt}\right.\\ &-\frac{\pi}{x}\ln\left[1-\left(\frac{xt}{\pi}\right)^2\right]-t\ln\frac{2\pi-xt}{2\pi+xt}+\frac{2\pi}{x}\ln\left[1-\left(\frac{xt}{2\pi}\right)^2\right]+t\ln\frac{3\pi-xt}{3\pi+xt}\\ &\left.-\frac{3\pi}{x}\ln\left[1-\left(\frac{xt}{3\pi}\right)^2\right]+\frac{xt^2}{4\pi}\right\}+2\sum_{m=1}^{\infty}\left[1-(-1)^m\frac{K_0(mx)}{m^2}.\end{aligned} \quad \text{(D6)}$$

Then substituting the values $x=\frac{\pi d_e}{4a}$ ($\{d_e/(4a)\} \ll 1$), $t=\frac{8L}{d}$, $xt=\frac{2\pi L}{a}$ ($\{2L/a\}<1$) in (D6), we get:

$$\sum_{m=5}^{\infty}[1-(-1)^m]\frac{1+\cos m\frac{2\pi L}{a}}{m^2}K_0\left(m\frac{\pi d_e}{4a}\right)$$
$$\cong\frac{\pi^2 L}{a}\left(1-\ln\frac{16L}{d_e}+\ln\frac{1-L/a}{1+L/a}-\ln\frac{1-2L/a}{1+2L/a}-\ln\frac{1-2L/(3a)}{1+2L/(3a)}\right)$$
$$+\frac{\pi^2}{2}\left\{\ln\left[1-\left(\frac{2L}{a}\right)^2\right]-2\ln\left[1-\left(\frac{L}{a}\right)^2\right]+3\ln\left[1-\left(\frac{2L}{3a}\right)^2\right]-\left(\frac{L}{a}\right)^2\right\}$$
$$+4\left[K_0\left(\frac{\pi d_e}{4a}\right)\sin^2\frac{\pi L}{a}+\frac{1}{9}K_0\left(\frac{3\pi d_e}{4a}\right)\sin^2\frac{3\pi L}{a}\right.$$
$$\left.+\sum_{m=5,7\ldots}^{\infty}K_0\left(m\frac{\pi d_e}{4a}\right)\Big/m^2\right]. \qquad \text{(D7)}$$

The expressions (D4) and (D7) give the final formula (99) after substitution in (D3).

REFERENCES

1. Bethe, H. A., "Theory of diffraction by small holes," *Phys. Rev.*, Vol. 66, 163–182, 1944.
2. Stevenson, A. F., "Theory of slots in rectangular wave-guides," *J. Appl. Phys.*, Vol. 19, 24–38, 1948.
3. Lewin, L., "Some observations on waveguide coupling through medium sized slots," *Proc. Inst. Elec. Eng.*, Vol. 107C, 171–178, 1960.
4. Sangster, A. J., "Variational method for the analysis of waveguide coupling," *Proc. Inst. Elec. Eng.*, Vol. 112, 2171–2179, 1965.
5. Levinson, I. B. and P. S. Fredberg, "Slot couplers of rectangular one mode waveguide equivalent circuits and lumped parameters," *Radio Eng. and Electron. Phys.*, Vol. 11, 717–724, 1966.
6. Khac, T. V., "Solutions for some waveguide discontinuities by the method of moments," *IEEE Trans. Microwave Theory and Tech.*, Vol. MTT-20, 416–418, 1972.
7. Rengarajan, S. R., "Analysis of a centered-inclined waveguide slot coupler," *IEEE Trans. Microwave Theory and Tech.*, Vol. MTT-37, 884–889, 1989.
8. Das, B. N., A. Chakraborty, and N. V. S. Narasimha Sarma, "S matrix of slot-coupled H-plane Tee junction using rectangular waveguides," *IEEE Trans. Microwave Theory and Tech.*, Vol. MTT-38, 779–781, 1990.

9. Yang, D., C. Liao, and W. Chen, "Numerical solution on coupling of UWB pulse into a rectangular cavity through slots," *Journal of Electromagnetic Waves and Applications*, Vol. 19, 1629–1638, 2005.
10. Das, S. and A. Chakrabarty, "A novel modeling technique to solve a class of rectangular waveguide based circuits and radiators," *Progress In Electromagnetics Research*, PIER 61, 231–252, 2006.
11. Das, S., A. Chakrabarty, and A. Chakraborty, "Characteristics of an offset longitudinal/transverse slot coupled crossed waveguide junction using multiple cavity modeling technique considering the TE_{00} mode at the slot aperture," *Progress In Electromagnetics Research*, PIER 67, 297–316, 2007.
12. Pandharipande, V. M. and B. N. Das, "Coupling of waveguides through large apertures," *IEEE Trans. Microwave Theory and Tech.*, Vol. MTT-26, 209–212, 1978.
13. Pandharipande, V. M. and B. N. Das, "Equivalent circuit of a narrow-wall waveguide slot coupler," *IEEE Trans. Microwave Theory and Tech.*, Vol. MTT-27, 800–804, 1979.
14. Sangster, A. J. and H. Wang, "A hybrid analytical technique for radiating slots in waveguide," *Journal of Electromagnetic Waves and Applications*, Vol. 9, 735–755, 1995.
15. Katrich, V. A., M. V. Nesterenko, and N. A. Khizhnyak, "Asymptotic solution of integral equation for magnetic current in slot radiators and coupling apertures," *Telecommunications and Radio Engineering*, Vol. 63, 89–107, 2005.
16. Khizhnyak, N. A., *Integral Equations of Macroscopical Electrodynamics*, Naukova dumka, Kiev, 1986 (in Russian).
17. Butler, C. M. and K. R. Umashankar, "Electromagnetic excitation of a wire through an aperture-perforated conducting screen," *IEEE Trans. Antennas and Propagat.*, Vol. AP-24, 456–462, 1976.
18. King, R. W. P., *The Theory of Linear Antennas*, Harv. Univ. Press, Cambr., MA, 1956.
19. Naiheng, Y. and R. Harrington, "Electromagnetic coupling to an infinite wire through a slot in a conducting plane," *IEEE Trans. Antennas and Propagat.*, Vol. AP-31, 310–316, 1983.
20. Bogolubov, N. N. and U. A. Mitropolsky, *Asymptotic Methods in the Theory Nonlinear Fluctuations*, Nauka, Moskow, 1974 (in Russian).
21. Philatov, A. N., *Asymptotic Methods in the Theory of Differential and Integral-differential Equations*, PHAN, Tashkent, 1974 (in Russian).

22. Garb, H. L., I. B. Levinson, and P. S. Fredberg, "Effect of wall thickness in slot problems of electrodynamics," *Radio Eng. Electron. Phys.*, Vol. 13, 1888–1896, 1968.
23. Warne, L. K., "Eddy current power dissipation at sharp corners: closely spaced rectangular conductors," *Journal of Electromagnetic Waves and Applications*, Vol. 9, 1441–1458, 1995.
24. Khac, T. V. and C. T. Carson, "Coupling by slots in rectangular waveguides with arbitrary wall thickness," *Electronics Letters*, Vol. 8, 456–458, 1972.
25. Nesterenko, M. V. and V. A. Katrich, "The method of induced magnetomotive forces for cavity-backed slot radiators and coupling slots," *Radioelectronics and Communications Systems*, Vol. 47, No. 1, 8–13, 2004.
26. Berdnik, S. L., V. A. Katrich, V. I. Kiiko, and M. V. Nesterenko, "Electrodynamic characteristics of the nonresonant system of transverse slots in the wide wall of rectangular waveguide," *Radioelectronics and Communications Systems*, Vol. 48, No. 1, 52–57, 2005.
27. Nesterenko, M. V. and V. A. Katrich, "The asymptotic solution of an integral equation for magnetic current in a problem of waveguides coupling through narrow slots," *Progress In Electromagnetics Research,* PIER 57, 101–129, 2006.
28. Whetten, F. L. and C. A. Balanis, "Meandering long slot leaky-wave waveguide antennas," *IEEE Trans. Antennas and Propagat.*, Vol. AP-39, 1553–1560, 1991.
29. Josefsson, L. G., "Analysis of longitudinal slots in rectangular waveguides," *IEEE Trans. Antennas and Propagat.*, Vol. AP-35, 1351–1357, 1987.
30. Katrich, V. A., V. A. Lyashchenko, and S. L. Berdnik, "Electrically long waveguide-slot antennas with optimal radiation and directivity characteristics," *Radioelectronics and Communications Systems*, Vol. 46, No. 2, 36–42, 2003.
31. Jia, H., K. Yoshitomi, and K. Yasumoto, "Rigorous and fast convergent analysis of a rectangular waveguide coupler slotted in common wall," *Progress In Electromagnetics Research*, PIER 46, 245–264, 2004.
32. Mittra, R. (ed.), *Computer Techniques for Electromagnetics*, Pergamon Press, Oxford-NY, 1973.
33. Katrich, V. A. and M. V. Nesterenko, "The near-zone field and resonant frequencies of narrow longitudinal slots in the broad face of a rectangular waveguide," *Telecommunications and Radio*

Engineering, Vol. 60, Nos. 1&2, 125–131, 2003.

34. Southworth, G. C., *Principles and Applications of Waveguide Transmission*, NY, 1950.
35. Chen, T. S., "Waveguide resonant-iris filters with very wide passband and stopbands," *Int. J. Electronics*, Vol. 21, No. 5, 401–424, 1966.
36. Bornemann, J. and R. Vahldieck, "Characterization of a class of waveguide discontinuities using a modified TE^x_{mn} mode approach," *IEEE Trans. Microwave Theory and Tech.*, Vol. MTT-38, 1816–1822, 1990.
37. Patzelt, H. and F. Arndt, "Double-plane steps in rectangular waveguides and their application for transformers, irises, and filters," *IEEE Trans. Microwave Theory and Tech.*, Vol. MTT-30, 771–776, 1982.
38. Beyer, R. and F. Arndt, "Efficient modal analysis of waveguide filters including the orthogonal mode coupling elements by an MM/FE method," *IEEE Microwave and Guided Wave Lett.*, Vol. 5, No. 1, 9–11, 1995.
39. Lewin, L., *Advanced Theory of Waveguides*, Iliffe & Sons, London, 1951.
40. Yang, R. and A. S. Omar, "Analysis of this inclined rectangular aperture with arbitrary location in rectangular waveguide," *IEEE Trans. Microwave Theory and Tech.*, Vol. MTT-41, 1461–1463, 1993.
41. Rud, L. A., "Axially rotated step junction of rectangular waveguides and resonant diaphragms based thereupon," *Telecommunications and Radio Engineering*, Vol. 55, No. 9, 17–26, 2001.
42. Mittra, R. and S. W. Lee, *Analytical Techniques in the Theory of Guided Waves*, The Macmillan Company, NY, 1971.
43. Gradshteyn, I. S. and I. M. Ryzhik, *Table of Integrals, Series, and Products*, Academic Press, NY, 1980.
44. Leontovich, M. A., "On the approximate boundary conditions for the electromagnetic field on surfaces of good conductive bodies," *Investigations of Radiowave Propagation*, Printing House of the Academy of Sciences of the USSR, Moscow-Leningrad, 1948 (in Russian).
45. Weinstein, L. A., *The Theory of Diffraction and the Factorization Method*, Golem Press, Boulder, Co., 1969.
46. Penkin, Y. M., "Admittance of slots with coordinate boundaries in a half-infinite rectangular waveguide with impedance endface," *Telecommunications and Radio Engineering*, Vol. 52, No. 9, 22–26,

1998.

47. Yoshitomi, K., "Radiation from a slot in an impedance surface," *IEEE Trans. Antennas and Propagat.*, Vol. 49, 1370–1376, 2001.
48. Takizawa, K. and O. Hashimoto, "Transparent wave absorber using resistive thin film at V-band frequency," *IEEE Trans. Microwave Theory and Tech.*, Vol. MTT-47, 1137–1141, 1999.
49. Brekhovskikh, L. M., *Waves in Layered Media*, Academic Press, NY, 1980.
50. Felsen, L. B. and N. Marcuvitz, *Radiation and Scattering of Waves*, Prentice-Hall, Inc., New Jersey, 1973.